Earth-Science Reviews 261 (2025) 104999

Contents lists available at ScienceDirect

Earth-Science Reviews

journal homepage: www.elsevier.com/locate/earscirev

Traversing the rift: A review of the evolution of the West and Central African Rift System and its economic potential

Nils Lenhardt [a,*], Erepamo J. Omietimi [a,f], Aitalokhai J. Edegbai [a,g], Lorenz Schwark [b], Octavian Catuneanu [c], James D. Fairhead [d], Annette E. Götz [e]

[a] Department of Geology, University of Pretoria, Private Bag X20, 0028 Pretoria, South Africa
[b] Institute of Geosciences, Christian-Albrechts-University, Ludewig-Meyn-Straße 10, 24118 Kiel, Germany
[c] Department of Earth and Atmospheric Sciences, University of Alberta, 1-26 Earth Sciences Building, Edmonton, Alberta T6G 2E3, Canada
[d] School of Earth and Environment, University of Leeds, Leeds, United Kingdom
[e] Department of Structural Geology and Geodynamics, Georg-August-University Göttingen, 37077 Göttingen, Germany
[f] Department of Geology, Niger Delta University, 560103 Amassoma, Nigeria
[g] Department of Geology, University of Benin, PMB 1154 Benin, Benin City, Edo State, Nigeria

ARTICLE INFO

Keywords
Continental rift
Rift basin
Cretaceous
Climate archive
Hydrocarbon reservoirs
Sequence stratigraphy
Gondwana breakup

ABSTRACT

The Cretaceous to recent West and Central African Rift System is a major geological feature in Africa, extending 4000 km from the west to the east. Its formation is related to the breakup of Gondwana and the separation of Africa from South America, during which a complex network of extensional, wrench and pull-apart basins formed. These basins can be separated into two coeval rift sub-systems, the West African Rift System and the Central African Rift System. Both systems are genetically related but are physically separated and show significant structural as well as sedimentological differences. However, despite its great importance for the history of the African continent, our understanding of its origins and evolution is limited due to a scarcity of geophysical and sedimentological data. In this review paper, we examine the sedimentary and igneous basin-fill of the major West and Central African Rift System basins using literature data from the previous five decades. We analyse basin evolution, sequence stratigraphy, changing environmental and palaeoclimatic conditions, and economic aspects of the basins. Furthermore, we address future needs and challenges in research and collaboration between academia and industry to better understand the vast economic potential of the West and Central African Rift System basins. Ultimately, our findings shed light on the complicated geological history of the West and Central African Rift System and offer vital insights for future research and development in the region.

1. Introduction

The West and Central African Rift System (WCARS) represents a unique geological feature in Africa that traverses major parts of the continent and extends ca. 4000 km from the Gao Basin in Mali to the Anza Basin in Kenya (Fig. 1). It is the only stable continental geological structure on Earth that is formed by large-scale topographic massifs (swells) (Ghomsi et al., 2022). Furthermore, the WCARS consists of a series of strike-slip shear zones related to extensional rift basins. These zones can be traced as continuous structures from Nigeria's Atlantic coast to southern Algeria and from Cameroon's coast to Kenya (Fairhead, 2023). The WCARS' complicated history included extension, shearing, and compression from the Early Cretaceous to the Paleogene (Keller et al., 2006) and is therefore significantly older than the East African Rift System (EARS) that did not start to form before the Eocene (Michon et al., 2022). The formation of the WCARS is linked to the opening of the Equatorial and South Atlantic oceans and the Indian Ocean, as well as the collision of the African with the Eurasian continent (e.g., Binks and Fairhead, 2019; Guiraud and Maurin, 1992; Peyve, 2015; Min and Hou, 2019; Nkodia et al., 2022), and hence to the geological history of four different continents: Africa, South America, Europe, and Asia.

Economically, the WCARS basins are considered to form extremely important hydrocarbon reservoirs (e.g., Liu et al., 2015; Fadul et al., 2020; Morakinyo et al., 2021; Chavom et al., 2022). Additionally, due to their wide stratigraphic range, the deposits of the WCARS basins

* Corresponding author.
E-mail address: nils.lenhardt@up.ac.za (N. Lenhardt).

https://doi.org/10.1016/j.earscirev.2024.104999
Received 19 August 2024; Received in revised form 14 November 2024; Accepted 22 November 2024
Available online 28 November 2024

constitute important archives to record climate changes, and may provide valuable information on several Oceanic Anoxic Events (OAE), such as OAE1a (Selli Event; early Aptian), OAE2 (Bonarelli Event; Cenomanian-Turonian) and OAE3 (Coniacian-Santonian), and potentially smaller and more localised events such as OAE1b (late Aptian to early Albian), OAE1c (middle Albian), OAE1d (Albian-Cenomanian) and MCE (middle Cenomanian) (e.g., Leckie et al., 2002; Wagreich, 2012; Beil et al., 2020, and references therein). Moreover, the WCARS deposits also record the Cretaceous-Paleogene (K-Pg) boundary event.

Research on the WCARS basins has always been strongly linked to hydrocarbon exploration, and it has often focused on identifying source and reservoir rocks.

So far, there is also a wealth of material available on the WCARS structural features and geophysical research (e.g., Fairhead, 1988, 2020, 2023; Fairhead and Green, 1989; Eyike et al., 2010; Fairhead et al., 2013; Eyike and Ebbing, 2015; Globig et al., 2016; Ghomsi et al., 2022; Baranov et al., 2023). A number of studies have also been conducted on the sedimentology, palynology, geochemistry, and petroleum geology of particular basins or parts of basins (e.g., Genik, 1993; Godet et al., 2014; Liu et al., 2015; Sarki Yandoka et al., 2015; Finthan and Mamman, 2020; Morakinyo et al., 2021; Ahmed et al., 2022; Chavom et al., 2022; Mbafor et al., 2023). However, a synthesis of these disparate pieces of information from many basins to provide context is currently lacking and urgently needed. This is the impetus behind the initiation of this review study.

Following an overview of the WCARS basins, their structures, and sedimentary infill, their context to sequence stratigraphy, palaeoenvironmental and palaeoclimatic changes, as well as the implications for economic aspects such as hydrocarbon reservoirs and geothermal energy potential, will be discussed.

2. Timing of WCARS formation and regional structure

The formation of the WCARS basins (Fig. 1) is closely related to the opening of the South and Equatorial Atlantic Ocean. Following the opening of the Central Atlantic Ocean during the Early Jurassic, which was associated with the formation of the Central Atlantic Magmatic Province (CAMP) and the subsequent breakup of Pangaea (Leleu et al., 2016), the South Atlantic Ocean began to form at around 150 Ma (Heine et al., 2013). After a period of expansion between the Paraná, Salado and Colorado basins in South America, and Africa, rifting began to occur progressively from south to north along reactivated older tectonic lineaments associated with extensive intracontinental deformation (Unternehr et al., 1988; Nürnberg and Müller, 1991; Eagles, 2007; Torsvik et al., 2009; Moulin et al., 2010; Seton et al., 2012). The timing of the onset of seafloor spreading was around 132 Ma, correlating with

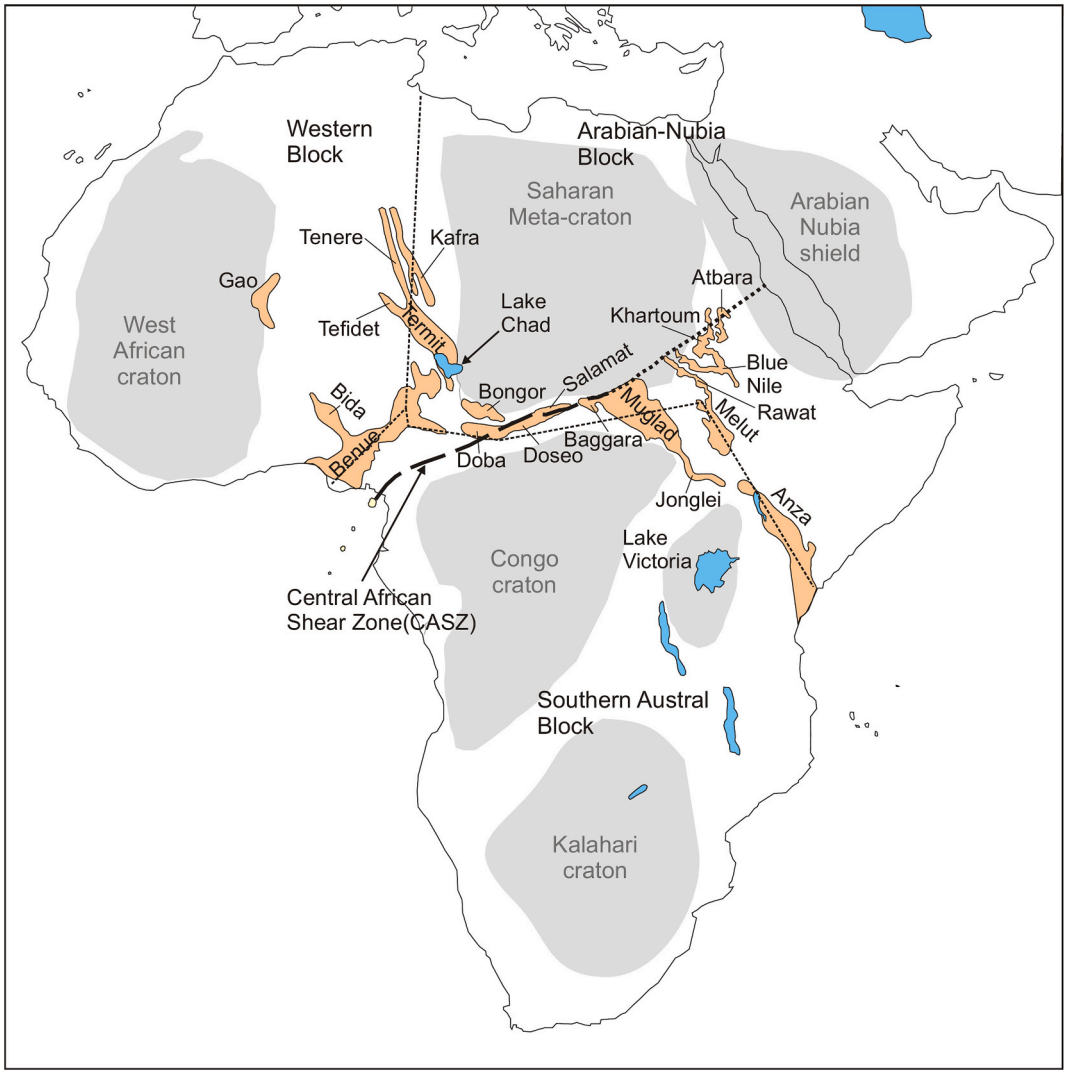

Fig. 1. Map showing the location of WCARS basins in between major cratonic areas in Africa, including the subdivision into a Western, Arabian-Nubia, and Southern Austral block (modified from Genik, 1993; Meert and Lieberman, 2008).

the peak of magmatism of the Tristan da Cunha mantle plume and the formation of the South Atlantic igneous province (Torsvik et al., 2009; Foulger, 2018) with the Paraná (Brazil) and Etendeka (Namibia) basalts (Beccaluva et al., 2020; Gomes and Vasconcelos, 2021) forming its main expression. This event coincided with the activation of the WCARS and the Central African Shear Zone (CASZ) (Binks and Fairhead, 2019; Genik, 1992; Guiraud and Maurin, 1992; Torsvik et al., 2009), which together with the Kandi Shear Zone (KSZ) extended towards the Pernambuco Shear Zone in South America (Bezerra et al., 2006). Pre-rift stages initiated along the future Gulf of Guinea and the Upper Benue area (Guiraud and Bellion, 1995) with half-graben formation in transtensional stress fields and the deposition of first coarse alluvial fan

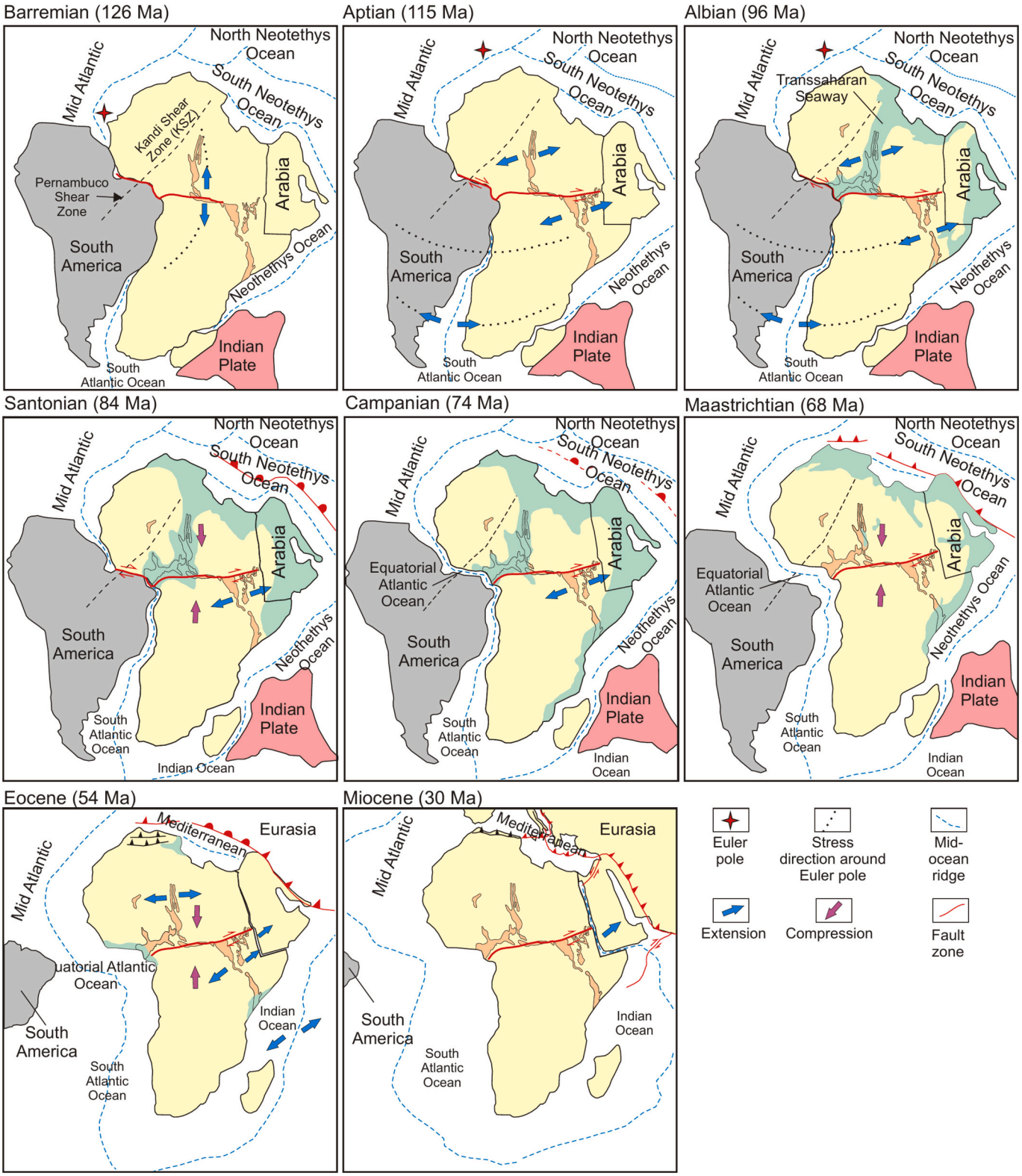

Fig. 2. Regional model of tectonic evolution and basin formation (modified from Genik, 1993; Scotese, 2014; Gao et al., 2023).

deposits and alkaline lava flows (Maluski et al., 1995). Rifting continued to propagate northward and into the African interior along the earlier-formed Pan-African mobile belts, which are assumed to have directly controlled the location of rift and failed rift systems during the Late Jurassic and Early Cretaceous (Bumby and Guiraud, 2005). The Benue Trough in Nigeria was active by at least 118 Ma (Nürnberg and Müller, 1991), although earlier extension may be possible (Torsvik et al., 2009). Furthermore, rifts developed along the Blue Nile Valley and the Anza Trough where marginal marine and fluvial deposits and basaltic lava flows were laid down following the opening of the Indian Ocean (Bosworth, 1992) (Fig. 2).

The rifts split the African plate into three blocks (Guiraud and Bellion, 1995): (1) the Western block to the west of the West African Rift, (2), the Arabian-Nubian block bound to the south and west by the WCARS, and (3) the Austral block south of the Central African rift (Fig. 1). The relative western movement of the Austral block was most probably attributed to the rifting direction of the South Atlantic, whereas the north-eastwards movement of the Arabian–Nubian block was related to opening of the Indian Ocean (Guiraud and Bellion, 1995). The equatorial part of the South Atlantic was the youngest to form with seafloor spreading assumed to have been between 120 and 100 Ma (Nürnberg and Müller, 1991; Eagles, 2007; Torsvik et al., 2009; Moulin et al., 2010).

The major part of the WCARS basin development can be attributed to the opening of the Atlantic Ocean and the separation of South America from Africa. However, the opening of the Indian Ocean additionally influenced crustal extension and basin formation by causing widespread faulting in Kenya and Sudan (Winn Jr et al., 1993; Fairhead, 2023). This probably took place during the Late Jurassic at 167 Ma with the oldest oceanic crust forming during the separation of eastern (India – Sri Lanka – Seychelles – Madagascar – Australia – Antarctica) from western (Africa – South America) Gondwana (Lawver et al., 1991). Rifting in the interior of Africa ceased at about 85 Ma (Seton et al., 2012). The sedimentary basins of the WCARS have undergone significant crustal extension and crustal thinning due to passive rifting (no active upper mantle processes), resulting in the isostatic response process of crustal subsidence (Fairhead, 2023), after which the basins were rapidly filled.

The development of the WCARS can be divided into three rift phases during the Early Cretaceous, the Late Cretaceous, and the Paleogene (Genik, 1992) (Fig. 3). The Early and Late Cretaceous rift phases took place in the majority of the WCARS basins, while the third (Paleogene) rift phase was generally confined to NW-SE trending basins, such as the Termit and Melut basins (Schull, 1988; McHargue et al., 1992; Genik, 1992, 1993). The first phase, corresponding to the Early Cretaceous (Fairhead, 1988), was a strong rifting stage. From 130 Ma (the opening of the South Atlantic) to 126 Ma, only minor actual rifting occurred, with the rift becoming fully developed between 126 and 98 Ma and the deposition of fully continental sedimentary strata (Genik, 1992). In the Bongor Basin north of the CASZ, the corresponding strata are capped by a regional unconformity (Genik, 1992), with all Late Cretaceous deposits missing. A similar situation can be seen in the Blue Nile Basin.

The second rift phase (Fig. 3), which corresponds to the Late Cretaceous (ca. 98–75 Ma), was associated with a short-lived period of rift followed by a long post-rift period of thermal subsidence (Genik, 1992),

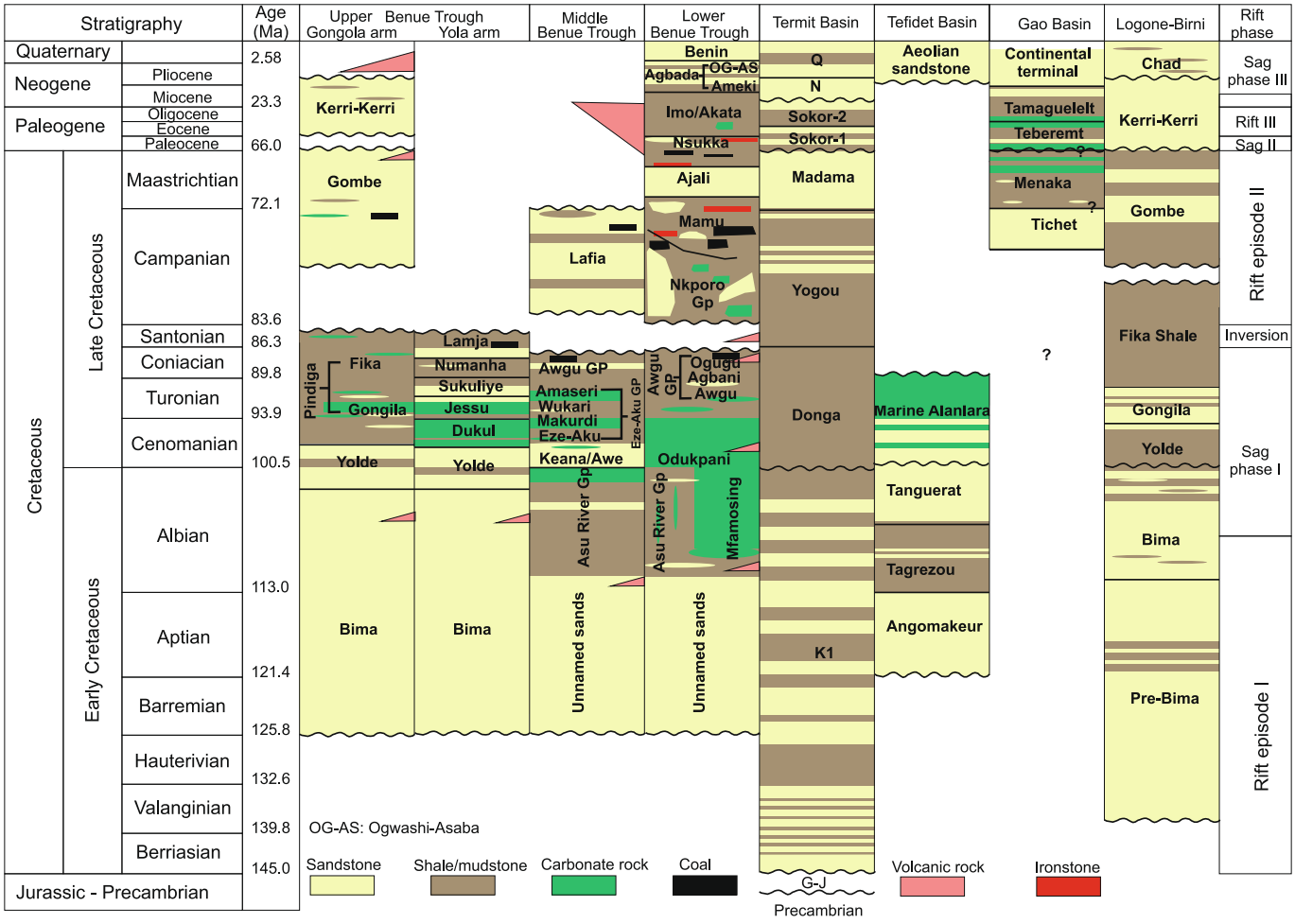

Fig. 3. Stratigraphy of the WARS (modified from Moody and Sutcliffe, 1991; Obaje, 2009; Loule and Pospisil, 2013; Zhou et al., 2017; Lai et al., 2018; Edegbai et al., 2019; Konaté et al., 2019; O'leary et al., 2019; Dou et al., 2022a; Wang et al., 2022).

which had the effect of deepening and widening the existing basins. This period coincided with a general sea-level rise that culminated in the late Cenomanian to Turonian, which is associated with the highest global Phanerozoic sea levels, resulting in extensive marine transgression over low-lying areas within the sagging rifts (Bumby and Guiraud, 2005; Guiraud et al., 2005). In particular, a marine transgression southwards from the Neothethys and northeastwards from the Gulf of Guinea occurred, flooding northern and west-central Africa and creating the Trans-Saharan seaway (Guiraud and Bellion, 1995; Edegbai et al., 2019). At about 80 Ma, the Trans-Saharan seaway attained its maximum eastern extent when it reached the western-most end of the Doba Basin in Chad (Genik, 1992). During this phase, the West African Rift basins were filled with several km-thick, primarily marine strata, while the Central African Rift basins received equal thicknesses of exclusively continental (lacustrine and fluvial) material. Additionally, during the Late Cretaceous, a compressional event occurred that is thought to be associated with a small change in the spreading direction and rate within the Atlantic Ocean and the initiation of the Alpine Belt by the collision of the African plate with the Eurasian plate along the NW African plate margin (Guiraud and Bosworth, 1997; Bachari et al., 2024): The N-S Santonian Compressional Event. The event is commonly recognised by the presence of folding and strike-slip faulting in most of the E–W to ENE–WSW trending basins in response to NE-orientated shortening, which resulted in the formation of transpressional flower structures (Bumby and Guiraud, 2005) and the inversion of most of the Cretaceous troughs between the Lower Benue Trough and westernmost Sudan (Guiraud et al., 2005). Because of their near-parallel orientation with the general Santonian shortening direction, the large-scale NW-SE trending troughs in Niger, Sudan, and Kenya continued to deepen during this event. This coincided with a reactivation of the Agadez lineament and the separation of the Termit from the northern Niger rifts (Genik, 1992). In addition, the Doba, Doseo, and Salamat basins, which up to this time had effectively been a single basin, were divided into four independent basins during that time by dextral movements along the Borogop fault (Guiraud et al., 1985, 1987; Fairhead and Binks, 1991; Genik, 1992; Chen et al., 2018).

A smaller, subsequent short-lived compressional episode known as the "Maastrichtian Compressional Event" or "End Cretaceous Event" had a compressional axis similar to that of the Santonian event and tended to emphasise the Santonian contraction features (Fairhead, 2023). Guiraud et al. (2005), however, suggest the age of this event as 55 Ma, which would place it into the Paleocene. As previously indicated, the compressional tectonics causing basin inversion appear to be restricted mainly to the E-W to ENE-WSW trending basins in North Africa, with the southern limits being the basins of the WCARS. Fairhead (2023) has thus suggested the WCARS has acted as a buffer zone, absorbing the effects of the short-lived N-S compressional events. The link between the timing of sedimentary unconformities (i.e., periods of crustal stress change) in the basins of the WCARS identified by Guiraud and Bosworth (1997) has been shown by Fairhead (2023) to closely relate to changes in the opening direction of the fracture zones within the adjacent Central Atlantic Ocean. Since the age of the oceanic crust is well constrained by the magnetic reversal patterns, this correlation helps to constrain the timing of tectonic events within the African basins.

The third rift phase (Fig. 3) between the late Eocene and early Miocene (50–15 Ma) predominantly occurred in the West African rift basins and few of the Central African basins such as the Muglad and Anza rifts and was terminated by a regional unconformity (Genik, 1992). Elsewhere, the basins were predominantly emergent. The deposits that formed during this phase were mainly continental. This phase is generally associated with continued rifting at the margins and within the African-Arabian plate (Lowell and Genik, 1972; Makris and Rihm, 1991). During this time, the Dead Sea-Red Sea-Gulf of Aden rift began to form with NE-SE extension, and N-S shortening in northern Africa (Bumby and Guiraud, 2005). This phase also coincides with the onset of magmatism associated with the Afar plume between 45 and 31 Ma (George et al., 1998; Burke et al., 2003) and the formation of the EARS, which has been active in recent times (Chorowicz, 2005). A large portion of the WCARS has remained essentially emergent during the past 30 million years, with major areas being elevated and eroded (Genik, 1992).

The WCARS can be separated into two coeval rift sub-systems: the West African Rift sub-system (WARS) and the Central African Rift sub-system (CARS) (Bosworth, 1992). Both are genetically related yet physically distinct, with structural differences. The Logone-Birni Basin in northern Cameroon can be considered a transitional zone between the two sub-systems (Eyike et al., 2010; Loule and Pospisil, 2013). The rift system generally follows older suture zones, i.e., the Pan-African orogenic belts in between the West African, the Saharan Metacraton, the Congo and Tanzania cratons, and the Arabian-Nubian Shield that are characterised by thicker crust (Fig. 1).

Particularly in Cameroon and Nigeria, the crustal structure of the WCARS is relatively well defined by seismological and gravimetric data (Fairhead, 2023). Geophysical investigations in Cameroon have revealed that the crust beneath the Yola Rift is relatively thin, with a thickness of 23 km. The crustal thickness beneath the Adamawa Uplift is 33 km (Stuart et al., 1985), whereas the Benue Trough has estimated crustal thicknesses of 20 to 23 km (Tokam et al., 2010; Akpan et al., 2016). According to the same authors, the adjacent, more elevated areas with crystalline basement have thicknesses of 35–40 km. In other areas of the WCARS, however, information is still very sparse. For instance, the only seismic data associated with the crustal structure of the CARS is found in Kenya for the Lake Turkana-Anza Basin area, where a Moho depth beneath Lake Turkana was found to vary from 20 to 23 km before increasing in depth southwards away from the Anza Basin trend from 28 to 33 km (Prodehl et al., 1994; Fairhead, 2023). Benoit et al. (2006) demonstrated that the average crustal thickness beneath the Lake Turkana area is 25 ± 5 km, which is 10–15 km thinner than the crust beneath the East African and Ethiopia plateaus. In addition, El Tahir et al. (2013) showed a crustal thickness beneath the Khartoum Basin in Sudan ranging between 33 and 37 km, with an average of 35 km.

The crustal thinning model associated with the WCARS major rift basins is based on regional gravity surveys in Nigeria/Cameroon (Fairhead and Okereke, 1987), Nigeria and Niger (Fairhead and Green, 1989; Fairhead, 2023), Sudan (Fairhead et al., 2013), and Kenya (Reeves et al., 1987), and is supported by seismic refraction studies across the Yola/Garoua rift in Cameroon (Stuart et al., 1985) and the Anza Basin in Kenya (Prodehl et al., 1994, 1997), as well as tele-seismic receiver function studies in Cameroon and Nigeria (Tokam et al., 2010; Akpan et al., 2016; Fairhead, 2023). These studies indicate that the major WCARS basins are associated with long-wavelength positive gravity anomalies resulting from major crustal thinning beneath them. In Cameroon and Nigeria, the crustal thicknesses over exposed basement areas to the NW and SE of the Benue Trough are 35–40 km, while within the Benue Trough and Yola rift, the crustal thicknesses are between 20 and 23 km. Similar findings over the Anza rift basin in Kenya are also found.

Although there have been many crustal tectonic models developed to explain the development of rift basins (McKenzie, 1978; Buck, 1991; Wernicke, 1985; Ziegler and Cloetingh, 2004; Unternehr et al., 2010), the only tectonic model that is consistent with the geophysical data for the WCARS is that of McKenzie (1978).

3. The West African Rift Sub-system (WARS)

3.1. Benue Trough, Nigeria

The Benue Trough is a prominent tectonic feature in the WARS (Fig. 1) covering an area of 1000 km by 100 km (Benkhelil, 1989) (Fig. 4). It is a polyhistory NE-SW trending collection of several mini-basins demarcated into three major segments: Lower, Middle, and Upper Benue troughs (Nwajide, 2013). The Gboko wrench fault (Whiteman,

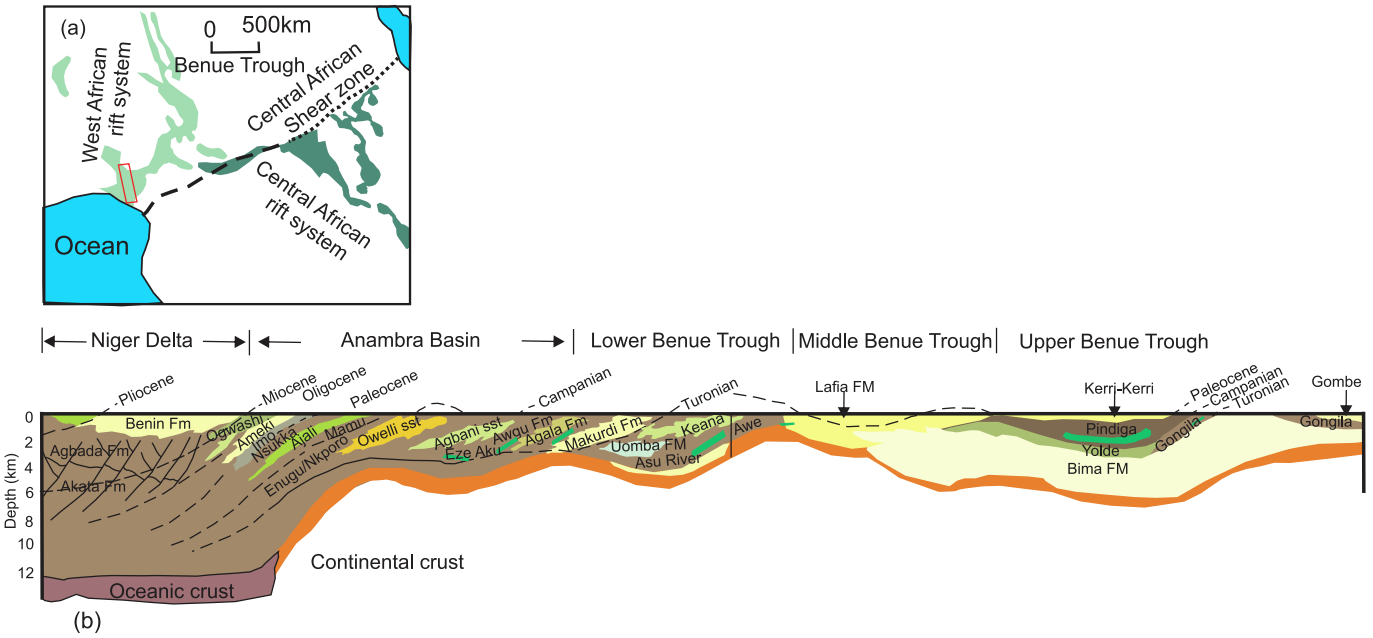

Fig. 4. a) Map showing the location of the Benue Trough within the West African and Central African Rift Systems. CASZ, Central African Shear Zone; b) Synthetic cross-section across the Benue Trough (after Benkhelil, 1989).

1982) separates the Lower from the Middle Benue Trough segments, while an arbitrary demarcation guided by major municipalities separates the Central Benue Trough from the Upper Benue Trough (Obaje, 2009; Nwajide, 2013). The Upper Benue Trough segment is subdivided into the Gongola and Yola sub-basins, which extend into Cameroon as the Garoua Basin. The initiation of the Benue Trough was preceded by the emplacement of the anorogenic Late Jurassic "Younger Granites" in the North Central Highlands of Nigeria and the northern Niger Republic (Burke and Whiteman, 1973; Whiteman, 1973; Offodile, 1980). Its basin fill is of variable thickness, comprising syn- and post-rift strata ranging from 3 km in the Central Benue Trough to 5 km and 6 km in the Upper and Lower Benue Trough, respectively (Ofoegbu, 1984). The pre-rift rocks (Fig. 3) are essentially Precambrian polycyclic crystalline basement rocks, which are overlain by an Aptian (or older) to mid-Albian syn-rift megasequence comprising continental to deltaic sedimentary strata of the Bima Formation (Upper Benue Trough) and the pre-Asu River Group (Middle and Lower Benue Trough), which are coeval with the Ise Formation in the adjoining transform margin Benin Basin (Allix and Popoff, 1983; Elvsborg and Dalode *in* Brownfield and Charpentier, 2006; Edegbai et al., 2019). Since the Asu River Group is widely accepted as the oldest strata in the Southern and Central Benue Trough, there are pieces of reliable geophysical and geochemical evidence supporting the occurrence of older continental feldspathic sandstone and siltstone strata below the Asu River Group (Bute et al., 2024; Maurin and Benkhelil, 1990; Etim et al., 1988; Olade, 1976). Recent seismic data from the adjoining Bornu and Benin basins show a break-up unconformity, which separates these syn-rift strata from the post-rift strata, arising from the final separation of the South American Plate from the African Plate. The first phase of marine incursion into the Benue Trough began in the mid-Albian, inundating the more proximal Southern and Central Benue Trough segments before reaching the more distal Upper Benue Trough in the early Cenomanian (Adeleye, 1975). Since the mid-Albian to Cenomanian transgression is evinced by the dominantly marine strata of the Asu River Group and Odukpani Formation in the Lower and Middle Benue Trough segments, the Cenomanian "transitional" Yolde and Gongila (bottom section) formations mark the onset of this ingressive phase in the Upper Benue Trough (Fig. 3) (Nwajide, 2013; Sarki Yandoka et al., 2017). Flooding progressed through to the Coniacian Stage (with minor regressions), establishing the Trans-Saharan Seaway with the maximum highstand at the Cenomanian-Turonian boundary (Reyment and Tait, 1972; Adeleye, 1975; Reyment and Dingle, 1987), and depositing richly fossiliferous (comprising gastropods, ostracods, and cephalopods) coeval strata across the Benue Trough, such as the Eze-Aku and Awgu groups (Lower and Middle Benue Trough), the Gongila (Gongola sub-basin) and the Dukul, Jessu, and Sekule formations (Yola sub-basin) (Fig. 3). This inland seaway was truncated due to the Santonian inversion of NE-SW trending faults (Suleiman, pers. comm., 2019) characterised by fault reactivation, folding, exhumation, and magmatism, which was more severe in the Southern Benue Trough. Since the southern and central parts of the Benue Trough were emergent during the inversion period, it is widely accepted that marine to estuarine depositional processes were active from the Turonian to the Campanian (?), depositing the Fika (Gongola sub-basin), Numanha, and Lamja formations (Yola sub-basin) (Fig. 3), implying that the inversion occurred at a later time (most probably the Maastrichtian) in the Upper Benue Trough (Abubakar et al., 2008). The penultimate phase of the Benue Trough's evolution is the post-inversion thermal sag phase, which followed a westward shift in depocenter towards the Gongola sub-basin, and the Anambra and Lafia (Central Benue Trough) basins, as well as the Afikpo sub-basin east of the Abakaliki anticlinorium. Sedimentation in these post-Santonian depocenters was characterised by Campanian to Danian strata of the Nkporo Group, the Mamu, Ajali, and Nsukka formations (Anambra Basin), and the Lafia and Gombe formations (Middle Benue Trough and Gongola sub-basin, respectively) that depict marine to estuarine palaeoenvironments (Abubakar et al., 2008; Nwajide, 2013; Edegbai et al., 2019). Other portions of the Benue Trough, such as the Yola sub-basin and most of the central segment, have had positive structures since the post-Santonian. There was short-lived compression in the early Paleogene, which is markedly visible in the Gongola and adjoining Bornu basins, demonstrated by the angular unconformity separating the Late Cretaceous Gombe Formation from the Paleogene continental Kerri-Kerri Formation that was deposited under thermal sag palaeotectonics (Fig. 3). The Niger-Delta Basin, which is a passive margin basin, represents the current phase in the Benue Trough's evolution. It is a siliciclastic wedge that has progressively prograded southwards through time into structures created in response to gravity spreading (Doust and Omatsola, 1990; Chima et al., 2019). Five of these structures, or depobelts, have so far

been recognised, each bounded by large regional and counter-regional bounding faults (Evamy et al., 1978; Doust and Omatsola, 1990). Available regional seismic lines along a N-S transect show varying structural domains, ranging from an extensional domain characterised by listric growth faults in the updip end, to a thrust fault-dominated compressional domain downdip (Evamy et al., 1978; Cohen and McClay, 1996). The sedimentary fill of up to 12 km (Short and Stauble, 1967) consists of three diachronous units: the marine Akata Formation, the middle paralic Agbada Formation, and the upper continental Benin Formation. The Niger and Benue River systems have supplied significant sediment volumes into the Niger-Delta Basin since the Eocene (Doust and Omatsola, 1990).

3.2. Termit Rift, Niger

The Termit Basin (Figs. 1 and 5), which covers approximately 27,000 km^2 in southeastern Niger, is one of the major Cretaceous-Paleogene rift systems within the WARS (Genik, 1993; Harouna and Philp, 2012; Mao et al., 2016; Tang et al., 2017; Fairhead, 2023). It is regarded as the second-largest expansive asymmetrical rift basin in the WCARS (Lai et al., 2018). Subsurface data indicates that the strata of the basin overlie the Precambrian-Jurassic crystalline complex, reaching a thickness of ca. 12 km (Dou et al., 2022a). In the Lower Cretaceous, around 149–97.8 Ma, the Termit Basin experienced rifting due to the fragmentation of Gondwana, marking the initial splitting of the African and South American lithospheric plates (Genik, 1992). During this period, a significant amount of Lower Cretaceous terrigenous siliciclastics (i.e., K1 Formation) accumulated (Lai et al., 2018; Wang et al., 2022) (Fig. 3).

Throughout the Upper Cretaceous period (~98.9–65.6 Ma), the basin experienced substantial thermal subsidence, which led to a widespread marine transgression from the Tethys Sea through Mali and Algeria in the north, and from the Atlantic Ocean through the Benue Trough in the south (Genik, 1993; Lai et al., 2018) (Fig. 2). Following this phase, seawater regression occurred until approximately 74 Ma (Lai et al., 2018). Within this sequence, three distinct formations can be identified, i.e., the Donga, Yogou, and Madama formations that make up the K2 Group (Fig. 3). During the Cenomanian-Campanian, the marine sedimentary rocks of the Donga and Yogou formations were deposited, composed of mudrocks, sandstones, and siltstones (Lai et al., 2018). The overlying Madama Formation was deposited in the Maastrichtian and primarily consists of sandstones, formed in braid-delta environments (Lai et al., 2018; Dou et al., 2022a; Wang et al., 2022). The Donga and Yogou formations align with the rise of global sea levels throughout the Late Cretaceous (Lai et al., 2018). The Sokor-1 Formation marks the onset of Paleogene sedimentation and consists of deltaic sandstones and shales. The Oligocene-aged Sokor-2 Formation comprises laminated shales deposited in a lacustrine environment and poorly to moderately sorted sandstones (Dou et al., 2022a). Four distinct widespread unconformities are identified in the Termit Basin (Fig. 3) (Dou et al., 2022a). During the Neogene to Quaternary, the basin underwent substantial faulting and uplift, subsequently accumulating extensive layers of alluvial plain and fluvial sedimentary rocks (Dou et al., 2022a).

3.3. Northern basins, Niger

In northern Niger, the Tefidet Trough (Fig. 6), trending in a NW-SE direction, constitutes one of the Cretaceous troughs within the western

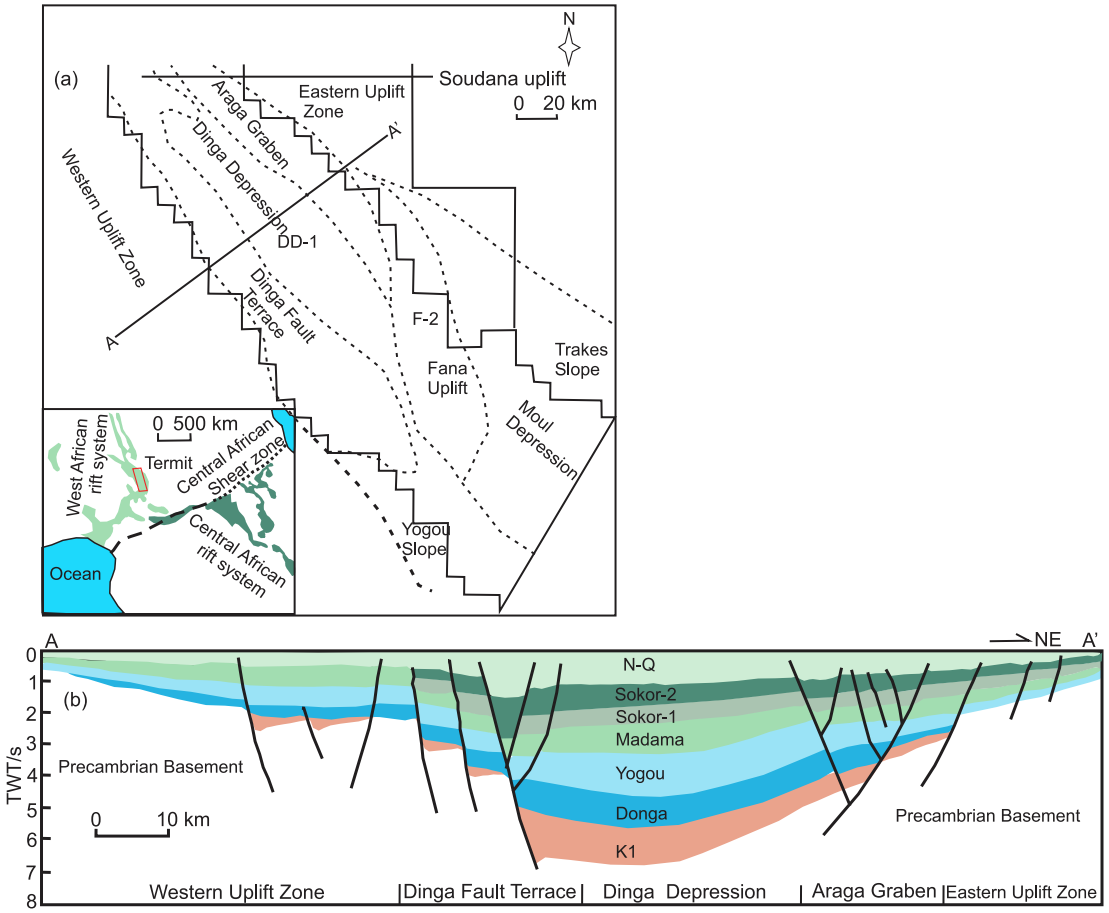

Fig. 5. a) Structural outline of the Termit Basin (after Wang et al., 2022). The inset shows the location of the Termit Basin within the West African and Central African Rift Systems. CASZ, Central African Shear Zone; b) cross-section through the Termit Basin (after Wang et al., 2022).

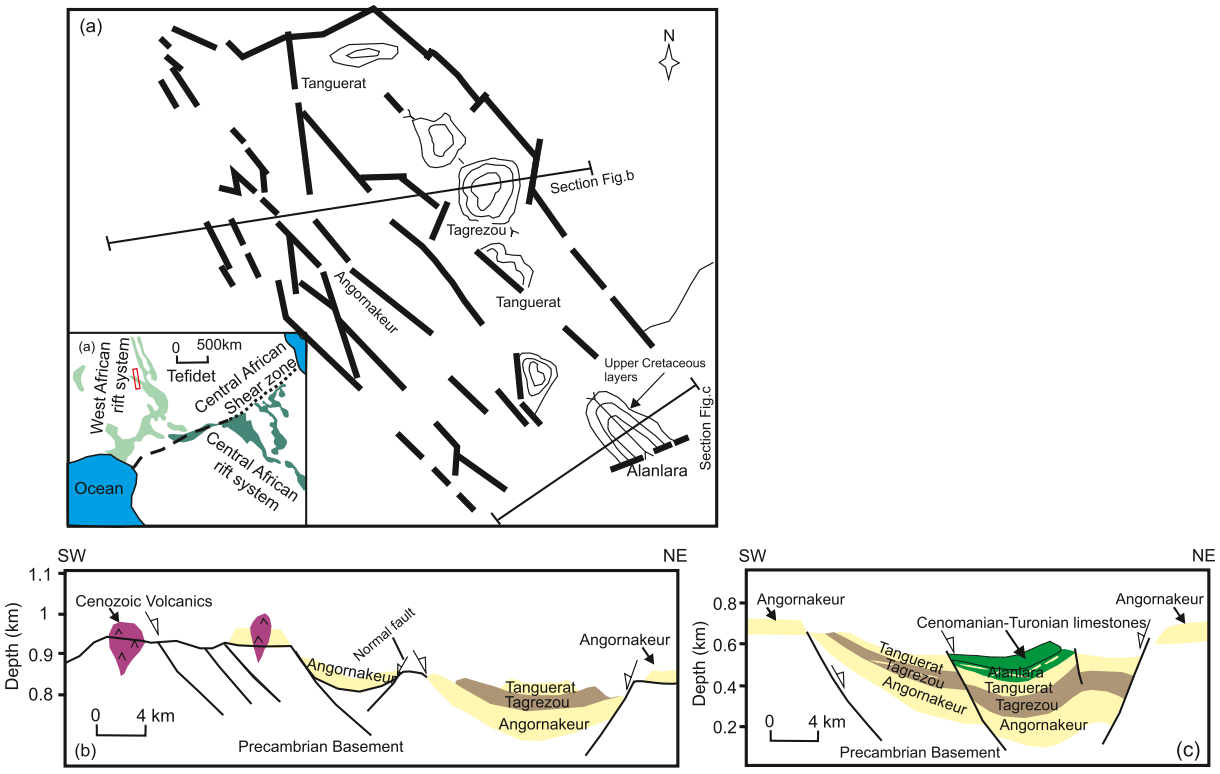

Fig. 6. a) Structural outline of the Tefidet Basin architecture (after Ahmed et al., 2016; Konaté et al., 2019). The inset shows the location of the Tefidet Basin within the West African and Central African Rift Systems. CASZ, Central African Shear Zone; b, c) cross-section profiles across the Tefidet Basin (after Konaté et al., 2019).

arm of the Tenere Graben (Fig. 7). In the Tenere, Grein, and Kafra troughs, the thickness of Cretaceous strata typically reaches up to 3 km (Liu et al., 2017a; Konaté et al., 2019). However, in the Tefidet Trough, this thickness does not exceed 1 km (Fig. 6) (Konaté et al., 2019). The formation of the Tefidet Trough and other Tenere grabens occurred concurrently with that of the Nigerian Benue Trough (Genik, 1993; Ahmed et al., 2016; Liu et al., 2017a; Konaté et al., 2019). It can be assumed that the N60° trending faults (i.e., the Charcot transform fault) of the Benue Trough may have functioned during the Cretaceous as a transfer fault, connecting the Tefidet extensive zone and the Atlantic opening (Benkhelil, 1982; Konaté et al., 2019). The fill of the Tefidet Basin primarily comprises Lower Cretaceous coarse-grained sandstones, mudrocks, and clayey sandstones, as well as Upper Cretaceous shallow-marine carbonates and siltstones and aeolian Quaternary sandstones. Konaté et al. (2019) constructed the stratigraphic framework of the Tefidet Basin through a combination of literature reviews and field investigations. The deepest southeastern part of the Tefidet Trough contains ca. 0.9 km of lacustrine and shallow-marine sedimentary rocks (Fig. 6). Meanwhile, moving north-westward within the trough, the thickness of the sedimentary sequences generally decreases. In some areas, only the Lower Cretaceous strata are visible, resulting in thin layers that are covered by Cenozoic volcanic structures (Konaté et al., 2019). The Tefidet Group comprises four sedimentary formations (see Fig. 3). The Angornakeur Formation consists of cross-stratified sandstones and thin clay lenses with an average thickness of 0.25 km. This formation sits unconformably on the crystalline Precambrian basement. Conglomeratic beds may be present, along with feldspathic layers exhibiting cross-stratifications. The overlying Tagrezou and Tanguerat formations consist of thin claystones and argillaceous siltstones, with vertebrate bones found within calcareous-enriched layers. The Cenomanian to Coniacian Alanlara Formation predominantly comprises black limestones with fine-grained sandstones, argillaceous limestones, and gastropod limestone-sandy facies. The Cenomanian-Turonian sequence (ca. 0.07 km in vertical thickness) consists of dark grey to dark fossilised (i.e., ammonites and gastropods) limestones and gypsum-rich shales containing sea urchins and oysters. The ammonites in the Cenomanian strata enable a good correlation with the northeast Nigerian Upper Benue Trough (i.e., Gongola and Yola sub-basins), indicating a connecting link between the Tenere Mega-system and the Upper Benue Trough during the Cenomanian-Turonian period in West Africa. Deposition continued in the Upper Cenozoic with the sedimentation of aeolian sandstone. So far, no formal name has been suggested for these Quaternary rocks (Fig. 3).

The Tenere Basin (Fig. 7), surrounded by the Tefidet and Grein grabens, trends in a NW-SE direction and spreads across 300 km north-south and 50–80 km east-west (Liu et al., 2017a). The oldest sedimentary sequences are uncomfortable with the Precambrian crystalline rocks, and the basin is split into structural units comprising the eastern depression I, the eastern depression II, and the western depression (Fig. 7) (Genik, 1992; Zanguina et al., 1998; Fairhead et al., 2013; Liu et al., 2017a; Yuan et al., 2022). The widespread rifting across West and Central Africa developed the Tenere and other WCARS basins. In the Albian period, rifting activities in the Tenere Basin led to a rapid subsidence and the subsequent accumulation of sediments from the continent in freshwater and marine environments (Liu et al., 2017a; Yuan et al., 2022). Consequently, fine-grained (mudrocks) and coarse-grained clastics (sandstones) in the basin can reach a vertical thickness of 2.0 km (Figs. 3 and 7). A significant shift in palaeogeographic conditions occurred during the Cenomanian period, marked by marine waters that entered the Niger and Chad basins through narrow passages from both the north (Neo-Tethys) and the south (Atlantic Ocean via the Benue Trough), forming the Trans-Saharan Seaway (Reyment, 1980; Reyment and Dingle, 1987; Genik, 1992; Maurin and Guiraud, 1993; Liu et al., 2017a; Yuan et al., 2022). Analysed microfossils (foraminifera, dinoflagellate cysts, and calcareous microalgae) and geochemical data from well SH-1 indicate that the Upper Cretaceous sequences were deposited in a marine environment (Liu et al., 2017a). Sedimentary layers consisting of sandstones and mudrocks were deposited in shallow marine to

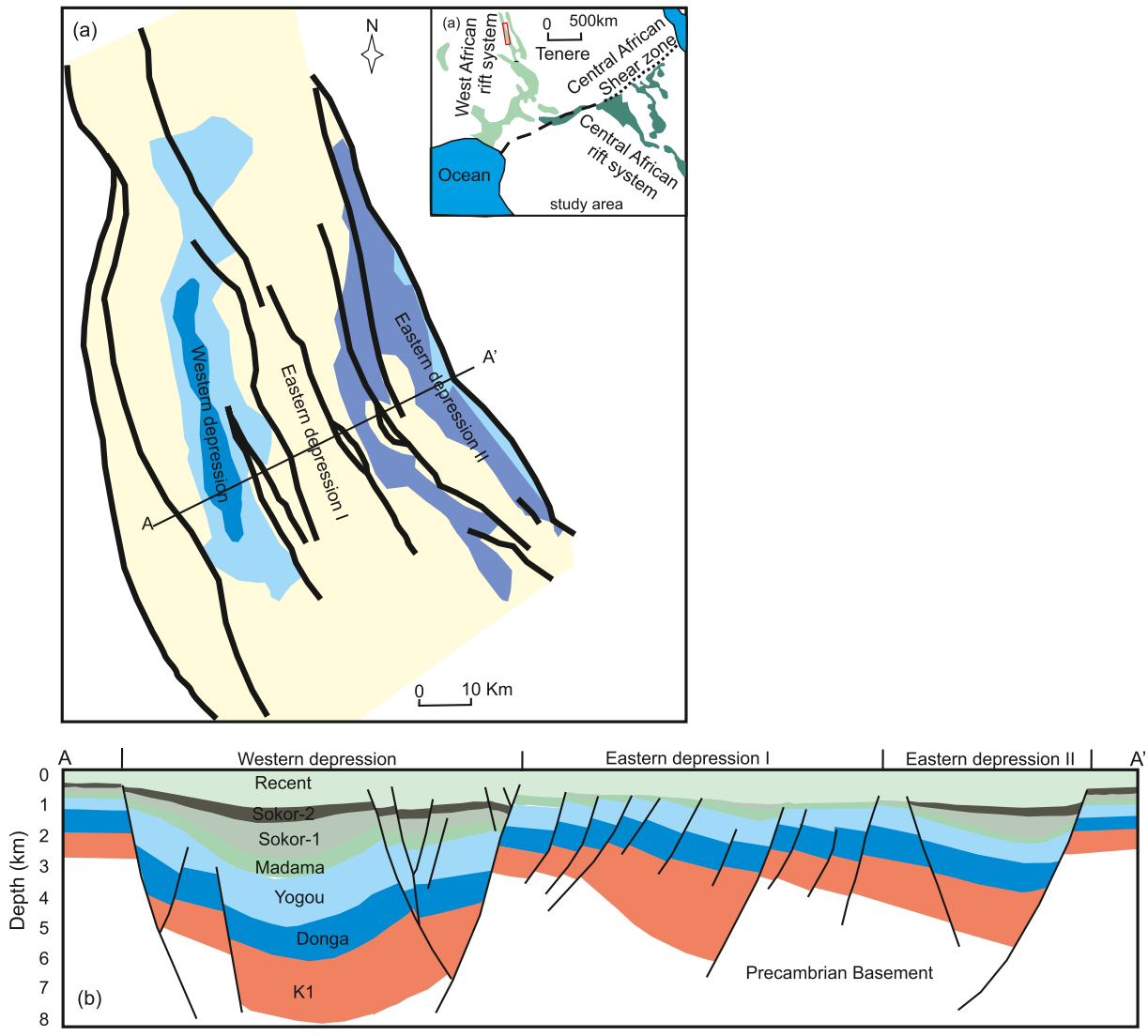

Fig. 7. a) Structural outline of the Tenere Basin architecture (after Genik, 1993; Liu et al., 2017a). The inset shows the location of the Tenere Basin within the West African and Central African Rift System. CASZ, Central African Shear Zone; b) East-West cross-section across the Tenere Basin (after Liu et al., 2017a).

paralic environments.

3.4. Gao Basin, Mali

During the Early Cretaceous, rifting activities created the Gao Basin in eastern Mali, which is classified as a graben, or potentially a half graben in some areas, and is bounded by a series of normal faults (Guiraud et al., 2005; Ye et al., 2017; O'leary et al., 2019). The Precambrian basement (i.e., igneous and metamorphic rocks) underlies the Cretaceous sequences in the basin (Moody and Sutcliffe, 1991). Although the basin is not linked to other parts of the WARS, it contains a comparably thick (>1 km) Cretaceous-Paleogene sedimentary sequence (O'leary et al., 2019). The succession consists of sandstones, conglomerates, shales, gypsum, and limestones that likely formed in marine to freshwater environments (Moody and Sutcliffe, 1991). Well data analysed by Merabet et al. (1971) suggests that the potential post-Turonian seaway channels in eastern Mali, particularly around Bourem and Gao, were relatively narrow, possibly less than 100 km wide (Moody and Sutcliffe, 1991). The Malian sequences that formed from the Trans-Saharan seaway exhibit similarities and lateral equivalence with the more extensively studied deposits in Nigeria and Niger (O'leary et al., 2019). During the Late Cretaceous and Eocene periods, the section of the Trans-Saharan Seaway that specifically filled the Gao Trench was identified as the Détroit Soudanais (Radier, 1959).

The Tichet and Ménaka formations are entirely subsurface, and no outcrop sections are known (O'leary et al., 2019). Nevertheless, they are the first formally described formations within the Gao basin fill. The upper Campanian Tichet Formation consists of fine- to coarse-grained sandstones that are green to orange in colour. The sandstones are characterised by cross-bedding and very large inclined foresets. The Maastrichtian Ménaka Formation is characterised by fissile shale layers with a significant quantity of mollusc shells and marly limestones. In addition, the formation consists of thin, fine-grained sandstones and conglomerate lenses. The overlying Teberemt Formation describes the lithostratigraphic sequence of open marine shales and carbonates that make up the Paleocene in Mali (Moody and Sutcliffe, 1991, 1993). Moody and Sutcliffe (1991) produced a composite graphic log for Mali and northern Nigeria that showed the fundamental stratigraphy of the Teberemt Formation, but their works did not provide a basis for the name "Teberemt" or specify a type locality (specific location where it was first identified). This type locality for the formation was eventually provided by O'leary et al. (2019). The Teberemt Formation consists of a 12–17 m-thick sequence of shales and limestone intervals below the Tamaguélelt Formation, and sits irregularly on top of the Ménaka Formation. The upper contact of the formation is identified by a limestone bed that is similar in thickness (1–5 m) and represents a shallow,

restricted marine environment in the Trans-Saharan Seaway deposits. In addition, the shales and limestone strata contain abundant echinoids, gastropods, and nautiloids, and there are many trace fossils, including a well-developed network of *Thalassinoides* burrows (O'leary et al., 2019). Age-diagnostic index fossils, including the dinoflagellate cyst *Spiniferites*, the nautiloids *Cimomia reymenti* and *Cimomia ogbei*, and the echinoid *Oriolampas michelini*, suggest a Maastrichtian-Paleocene age for the Teberemt Formation.

The Tamaguélelt Formation consists of a 13–16-m-thick sequence mainly composed of fissile shales and siltstones, with occasional phosphate and conglomerate lenses of varying thickness and rare sandstone beds. This formation sits above the Teberemt Formation and below the Continental Terminal. The fissile shales in the Tamaguélelt Formation are notably more orange to yellow compared to those in the Ménaka or Teberemt formations and often contain iron oxide nodules. The upper boundary of the Tamaguélelt Formation is marked by ferruginous sandstones, which are at the base of the Continental Terminal sedimentary strata (O'leary et al., 2019).

3.5. Logone-Birni Basin, Cameroon

The sedimentary deposition in the Logone-Birni Basin (LBB) in northern Cameroon occurred during the Lower Cretaceous period. Gravity, magnetic, and seismic investigations have revealed that the basin contains approximately 6 km of siliciclastic rocks in its centre, which directly overlie the crystalline basement (Manga et al., 2001; Loule and Pospisil, 2013; Nguimbous-Kouoh et al., 2017).

Based on the tectonic development, the initial sedimentation in the LBB can be traced back to the Valanginian–Barremian, comprising the oldest deposits in the basin (Manga et al., 2001). These sedimentary layers with a thickness of 3600 m consist of coarse- and fine-grained clastics (i.e., sandstone and shale) deposited in alluvial and fluvial settings, associated with the Pre-Bima Formation (Figs. 3 and 8) (Loule and Pospisil, 2013). The overlying Bima Formation, Albian in age, consists mainly of continental sandstone facies that were free from reflections from seismic surveys. This is followed by the Cenomanian-Turonian Gongila Formation, comprising alternations of sandstone, shale, and limestone layers. In the Turonian to Campanian, the reflection-free Fika Formation was deposited. The overlying Gombe Formation is characterised by irregular and discontinuous reflectors. The formation is made up of alternating shale and sandstone lithologies and was deposited in the Santonian-Maastrichtian period. It is laterally equivalent to the Gombe Formation in the Northern Benue Trough. At the end of the Maastrichtian, there was a basin-wide unconformity due to a short-lived compressional episode (Fairhead, 2023). In the Eocene-Oligocene, deposition in the basin continued with sedimentation of the Kerri-

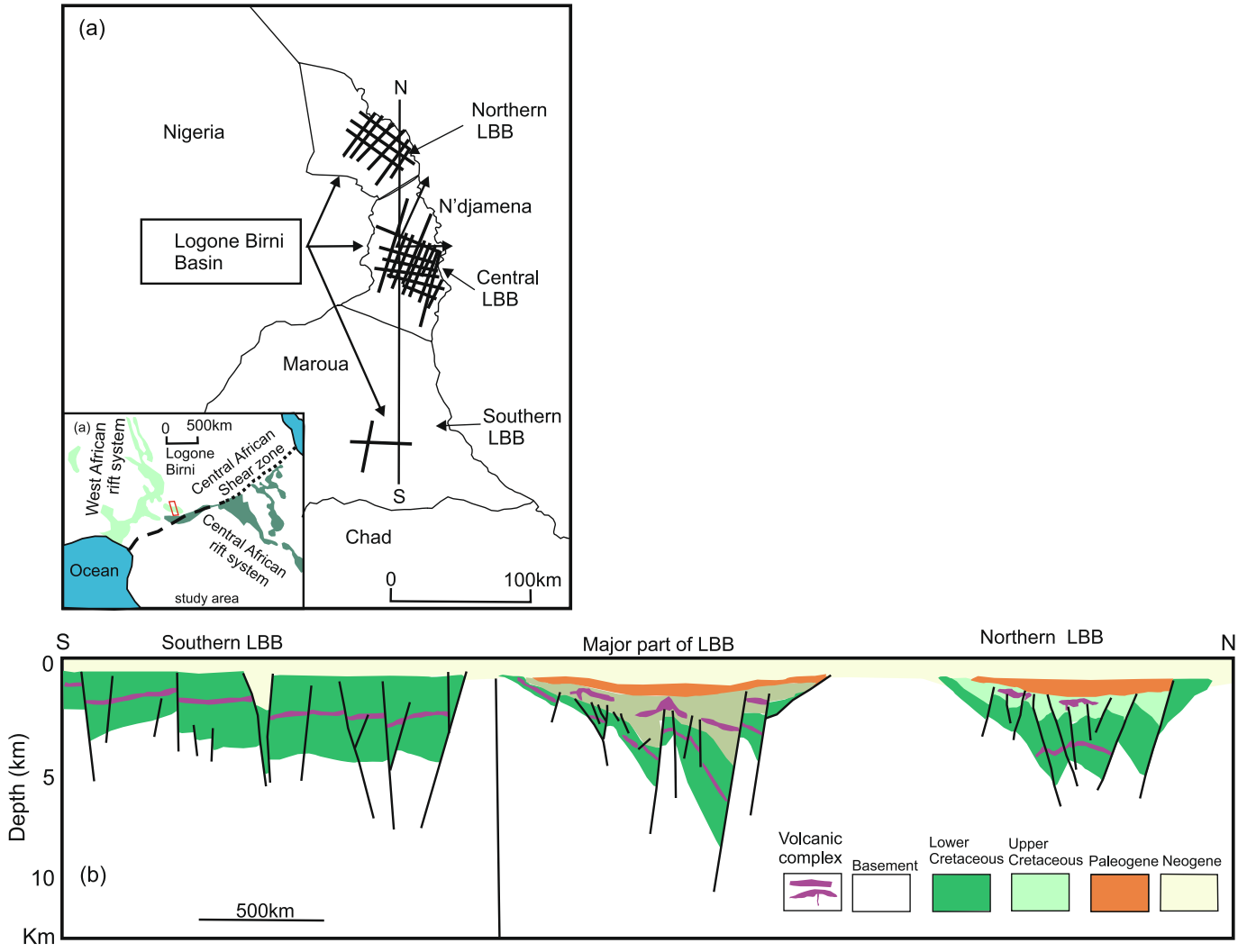

Fig. 8. a) Structural outline of the Logone Birni Basin (after Loule and Pospisil, 2013). The inset shows the location of the Logone Birni Basin within the West African and Central African Rift System. CASZ, Central African Shear Zone; b) South-North schematic cross-section across the Logone Birni Basin (after Loule and Pospisil, 2013).

Kerri Formation, comprising argillaceous sandstones and sandstone units (Manga et al., 2001; Loule and Pospisil, 2013). The Plio-Pleistocene Chad Formation, the most recent geological unit in the basin, comprises sandstones with clay lenses deposited in lacustrine and fluvial environments (Manga et al., 2001).

4. The Central Africa Rift Sub-system (CARS)

Based on their orientation, the CARS basins can be subdivided into two basin groups (Fig. 1): The Central Rift Basin Group encompassing the Bongor and Doba-Doseo-Salamat rift basins is aligned in a roughly E-W direction and is related to the large-scale strike slip fault of the CASZ. The Muglad, White Nile, Blue Nile, Shendi-Atbara, and Anza basins that are aligned in a roughly N-S direction and are related to oblique extension belong to the Eastern Rift Basin Group (Khain, 1992).

4.1. Bongor Basin, Chad

The lacustrine-to-fluvial Bongor Basin (Fig. 9) in the southwest of Chad lies to the north of the CARS (Fig. 1). The basin, a NW-SE trending half graben, was formed by the extensional movement of the CASZ within its dextral shear stress field, and is separated from the adjacent basins to the south by a basement high (Shellnutt et al., 2015).

The Bongor Basin, with an area of ca. 18,000 km^2 (Genik, 1992; Tan et al., 2017) (300 km in length and 40–80 km in width), is delimited by a series of deep-seated rift-influenced faults and can be divided into six structural units: the Northern Slope, the Northern, Western, and Southern Uplifts, the Southern sub-basin, and the Central sub-basin, which can be divided into the Moul, Mango, Cola, and Annona sags or depressions (Tan et al., 2017; Chen et al., 2018; Dou et al., 2020a) (Fig. 10). The basin formed on a Late Proterozoic to Pan-African crystalline basement composed of granite, migmatitic granite, and gneiss (Lu et al., 2009a; Dou et al., 2015; Shellnutt et al., 2015; Li et al., 2017). The rocks are heavily sheared and fractured by multi-stage and multi-angle fractures (Chen et al., 2018), forming an excellent fractured reservoir. Lower Cretaceous and Neogene continental strata with a thickness of up to 10 km make up the basin fill (Genik, 1992) (Fig. 9). The absence of Upper Cretaceous strata is related to the Santonian Compressional Event (Guiraud and Maurin, 1992; Genik, 1993), which resulted in the erosion of over 1 km of sedimentary rocks (Tan et al., 2017) and caused an unconformity between the Cretaceous and Paleogene layers. Another unconformity can be observed between the basement and the Cretaceous strata.

The Lower Cretaceous rocks can be divided into five stratigraphic formations: the Prosopis (Valanginian), Mimosa (Hauterivian), Kubla (Barremian), Ronier (Aptian), and Baobab (Albian) formations (Fig. 9). The biostratigraphic ages of the formations have been determined from palynomorph assemblages, ostracods, and charophytes (Dou et al., 2018).

The syn-rift Prosopis and Mimosa formations are composed of fan-deltaic and sub-lacustrine fan conglomerates interbedded with deep lacustrine dark mudstones and shales (Tan et al., 2017). The coarse-grained sandstones are primarily poorly sorted, indicating a local origin (Yang et al., 2020). Many of the sand- and mudstones of these

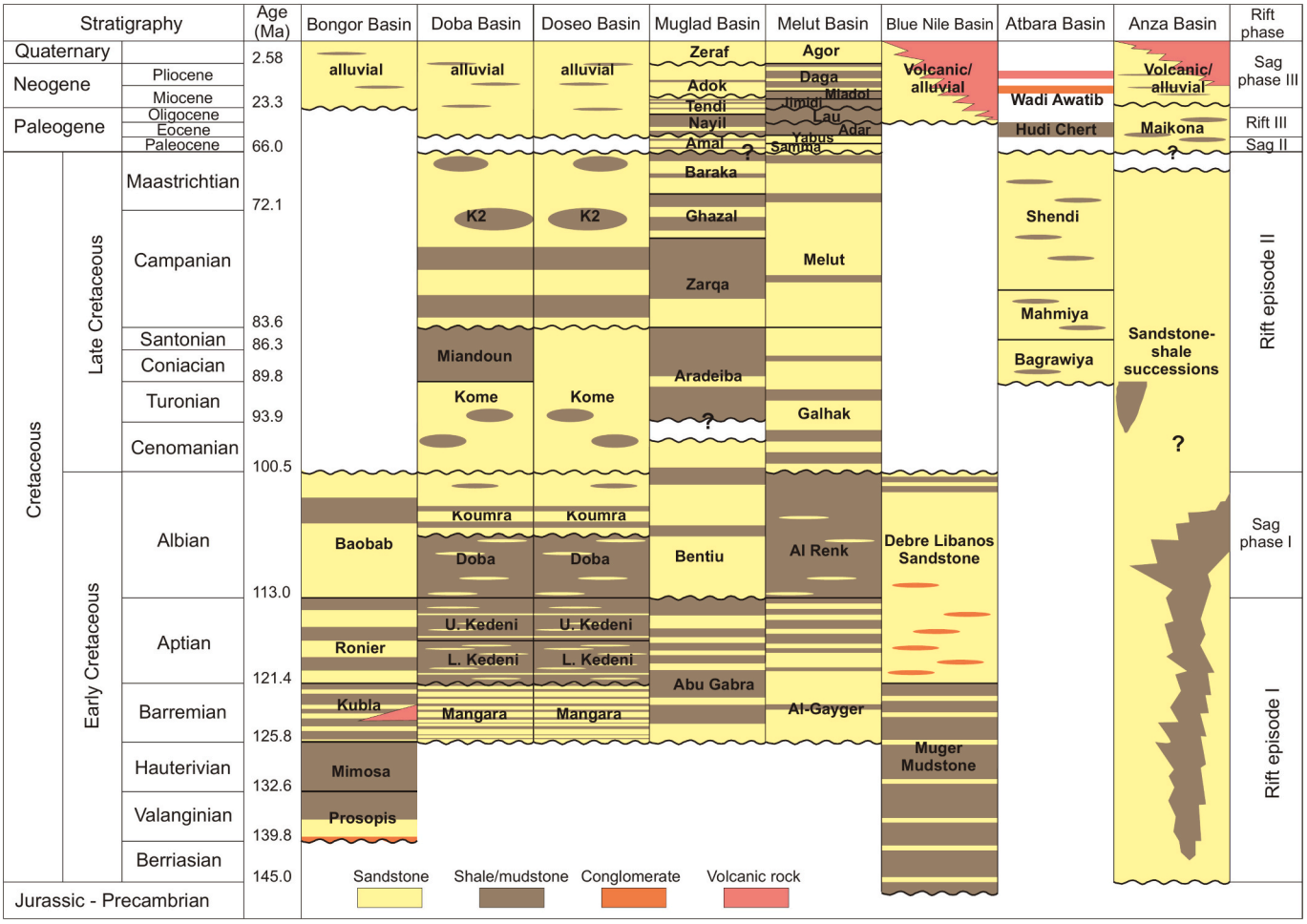

Fig. 9. Stratigraphy of the CARS (modified from Schull, 1988; McHargue et al., 1992; Guiraud and Bosworth, 1997; Gani et al., 2009; Wolela, 2009; Dou et al., 2013, 2018, 2023a; Liu and Chen, 2014; Eisawi et al., 2015; Mohamed et al., 2016; Bussert et al., 2018; Yassin et al., 2017; Mohammedyasin et al., 2019; Gao et al., 2023).

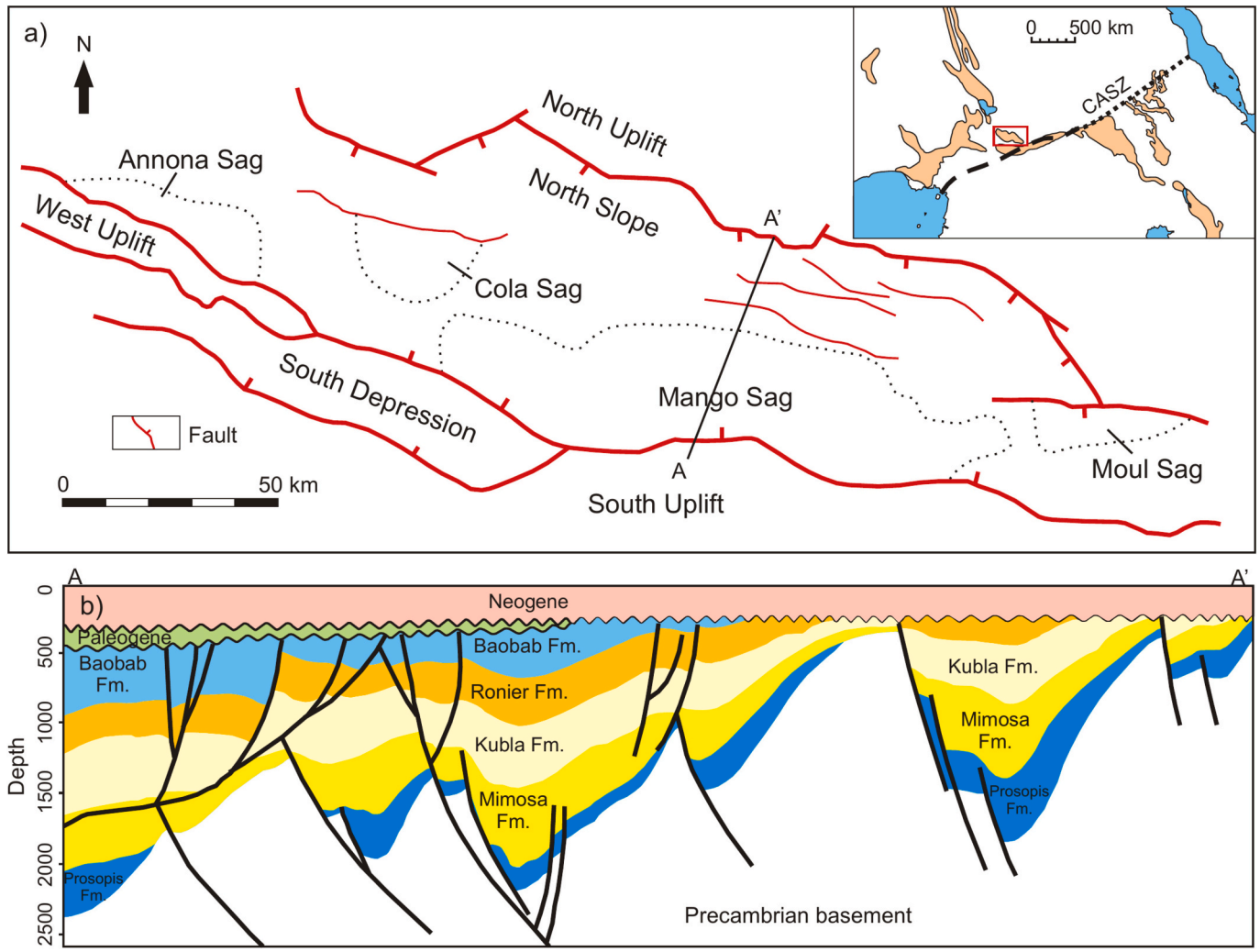

Fig. 10. a) Structural outline of the Bongor Basin (after Chen et al., 2018). The inset shows the location of the Bongor Basin within the Central African Rift System. CASZ, Central African Shear Zone; b) cross-section through the Bongor Basin (after Dou et al., 2011). For location of A-A' see 10a.

formations have been interpreted as gravity-flow deposits in the fan-delta front, sub-lacustrine fan, or slump deposits (Tan et al., 2017). Yang et al. (2020) provided the most comprehensive account of the Prosopis Formation to date and described the fan deltas as having relatively high gradients, being dominated by the arid fan-delta type, which mainly developed debris-flow deposits with several sub-facies: fan-delta plain, fan-delta front, and pro-delta sub-facies. The sub-lacustrine-fan systems were particularly developed along the margin faults.

The early period of the Prosopis Formation was characterised by rapid subsidence with the development of fan deltas on gentle-slope margins and sub-lacustrine fans near the border faults. The late period of the Prosopis Formation was characterised by a phase of tectonic quiescence. During this time, fan-delta deposits prograded into the deep-water setting. Sub-lacustrine fans were controlled by the activities of step faults and slumping or turbidite deposits from the deltas (Yang et al., 2020).

The Kubla Formation consists of fan-deltaic and braided-river-deltaic sandstones and pebble conglomerates, shallow lacustrine mudstones, and silty mudstones interbedded with basalts (Tan et al., 2017). At the onset of the deposition of the Kubla Formation, water depths decreased and the sand content increased in the system (Dou et al., 2020a). The overlying Ronier Formation exhibits fluvial-deltaic sandstones that are interbedded with grey, shallow lacustrine mudstones. The formation has been intruded by dolerite sills dated to 67.5 ± 3.1 to 51.9 ± 1.7 Ma (Lu et al., 2009a, 2009b) and 52–56 Ma (Genik, 1992) in the Ronier-1 and Naramay-1 wells, respectively. Finally, the Baobab Formation is composed of fluvial-plain sandstones and intercalated mudstones (Tan et al., 2017). As a result of lateral facies variations and syn-sedimentary extensional faulting, the thicknesses of the formations vary laterally. The total preserved thickness of the formations ranges from 9 km in the Mango Depression to zero at the basin's eroded margins (Dou et al., 2020a). Upper Aptian strata are absent from the Northern Slope due to erosion but preserved elsewhere in the basin. This may indicate a tilting of the strata and more intensive erosion in the NE than in the SW (Dou et al., 2020a).

The overlying Cenozoic succession unconformably overlies the Baobab Formation and consists primarily of unconsolidated sandstones with some interbedded thin mudstones and has an average thickness of 300–500 m (Dou et al., 2020a). No formal names for the Cenozoic formations have been proposed to date.

Samples from exploration wells from the northern slope area of the basin revealed terrestrial palynofloras dominated by *Classopollis* pollen. This pollen is considered to have come from xerophytic coniferous plants of the Cheirolepidiaceae Family, which prefer a sandy substrate on low-lying coastal plains, and arid or semi-arid climatic conditions (Srivastava, 1976; Dou et al., 2020a).

4.2. Southern Chad Basin (Doba, Doseo (Ngaoundere), and Salamat basins)

The Doba, Doseo, and Salamat basins are collectively known as the Southern Chad Basin (Genik, 1993) (Fig. 11). Since the China National Petroleum Corporation (CNPC) began conducting extensive hydrocarbon exploration in the first two basins over the previous two decades, the basins have become relatively well documented (Dou et al., 2022b). Nevertheless, despite being described as having the highest hydrocarbon potential of the three basins, very little information has been published (particularly in English) on the Doba Formation (Mohd Sumery et al., 2017), with the Doseo Basin receiving the majority of attention. Since the Salamat Basin is regarded to have the lowest hydrocarbon potential, basically no information is accessible on it.

The thickness of the sedimentary sequences in the Doseo Basin is ca. 8 km (Fig. 9), which is slightly less than in the Doba Basin (10 km) and greater than in the Salamat Basin (6 km) (Dou et al., 2023a). All three basins, like the Bongor Basin in the north, are inverted rift basins that formed directly on the Pan-African crystalline basement (Guiraud and Maurin, 1992; Genik, 1992, 1993; Shellnutt et al., 2017), which yielded radiometric ages of 434–594 Ma (Genik, 1992). In the Doba Basin, in addition to the Precambrian rocks, a late Permian (257 ± 1 Ma) gabbro was discovered in one of the drill cores, which may have been tied to a period of magmatism and tectonics associated with the formation of the Variscan orogen (Shellnutt et al., 2015, 2016).

All three basins are primarily lacustrine (Genik, 1993; Mohd Sumery et al., 2017; Dou et al., 2022b; Gao et al., 2023) and experienced three phases of rift development, corresponding to the three rift stages outlined earlier: intensive strike-slip and extension in the Early Cretaceous, weaker extension in the Late Cretaceous, and minor extension and

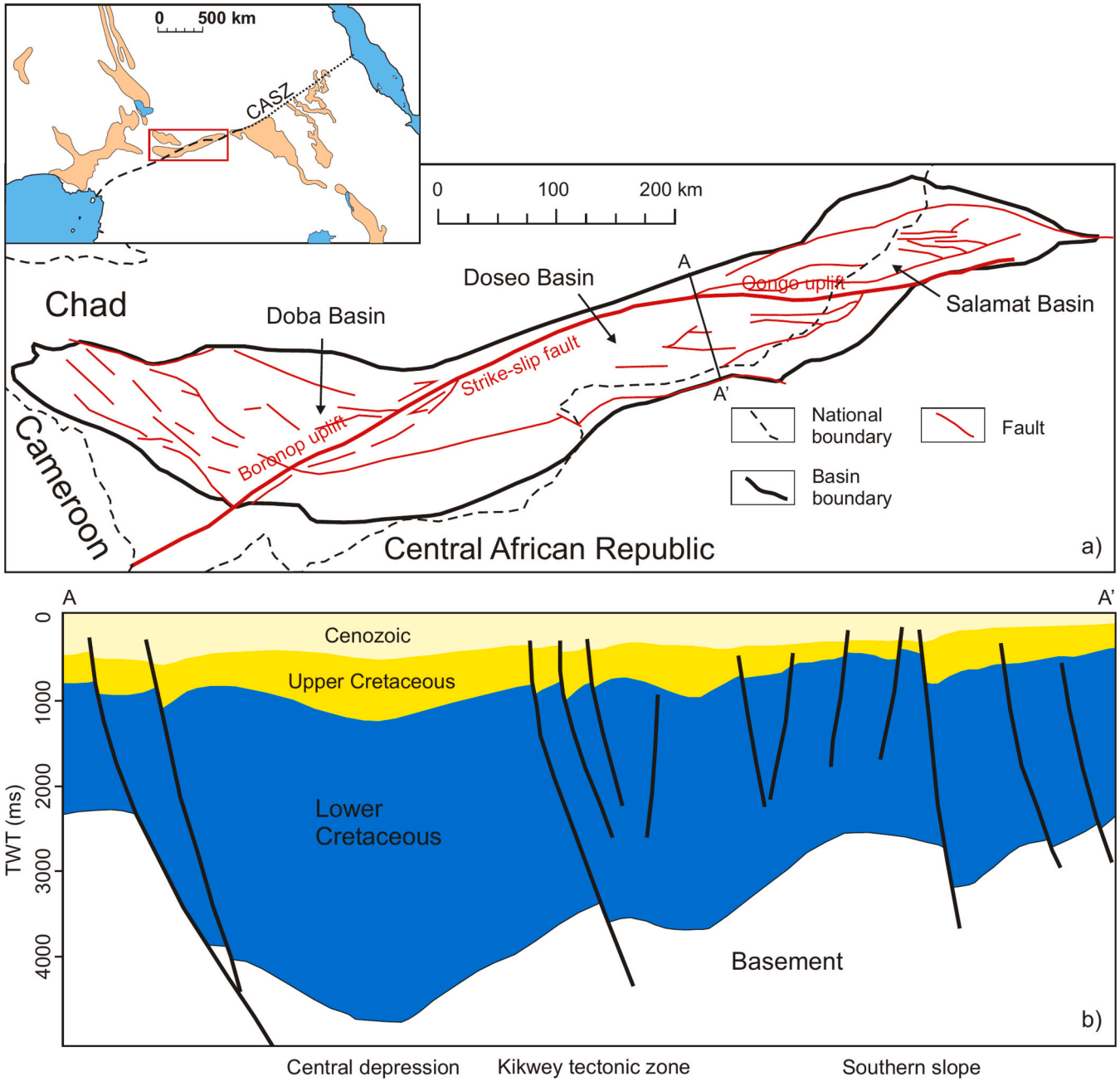

Fig. 11. a) Structural outline of the Doba, Doseo, and Salamat basins (after Dou et al., 2023a). The inset shows the location of the basins within the Central African Rift System. CASZ, Central African Shear Zone; b) cross-section through the Doseo Basin (after Dou et al., 2023b). For location of A-A' see 11a.

eventually sagging in the Paleogene.

The effect of the previously described Santonian compression and inversion event has been identified as relatively insignificant in the Doseo Basin (El Hassan et al., 2017). However, the basin experienced extensive inversion and denudation during the late Paleogene. Seismic stratigraphic correlation indicates that around 40 Ma, ca. 800–1000 m of sedimentary material was lost to erosion, which is equivalent to the magnitude of erosion in the Bongor Basin (Dou et al., 2021, 2022b).

The Doseo Basin extends from ENE to WSW and is made up of a sequence of half-grabens and grabens that are faulted in the north and overlap in the south. It is separated from the Doba Basin in the west and the Salamat Basin in the east by the Borogop Fault belonging to the CASZ. Before its development, the three basins were effectively a single basin (Genik, 1992). The Doseo Basin, a transtensional asymmetric complex rift (Genik, 1992), is 70–100 km wide and 550 km long, encompassing an area of ca. 50,000 km^2 (Dou et al., 2022b). The basin is structurally separated into Northern, Southern, Western, and Eastern depression zones, a Northern and Southern Slope, and a Central Uplift (Guiraud and Bosworth, 1997; Reynolds and Jones, 2004). The Northern Depression Zone is faulted in the north and south, while the Southern Slope, located on the southern margin of the Southern Depression Zone, is faulted in the north but overlaps in the south (Dou et al., 2022b).

The basin fill is composed of sedimentary rocks that range in age from the Early Cretaceous to the Neogene, with five unconformities separating the lithological units. The Lower Cretaceous Series is separated into four units that were formed during two sedimentary cycles: the Mangara Group and the Kedeni, Doba, and Koumra formations.

The 1–3 km-thick Mangara Group (Barremian?) contains lacustrine mudstone and fluvial-deltaic sandstones and was formed during a complete transgressive-regressive cycle in the early stage of rifting (Dou et al., 2022b; Gao et al., 2023; Zhang et al., 2024a).

The Kedeni Formation follows an unconformity that formed locally on top of the Mangara Group (Dou et al., 2022b). The Kedeni Formation is 600–1200 m thick and composed of lacustrine mudstones intercalated with braided-delta or fan-delta sandstones (Dou et al., 2022b; Gao et al., 2023). The formation underwent two complete third-order sedimentation cycles from top to bottom, resulting in the upper and the lower Kedeni members (Zhang et al., 2024a). The rapid rise of the lake water level during the deposition of the lower Kedeni Member resulted in the predominance of shale with thinly bedded sandstone. During the upper Kedeni Member, multiple thick layers of sandstone were deposited as a result of short-term uplifting (Zhang et al., 2024a).

The thicknesses of the overlying Doba and Koumra formations are 400–700 m and 300–600 m, respectively. Both formations are composed of lacustrine to fluvial-delta sandstones and mudstones (Gao et al., 2023). With continuing lake transgression and limited sediment supply, thick-bedded shale predominated in the early phases of Doba Formation deposition, which occurred on top of an unconformity. Sand bodies became more prominent as the lake level began to fall again during the late stage of deposition (Koumra Formation) (Zhang et al., 2024a).

The Upper Cretaceous strata are fluvial-lacustrine deposits with a thickness of 500–1100 m. So far, only the lower Upper Cretaceous Kome Formation has been named. The formation, along with the overlying K2 unit (which extends into the Paleogene, and is separated from the Kome Formation by an unconformity caused by the Santonian event), consists primarily of lacustrine-delta sandstones. During the Paleogene, the sedimentary environment was a shore-shallow lacustrine delta, which progressively transitioned into a shore-shallow lake and an alluvial plain in the Neogene. The Neogene sandy deposits are weakly consolidated, with residual thicknesses ranging from 250 to 450 m (Dou et al., 2022b).

The Early Cretaceous saw the development of a rifted lacustrine basin, in which well-sorted medium-fine grained quartz sand bodies of delta and fan-delta deposits with relatively distant provenance emerged in the northern and southern depressions, respectively. Delta and braided-delta deposits dominated the southern margin. In contrast, fan delta or braided delta deposits were deposited on the northern margin of the basin. Semi-deep-lacustrine and deep-lacustrine mudstones, intercalated with turbidite sandstones and distal-bar sandstones, formed in the basin centre. Semi-deep refers to lacustrine strata that did not form in environments as shallow as littoral zones but not as deep as the central parts of large lakes. Although the term is widely used in literature, there is not a universally fixed depth for “semi-deep” deposits or basins.

The Early Cretaceous began with a transgression during which the lacustrine basin expanded and deepened. Following the initial transgression phase, during mid-Early Cretaceous times, delta sand bodies started to accumulate. Later, sandstones became thicker and coarser as the sand bodies prograded. The Late Cretaceous to Paleogene are compressing-inverting periods in which the basin was uplifted and its deposits eroded (Dou et al., 2022b). The overlying strata of Palaeogene and Neogene age are predominantly made up of sandstones and intercalated shales of shore-shallow lacustrine, deltaic, and alluvial plain origin (Dou et al., 2023a).

The Doba Basin, a rotated, wrench modified rift, is ca. 300 km long and 150 km wide, containing Barremian to recent non-marine sandstones, shales and mudstones (Genik, 1992). Similar to the Doseo Basin, this depository has been described to contain the Lower Cretaceous Mangara Group as well as the Kedeni, Doba, and Lower Kome formations. The Upper Kome and Miandoum formations comprise the Upper Cretaceous (Mohd Sumery et al., 2017).

The Salamat Basin, with a length of 300 km and a width of 60 km, is the least studied of the three basins that have been discussed in this section. It has been classified as a transtensional complex rift at the eastern end of the Borogop fault zone (Genik, 1992). The sedimentary infill of the basin is primarily made up of continental fluvial to lacustrine deposits, with up to 6 km of sandstones and shales that may form potential source rocks (Genik, 1993).

4.3. *Muglad Basin, Sudan and South Sudan*

The NE-SW-trending Muglad Basin is the largest of the rift basins along the CASZ. Like all CAS basins, it is linked to the right-lateral strike-slip movement of the CASZ (Genik, 1993). The basin is up to 1200 km long and 300 km wide, with an area of approximately 120,000 km^2 that is distributed across the Republic of Sudan and South Sudan (Schull, 1988; McHargue et al., 1992; Makeen et al., 2021). Nevertheless, there is presently no surface expression of the rift basin (Mohamed et al., 2001) (Fig. 12). The Muglad Basin may connect with the Anza rift in Kenya to the south via the South Sudan Shear Zone (Fairhead, 1988; Bosworth, 1992). The basin can be separated into the Abu Sufyan, Nugara, Fula, Bamboo, and Unity sub-basins, the Kaikang Trough, the Babanuse Uplift, and the Abei Slope (Dou et al., 2013; Yassin et al., 2017). To the north, the basin is separated from the Baggara Basin by a structural high. Nevertheless, the stratigraphy of the Baggara Basin matches that of the Muglad Basin (El Hassan and El Nadi, 2015) for which reason the former basin can be seen as a continuation of the latter.

According to seismic data, the greatest thickness of sediment fill within the basin is 13 km (Schull, 1988; Mohamed et al., 2001). The crystalline basement underlying the basin is primarily Precambrian, i.e., Pan-African in age. However, during the Late Triassic to Early Jurassic (225–195 Ma), the Precambrian basement was also intruded by younger granites, syenites, diorites, and monzonites (Zhao and Dou, 2022). The sedimentary infill directly overlying the crystalline basement is made up of three cycles of rift-related fluvio-lacustrine deposits, which correlate to three episodes of extension, with each cycle being separated by an angular unconformity. Furthermore, each tectonic cycle is represented by a coarsening-upward cycle, i.e., a gradation from lacustrine shale to fluvial sandstone (McHargue et al., 1992). The Muglad Basin generally received its sediments from the surrounding Nuba Mountains (Fadul et al., 2020).

In the first rift cycle (Barremian-Aptian), the Sharaf and Abu Gabra formations consist mainly of lacustrine shales and clays with thin intervals of sandstone (Abdalla et al., 2001; Abdelhakam and Ali, 2008)

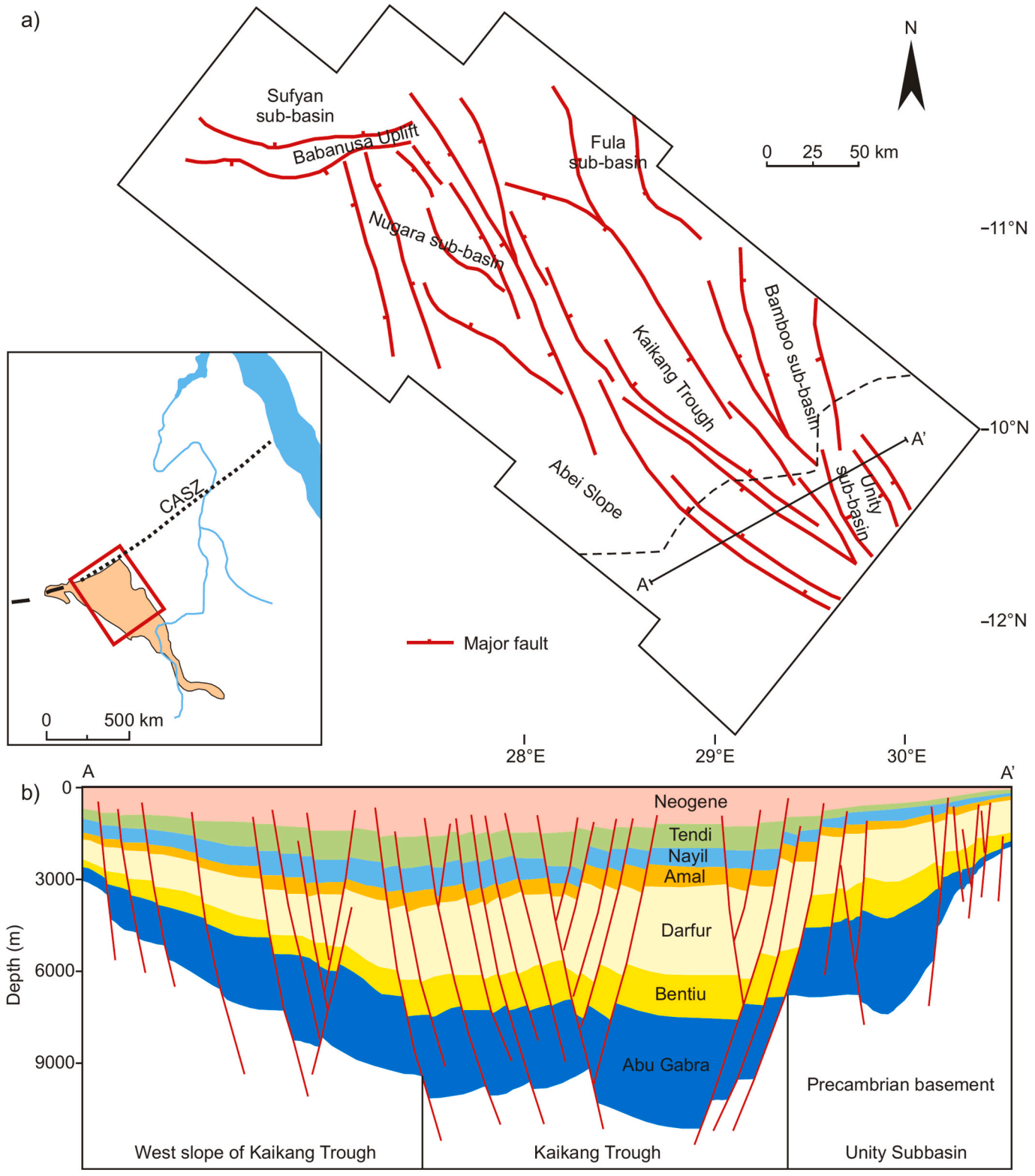

Fig. 12. a) Structural outline of the Muglad Basin (after Dou et al., 2013). The inset shows the location of the Muglad Basin in East Africa. CASZ, Central African Shear Zone; b) cross-section through the Muglad Basin (after Shi et al., 2014). For location of A-A'see 12a.

(Fig. 9). Since Dou et al. (2013), the two formations are usually shown combined in the Abu Gabra Formation. The shales are interpreted to have formed in stratified lakes as distal dysoxic to anoxic facies (Mustafa and Tyson, 2002). Sandstone increases in frequency upwards and is prevalent in the post-rift strata of the ca. 1000 m thick (Albian-Cenomanian) Bentiu Formation (Schull, 1988), consisting of medium- to coarse grained sandstones (Dou et al., 2013).

The second depositional cycle (Turonian-Maastrichtian) is characterised by the up to 4000 m-thick, shallow-water lacustrine and floodplain mudstones and sandstones of the Darfur Group (Dou et al., 2013). The group can be divided into the Aradeiba, Zarga, Ghazal, and Baraka formations. The Aradeiba Formation at the base of the group is largely

composed of fluvial and deltaic shales. Afterwards, there is a steady increase in sandstones from the Zarga to the Baraka Formation (Makeen et al., 2015a). There is still some disagreement over the Muglad Basin's stratigraphy, particularly the age and extent of the Darfur Group, with some authors considering it to be Cenomanian to Turonian in age, whereas others place it from the Turonian or Santonian to the Maastrichtian (cf., Dou et al., 2013; Yassin et al., 2017; Makeen et al., 2021). This can cause a lot of misunderstanding and must certainly be addressed in future stratigraphic work.

The overlying post-rift strata of the Amal Formation are largely massive sandstones (Mohamed et al., 2001; Dou et al., 2013).

The strata of the third rift cycle (Late Eocene-Oligocene) are up to 4100 m thick (Mohamed et al., 2001) and are contemporaneous with the initial opening of the Red Sea (Lowell and Genik, 1972) and the EARS (Patton et al., 1994). This period is marked by lacustrine and floodplain mudstones and siltstones of the Nayil and Tendi formations that transition to coarse sandstones of the Adok Formation (along with the Nayil and Tendi formations belonging to the Kordofan Group), which are

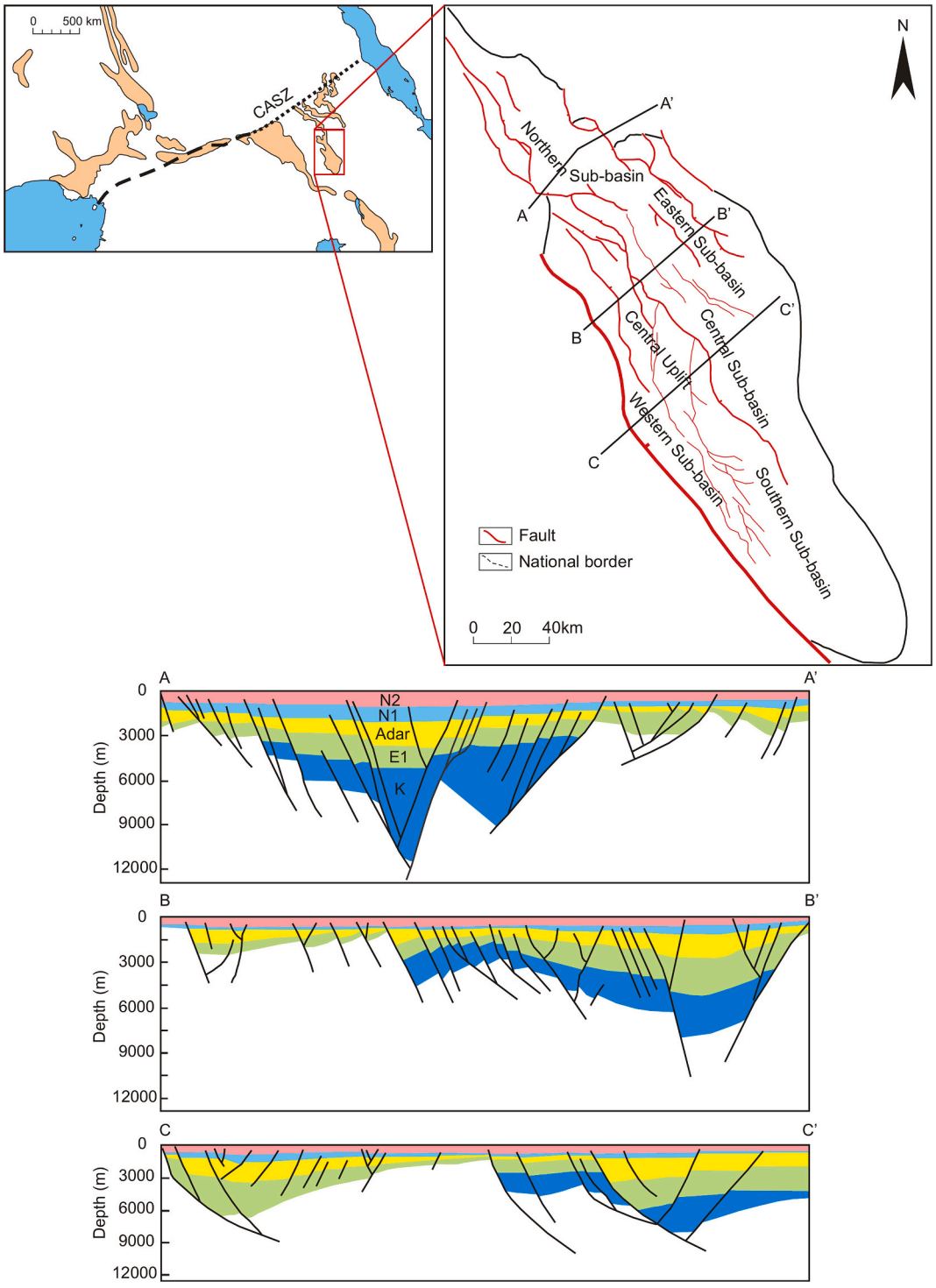

Fig. 13. a) Structural outline of the Melut Basin (modified from Dou et al., 2007). The inset shows the location of the Melut Basin within the West and Central African Rift System; b) cross-sections through the Melut Basin (after Dou, 2005). For locations of A-A', B-B′, and C-C′ see Fig. 13a.

thickest in the Kaikang Trough (Schull, 1988; McHargue et al., 1992). A sandstone-dominated Miocene succession, which formed during post-rift thermal subsidence, overlies the syn-rift succession unconformably (Dou et al., 2013). The Zeraf Formation, which consists of fluvial-alluvial sands and clays, represents these post-rift sedimentary strata. McHargue et al. (1992) classified the shale and mudstone formations within each cycle as syn-rift sediments, whereas the sandstone formations at the top of each cycle were classified as post-rift (thermal sag) sediments, together with sandstones deposited at the beginning of the following rift episode.

4.4. White Nile Basin, Sudan, South Sudan, and Ethiopia

The White Nile Basin is separated into two unique and distinctive sub-basins: the Rawat sub-basin in the north and the Melut sub-basin in the south.

The Melut sub-basin is the southeastern extension of the White Nile rift basin, spanning from south of the Sudan to Ethiopia where it is also known as the Gambella Basin (Fig. 13). It was formed by strike-slip and associated pull-apart along the CASZ (Guiraud and Maurin, 1992; McHargue et al., 1992). The basin constitutes the second-largest rift basin in the CAS. Early and Late Cretaceous rifting resulted in the formation of NWW-SEE trending faults due to the strike-slip of the CASZ. Furthermore, Paleogene rifting generated a set of NW–SE trending faults and structures under an NE–SW extensional stress field (Dou et al., 2007).

The basin has a size of over 33,000 km^2, a length of ca. 400 km, and a maximum width of ca. 200 km. Southwards, similar to the Muglad Basin, the Melut Rift may link up with the Anza Rift in Kenya (Dou et al., 2007). Based on geophysical data, the basin can be subdivided into six sub-basins and one high (Guiraud and Maurin, 1992), which are the northern, southern, eastern, western, and central sub-basins, and the central high. Pan-African schist, gneiss, and Cambrian granite dominate the surrounding areas as well as the basement of the basin (Schull, 1988). The Cretaceous to Paleogene sedimentary infill is up to 10 km thick.

Four depositional cycles developed in the Melut Basin during the Cretaceous, Paleogene, and Neogene–Quaternary periods. These cycles are linked to three rifting episodes and a final sagging phase and resulted in the formation of a sedimentary infill that reaches a thickness of up to 10 km (Dou et al., 2007). Each cycle is preceded by angular unconformities that are associated with significant erosional processes that removed 200–600 m of sedimentary strata (Hakimi et al., 2022).

Of the three rifting episodes, the Early Cretaceous extension was the largest, resulting in the formation of a vast lacustrine basin. The widening during this period accounted for nearly 50 % of the total extension of the basin (Dou et al., 2008). By contrast, the Late Cretaceous extension was relatively modest, leading to subsidence and the deposition of fluvial to shallow lacustrine sandstones and minor mudstones. The extension during the third rifting phase in the late Eocene-Oligocene (Bosworth, 1992), associated with the opening of the Red Sea and EARS (Patton et al., 1994), caused a reactivation of the boundary faults and intra-basinal extensional structures (McHargue et al., 1992). This phase is primarily marked by the thick sequence of lacustrine and floodplain mudstones and siltstones. Particularly the deposition of the Lau Formation, however, may have been influenced by a marginal marine transgression that entered the region from the south (Mustafa et al., 2022).

Following this phase, the basin entered a post-rift subsidence or sagging stage. From the Miocene to the present, separated by a regional unconformity from the underlying Oligocene sequences, the deposition became more sandy throughout the basin (Dou et al., 2007).

The Lower Cretaceous Al-Gayger and the Al Renk formations are together up to 3000 m thick and indicate a time of major lake development (Fig. 9). Thick fluvial-deltaic sandstones are interbedded with thin shales to form the Al-Gayer Formation (Dou et al., 2007). These lithologies transition upwards to the Al Renk Formation with thicker shales and thin intercalated sandstones, which formed in a semi-deep to deep lacustrine environment (Zhao et al., 2020). According to Shi et al. (2017), the Al Renk Formation attains a maximum thickness of 1000 m in the centre of the basin and 200–500 m along its margins.

After an unconformity, the Upper Cretaceous is made up of the Galhak and Melut formations (up to 1593 m combined thickness; Dou et al., 2007). The medium- to fine-grained sandstones and mudstones of the Galhak Formation (late Cenomanian–Turonian) developed in a braided delta and shallow lacustrine environment. The thickness of this unit averages 290 m (Dou et al., 2007). The predominance of thick sandstones interbedded with thin mudrocks in the overlying Melut Formation indicates that the water became gradually shallower with time (Dou et al., 2007). The Late Cretaceous ended with the deposition of increasing coarser-grained strata. They were deposited in shallow lacustrine and sand-rich fluvial environments that prograded from the basin margins. Furthermore, some basaltic rocks of potentially Late Cretaceous age have been described from several wells (Vail, 1989).

The Paleogene sedimentary strata attain a maximum thickness of ca. 2500 m in the deepest part of the basin (Dou et al., 2007). The Paleogene formations are referred to as Samma, Yabus, Adar, and Lau. In the deepest portion of the basin, they reach a maximum thickness of about 2500 m (Dou et al., 2007). Thick, coarse- to medium-grained sandstones with interbedded mudrocks make up the Samma Formation. The overlying Yabus Formation is finer-grained and contains less (subarkosic) sandstone, reaching thicknesses of up to 220 m (Mahgoub et al., 2016). Both formations formed in progressive braided (Samma Formation) and meandering (Yabus Formation) delta, marginal, and shallow lacustrine environments (Dou et al., 2007; Mahgoub et al., 2016).

The Adar Formation was deposited in a shallow to semi-deep lacustrine environment, as indicated by its predominant occurrence of shales and interbedded siltstones and sandstones within the centre of the basin (Dou et al., 2007). Towards the edges of the basin, the deposits change to coarser alluvial strata. The maximum thickness of the Adar Formation is 900 m.

The up to 500 m-thick Lau Formation follows after an unconformity. It exhibits an upward-fining cycle, and, according to Dou et al. (2007), it was formed in a shallow lacustrine to braided river environment. In contrast, Mustafa et al. (2022) interpreted the sandstones of the Lau Formation as shallow marine beach sands.

Massive sands and mudstones make up the Miocene Jimidi (~210 m thick) and Miadol (~290 m thick) formations, respectively. The Jimidi and Miadol formations are also thought to correlate positively with the post-rift succession in the Anza Graben to the south (Hassan et al., 2024).

The sandstone-rich Pliocene Daga Formation was deposited following an unconformity. The Quaternary Agor Formation, which is primarily composed of loose sands, was the last formation to form within the basin (Dou et al., 2007). All these younger deposits are interpreted to have been deposited in alluvial and fluvial braided river environments (Mustafa et al., 2022).

Apart from some accounts from Fairhead (1988) and Schull (1988), relatively little research has been done so far on the northern Rawat Basin, which can be further subdivided into north, east, south, west and central sub-basins with an up to 6000 m thick sedimentary sequence in the central part (Awad, 2015). The Rawat Basin is ca. 175 km long and 50 km wide and is located ca. 350 km south of Khartoum, the capital of Sudan (Hassan et al., 2024). The stratigraphy of the Rawat Basin is very similar to that of the southern Melut Basin and is directly comparable (Hassan et al., 2024; Babai et al., 2024).

4.5. Blue Nile, and Shendi-Atbara basins, Sudan

The Blue Nile (or Abay) Basin, with the Khartoum sub-basin as its northern extension, comprises ca. 120,000 km^2 and contains a ca. 3000 m thick sedimentary sequence (Wolela, 2007). Like the other basins of the CARS, the Blue Nile Basin is a NW-SE-oriented rift basin that

terminates against the CASZ (McHargue et al., 1992). The Khartoum sub-basin is different from the rest of the Blue Nile Basin, as it is a "sag" basin, i.e., its boundaries do not appear to be governed by major bounding faults, and it is rather shallow, with a maximum sediment thickness of only a few km (Mohammed, 1997). Moreover, the Blue Nile Basin in itself is not the typical CARS basin as it appears to be older than the other basins and already started to form during Permo-Triassic times as a "Karoo-age" basin (Wolela, 2007). Nevertheless, due to its relationship to the CASZ, and its extension parallel to basins such as the White Nile and Muglad basins, it is usually counted as one of the CARS basins.

The basement beneath the Blue Nile Basin is characterised primarily by quartzites, granites, gneisses, and metavolcanics of the Alghe Group (Kazmin, 1975; Mengesha et al., 1996; Wolela, 2009). Overlying the crystalline basement, ca. 1200 m of Permo-Triassic to Early Jurassic sandstones, shales, and conglomerates related to a first phase of Karoo rifting can be found that were all deposited within fluvial and alluvial fan environments (Wolela, 2008, 2009) (Fig. 14). During the Early to Middle Jurassic, a second phase of rifting led to a marine transgression and the deposition of clastic material, carbonates, and evaporites

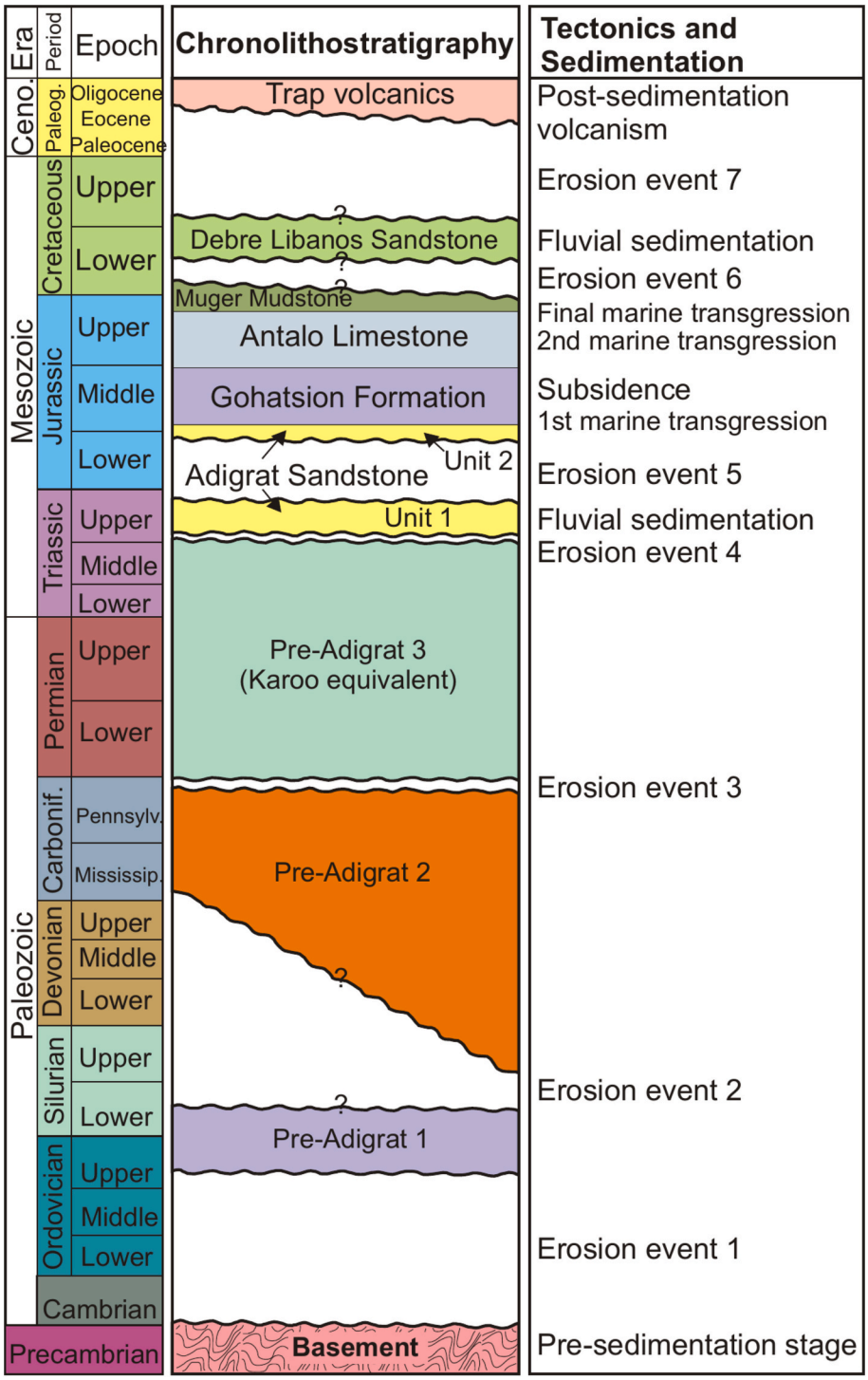

Fig. 14. Chrono- and lithostratigraphy and summarised tectonic and sedimentation history of the Blue Nile Basin (Mohammedyasin and Wudie, 2019). For interpretation of the references to colour in this figure legend, the reader is referred to the web version of this article.

(Salman and Abdula, 1995; Bunter et al., 1998). A regression during the Early Cretaceous resulted in the deposition of the shallow-marine Muger Mudstone (mudstone with intercalations of fine-grained sandstone), and the fluvial Debre Libanos Sandstone (fine- to medium-grained sandstone with intercalated conglomerates and mudstone towards the top), which reach 320 m and 280 m in thickness, respectively (Wolela, 2009). This might be the only depositional period that coincides with the typical WCARS depositional phases. The regression probably formed as a result of the WCARS wide basin inversion. The Late Cretaceous is primarily characterised by non-deposition (Wolela, 2009). However, at the end of the Cretaceous, rifting began in the Gulf of Aden area and led to the formation of the Red Sea and the Main Ethiopian Rift (Bunter et al., 1998; Korme et al., 2004; Wolela, 2008, 2012). As a consequence, the Blue Nile rift system is dissected by the main Ethiopian rift. Furthermore, most of the Blue Nile Basin rocks are overlain by 500–2000 m-thick early to late Oligocene and ca. 300 m-thick Quaternary volcanic rocks (Hofmann et al., 1997; Gani et al., 2009).

The Shendi-Atbara Basin towards the East of the Blue Nile Basin is a half-graben structure and contains ca. 3 km of sedimentary infill (Jorgensen and Bosworth, 1989).

The main sedimentary units of the basin include Cretaceous strata, which lie unconformably on the Basement Complex (Whiteman, 1971). The Coniacian to Santonian Bagrawiya Formation is overlain by the Santonian to Campanian Mahmiya Formation, which in turn is overlain by the Campanian to Maastrichtian Shendi Formation that formed during a phase of thermal sagging after the Cenomanian-Turonian rifting event of the WCARS (Eisawi et al., 2015; Bussert et al., 2018; Babkir et al., 2023). The rocks of these formations are all terrestrial sandstones, conglomerates, and shales that formed within a fluvial setting (Babkir et al., 2023).

4.6. Anza Basin, Kenya

The Anza Basin has received little academic or industry attention. This is mostly due to the lack of rift-fill exposures in the basin, which is covered by Pliocene-Quaternary volcanic and sedimentary rocks. The available information on the basin is largely based on well data from five wells drilled by Amoco Kenya and Total Kenya in the late 1980s (Winn Jr et al., 1993). Stratigraphic subdivision of its sedimentary infill into groups and formations is yet to be completed.

The Anza Basin is located in north-central Kenya and borders the Lamu Basin to the south. The Anza Basin is ca. 560 km long and appears to be deepest towards its northeast side, where the rift spans 130 km. According to Reeves et al. (1987) and Bosworth (1992), the Anza Basin's sedimentary infill spans from ca. 7 to 10 km. The basin is divided into the Chalbi and Kaisut sub-basins in the northwest, the Yamicha sub-basin in the east and southeast, and the Intermediate Tilted Blocks and the Matasade Uplift in the middle (Fig. 15). The Yamicha sub-basin contains the thickest Cretaceous deposits, with up to 13 km of fill preserved in the centre (Dou et al., 2023b).

Seismic reflection measurements indicate the existence of a few syn-rift magmatic intrusions within the sedimentary succession (Reeves et al., 1987; Bosworth, 1992). According to Bosworth (1992), rifting may have begun in the Late Jurassic, followed by extensional pulses in the Turonian to late Senonian-Paleocene and late Eocene-Oligocene (which may have continued into the early Miocene). However, no wells have yet penetrated the basement of the basin. Nevertheless, Bosworth and Morley (1994) propose that the Anza rift may have been initiated in the Late Jurassic, along with extensions to the south in the Lamu embayment and to the north in the Blue Nile rift of Sudan. This rifting in the Late Jurassic was most likely associated with an extensive transgression (Reeves et al., 1987), which included platform formation on top of the Precambrian basement and the deposition of shallow-water carbonates on the Matasade High in the basin's western region. This phase was most likely related to the separation of Madagascar from East Africa (Bosworth and Morley, 1994). With the beginning of the Cretaceous period, a regression occurred, coinciding with a return to continental depositional conditions (Reeves et al., 1987). The Cretaceous sedimentary rocks are primarily shales and sandstones that formed in fluvial, floodplain, deltaic, and lacustrine environments (Schull, 1988). Furthermore, aeolian sandstones have been described (Sewe, 1995), indicating the presence of potential dune fields.

By the Late Cretaceous, a system of steeply dipping faults was established that produced a deep basin without significant rotation of strata in the north and only minor rotation in the south. This basin geometry favoured the establishment of large, deep lakes, which occasionally were connected to the sea (Sewe, 1995), leading to marine incursions during the Cenomanian, Campanian, and Maastrichtian (Bosworth and Morley, 1994). The marine influence mostly affected the Lamu embayment in the south of the basin but may have reached the central Anza rift in the Cenomanian when a variety of deep marine shales were deposited in these areas. In contrast, at the same time, the north-west was characterised by the deposition of coarse clastic fluvial deposits. Coarse fluvial deposits generally dominate within the basin. The Cretaceous deposits are overlain by the Paleogene fluvial sandstones of the Maikona Formation, followed by up to 3 km of Miocene to recent fluvial and lacustrine deposits and the flood basalts of the EARS (Bosworth and Morley, 1994).

5. Discussion

5.1. Sequence stratigraphy

The sedimentary fill of the WCARS qualifies as a 'first-order' stratigraphic sequence defined by deposition in a rift setting (Catuneanu, 2022). Rift basins are complex, with multiple segments and depocenters that may undergo subsidence at different times, but do generally follow a predictable pattern of evolution, with subsidence rates first increasing during the formation of the basin and decreasing towards the end of rifting, commonly within a range of 10^{-3}–10^{0} m/kyr (dePolo and Anderson, 2000). As a result, subsidence typically starts with low rates in the early stage of rift initiation, continues with higher rates during the main stage of basin development, and ultimately ends with low rates in the late stage of rifting (Fig. 16). These stages result in changes in the balance between accommodation and sedimentation during the evolution of rifts, with an impact on the depositional environments that can occur within a basin at times of overfilled (i.e., with all marine or lacustrine accommodation consumed by sedimentation, resulting in a fully continental environment across the basin) or underfilled (i.e., with marine or lacustrine environments still present within the basin) accommodation (Fig. 17; Catuneanu, 2024).

The three stages of basin development that define the first-order rift cycle (Figs. 16 and 17) generate total amounts of subsidence in a range of 10 km, sometimes even exceeding 10 km (Bosence, 1998; Allen and Allen, 2013). However, this subsidence is differential, with higher rates adjacent to the boundary faults of the half-grabens and gradually decreasing rates towards the flexural basin margins. As a result, the basin fills are asymmetrical and wedge-shaped, with the depocenters located closer to the boundary faults where greater amounts of accommodation are generated. This asymmetry also implies that the balance between accommodation and sedimentation may vary at any given time across a basin in a dip direction as well as in a strike direction due to variations in the rates of subsidence and sedimentation along the rift axis. Nevertheless, each stage of rift development records distinctive trends in terms of depositional environments and the degree in which the accommodation made available by extensional subsidence is consumed by sedimentation.

As rifting is typically initiated in a continental setting, the **early stage** of basin development is prone to continental or shallow-water environments enabled by relatively low subsidence rates that are matched by sedimentation (Fig. 17). This depositional setting is maintained for as long as accommodation and sedimentation are in relative

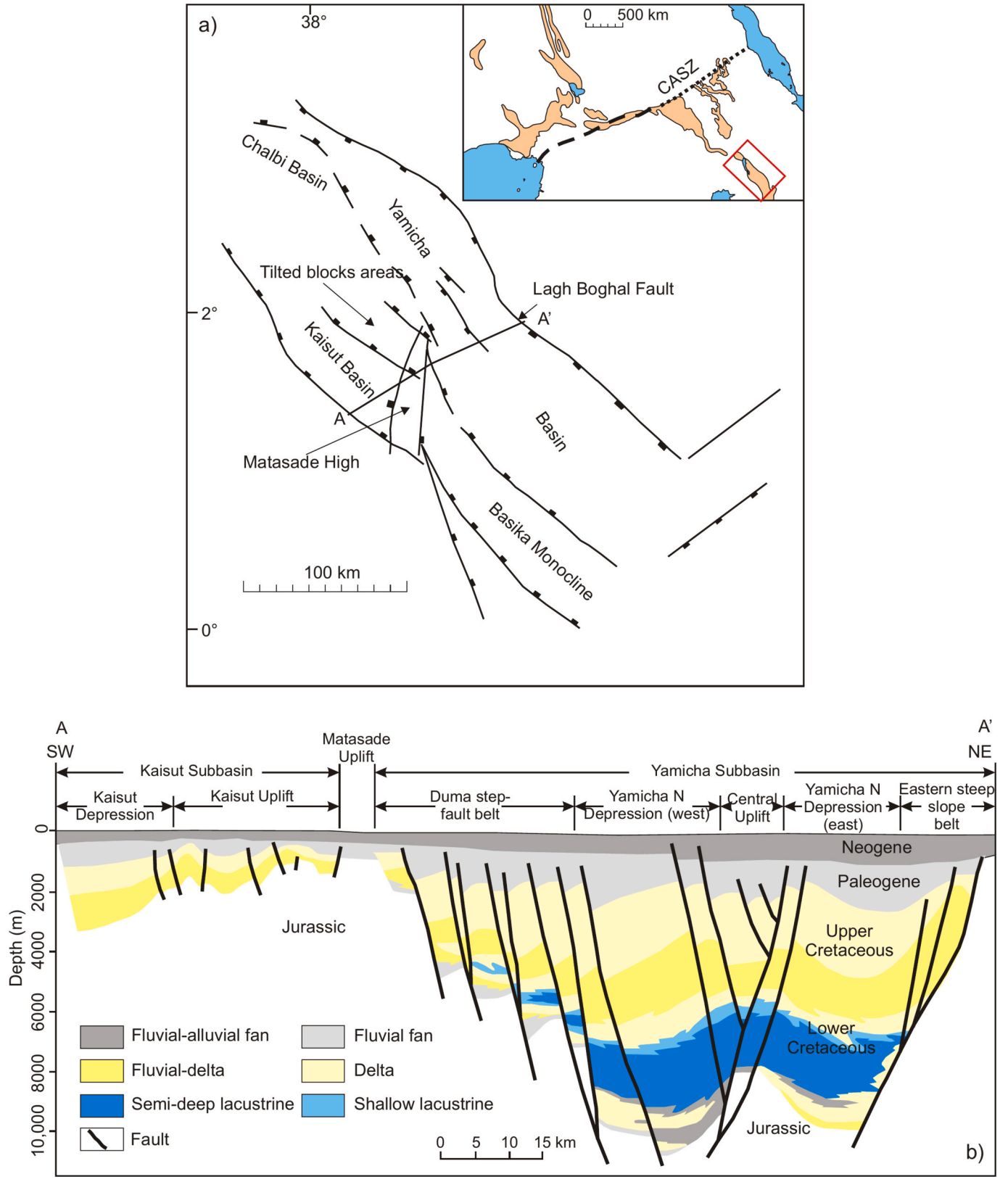

Fig. 15. a) Structural outline of the Anza Basin (modified from Sewe, 1995). The inset shows the location of the Anza Basin within the West and Central African Rift System; b) cross-sections through the Anza Basin (after Dou et al., 2023b). For locations of A-A', B-B′, and C-C′ see Fig. 15a.

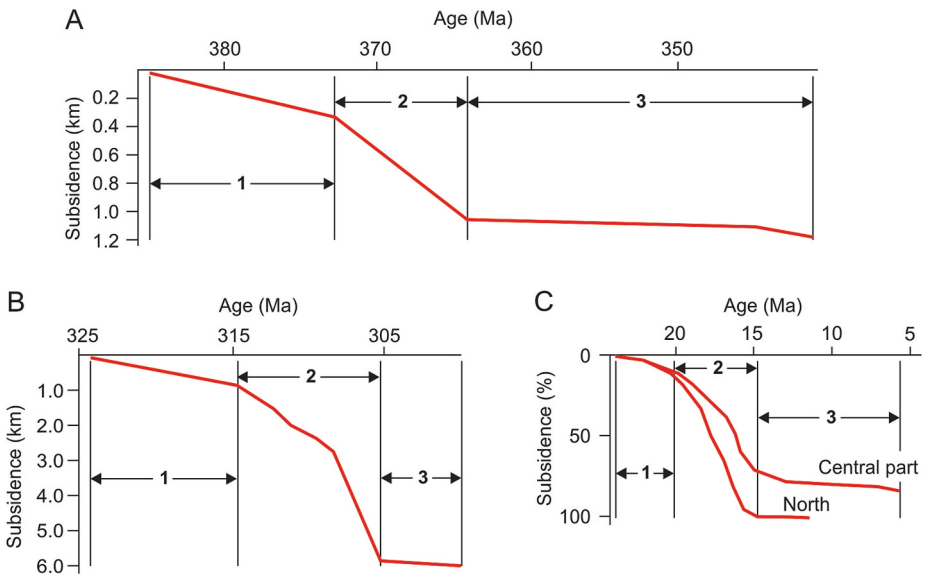

Fig. 16. Subsidence curves in rift basins: A – Dnieper–Donets Basin, Ukraine; B – Asturias Basin, Spain; and C – Suez rift, Egypt (from Catuneanu, 2024; modified from Moretti and Colletta, 1987; Van Wees et al., 1996; Izart et al., 2003; Holz et al., 2017). Stages of basin development: 1 – early stage of low subsidence rates; 2 – main stage of high subsidence rates; and 3 – late stage of low subsidence rates.

balance, resulting in overfilled or partially underfilled basins that commonly host alluvial, fluvial, aeolian, and lacustrine environments. In this early stage of evolution, the rift system is fragmented, with multiple isolated depocenters dominated by a half-graben geometry controlled by single boundary faults. Fluvial drainage may be restricted to each half-graben, with no through drainage across the entire rift basin, and lakes may form in the deeper and underfilled parts of the depocenters. During this stage, deposition may be either upstream-controlled, in the case of overfilled basins, or downstream-controlled, where lake-level changes influence shoreline trajectories and the related stratal stacking patterns. In the case of the WCARS basins, this early stage of basin evolution approximately ranges from the Valanginian to the end of the Barremian (Fig. 18). In the Termit, Blue Nile, and Anza basins, where the onset of sedimentation is as yet unknown, this early stage may already have started during the Berriasian (Figs. 3 and 9).

The **main stage** of rift development is characterised by high subsidence rates, which typically outpace the rates of sedimentation across most of the basin. As a result, the rift becomes underfilled and dominated by deeper lacustrine or marine environments (Figs. 16 and 17). During this stage, the boundary faults of the individual half-grabens grow and coalesce into more regional extensional faults, which outline larger depocenters along the rift axis. Sediment supply to these lakes or interior seas may come from either side of the rift and may feed gravity flows directed to the depocenters and possibly along the rift axis if sufficient tilt supports the sediment transport in a strike direction. The resulting turbidites and debrites are commonly interbedded with fine-grained suspension sediment, which may generate economically significant petroleum source rocks. Such rift source rocks become important not only for the petroleum systems of rifts but also for the prospectivity of other juxtaposed basins (e.g., overlying 'passive-margins' in the case of rifts that lead to continental breakup). The underfilled nature of the basin at this time also implies that deposition is downstream-controlled, whereby the lake/sea-level changes influence shoreline trajectories and the related stratal stacking patterns. For the WCARS basins, the main stage of basin evolution lasted from the Aptian to the end of the Oligocene (Fig. 18). Particularly, the WARS basins, such as the Benue Trough, and the Tefidet and Gao basins exhibit a high amount of marine sediments during that time (Fig. 3). In contrast, the CARS basins are predominantly characterised by lacustrine deposition. An exception is the Anza Basin, which exhibits marine deposits of this age in its southern part (Fig. 9).

The **late stage** of rift evolution is defined by declining subsidence rates, which change the balance between accommodation and sedimentation in favour of the latter. As a result, rifts become overfilled and dominated by continental environments (Figs. 16 and 17). It is thus common to find fluvial or aeolian sediments towards the top of rift sequences, below the first-order sequence boundaries (Kress et al., 2021). Deposition may still be, at least in part, downstream-controlled during the transition from the main stage (underfilled basin) to the late stage (overfilled basin) of rift evolution and typically becomes upstream-controlled once all accommodation is consumed by sedimentation. The complete infill of rifts by the end of the first-order rift cycles explains the formation of unconformities at the top of rift sequences, which mark breaks in sedimentation before subsidence resumes following the formation of a new basin. For example, in the case of rifts that lead to the opening of new oceans, rift sequences are overlain by 'passive margin' sequences, with the intervening first-order sequence boundaries represented by 'breakup' unconformities, which mark a change in the tectonic setting from rifts dominated by extensional subsidence to 'passive margins' dominated by thermal subsidence. The late stage of the WCARS basins ranges from Miocene to recent and shows a pronounced return from marine and lacustrine to alluvial deposition (Figs. 3, 9, and 18).

First-order rift sequences are typically bound by regional unconformities at the base and at the top, which mark changes in the tectonic setting and the dominant subsidence mechanisms. At the base, the 'syn-rift' unconformity marks the onset of rifting and continues to develop during rifting in response to the thermal uplift of the flexural basin margins (Bosence, 1998; Holz et al., 2017; Fig. 17). The fragmentation of the rift zone into multiple half-grabens, especially during the early stage of rift development, implies that the syn-rift unconformity may be a composite and diachronous surface, consisting of smaller fragments of local significance. At the regional rift scale, however, the syn-rift unconformity may be mapped as a throughgoing first-order surface at the base of the rift sequence, especially in low-resolution studies such as those afforded by seismic data. The top of the first-order rift sequence is also marked by a regional unconformity, which signifies the cessation of sedimentation following the complete infill of the rift basin at the end of the first-order rift cycle. This first-order sequence boundary can also be diachronous, reflecting variations in the rates of subsidence and sedimentation along the rift axis that affect

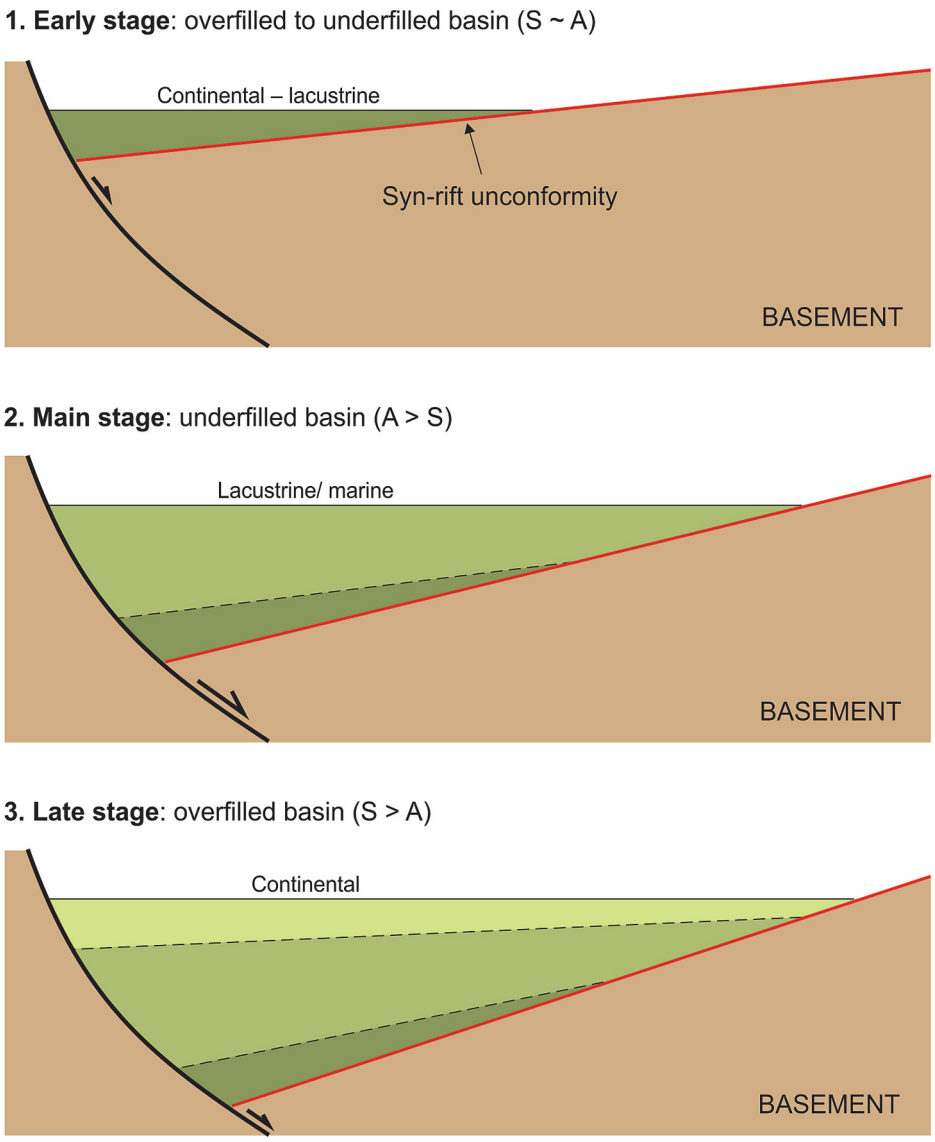

Fig. 17. First-order rift cycle – stages of basin development: 1. low subsidence rates in relative balance with sedimentation; 2. high subsidence rates and basin deepening; and 3. low subsidence rates and basin infill (from Catuneanu, 2024). Variations in the rates of subsidence and sedimentation across the basin may result in the formation of different but age-equivalent systems tracts along dip and strike directions (see text for details). Abbreviations: A – accommodation; S – sedimentation.

the timing of the end of rifting at any location. However, this unconformity is more likely to form a physically continuous surface across the rift basin, following the coalescence of half-grabens during the main stage of rift development. In the case of the WCARS basins, the lower unconformity of the first-order sequence coincides with the early stage of basin formation and varies in age between individual basins between the Valanginian and the Berriasian (Figs. 3, 9, and 18).

Within the first-order rift sequence, lower rank sequences and bounding unconformities may also form in relation to the higher frequency cycles of fault reactivation and tectonic quiescence that punctuate the rift development during each of the three stages of the first-order rift cycle. These higher frequency cycles subdivide the first-order rift sequence into second-order and lower rank sequences. Second-order cycles within the WCARS basins, for instance, range from the Valanginian to the end of the Albian, from the Cenomanian towards the end of the Maastrichtian, and from the Paleocene to the Holocene (Figs. 3, 9, and 18). Third-order cycles would be on a formation level and require further lithostratigraphic observations. The origin of some of the lower rank unconformities relates to the thermal uplift that affects the flexural basin margins, which may become the dominant control on accommodation and sedimentation at times of tectonic inactivity along the basin-margin faults. Periods of tectonic quiescence may also produce stratigraphic hiatuses, even in the absence of thermal uplift, particularly in overfilled basins where deposition gives way to sediment bypass once graded profiles are attained, until subsidence resumes and starts a new sedimentation cycle. Fluctuations in the lake/sea level during stages of underfilled accommodation may also generate lower rank depositional sequences, further complicating the stratigraphic architecture of rift basins. However, tectonism, including extension and tectonic inversion, remains the dominant underlying control on the formation and evolution of rifts, as well as on the stratigraphic cyclicity observed at larger scales (Figs. 16 and 17).

The long-term stages in the evolution of rifts are commonly depicted with one-dimensional or two-dimensional diagrams, which capture the essence of the overall subsidence and sedimentation trends during the first-order rift cycles (Figs. 16 and 17). However, the rates of subsidence and sedimentation at any given time vary across a rift basin, leading to potentially out-of-phase bathymetric and/or depositional trends along

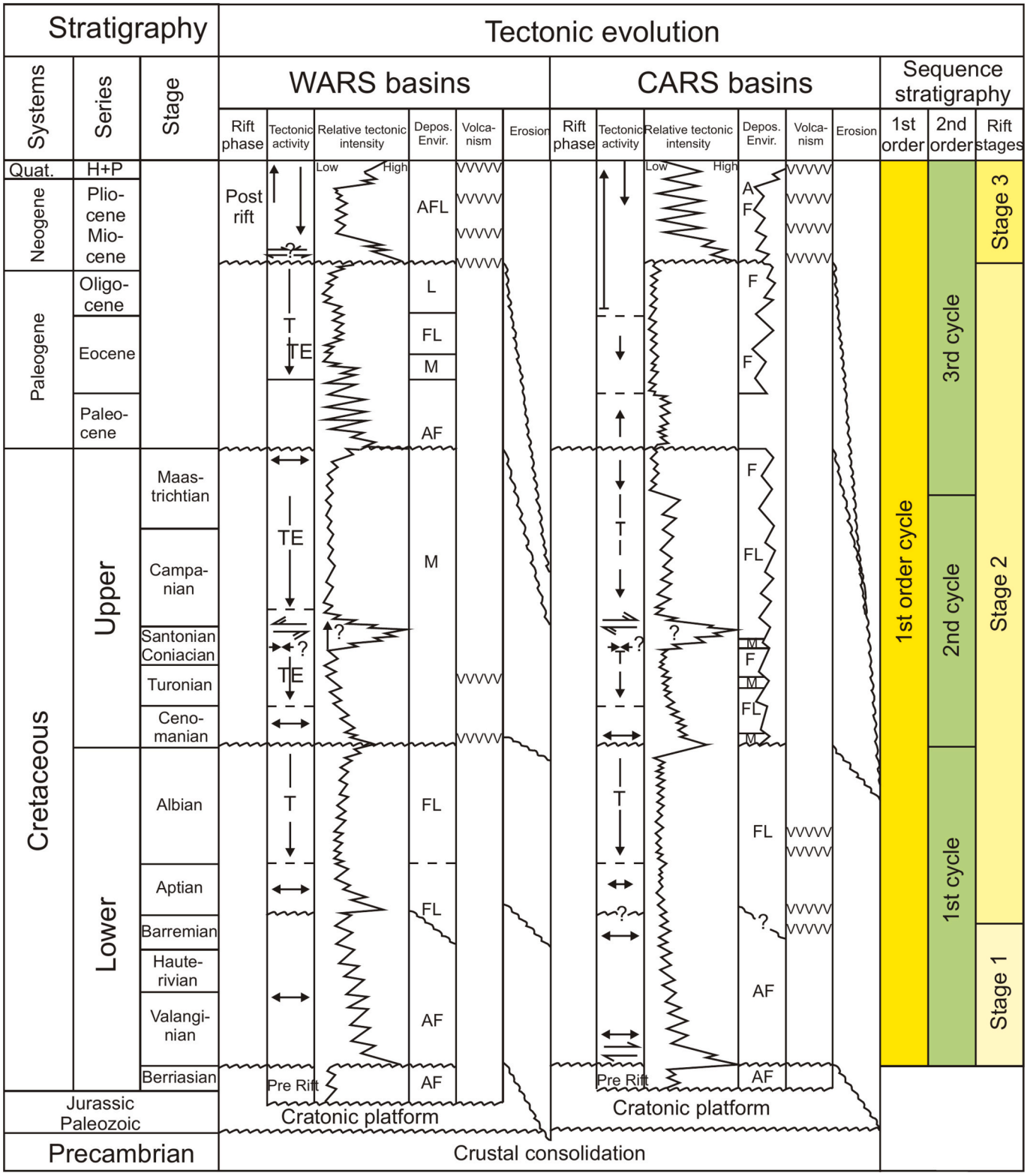

Fig. 18. Paleotectonic evolution of the WCARS basins (modified from Genik, 1993).

dip and strike directions. This three-dimensional variability affords the coeval development of different types of systems tracts across a basin, e.g., in relation to contrasts between the proximal and distal shorelines along the faulted vs. the flexural basin margins, or along the same shoreline in a strike direction (Fig. 19). These variations affect the timing and the systems-tract composition of the lower rank sequences that form during each stage of rift development, but may also offset the timing of the main stages of the first-order rift cycle along the rift axis. Therefore, different areas of a rift basin may record their own subsidence history (e.g., Fig. 16C) and corresponding timing of the early, main, and late stages of the rift cycle.

At times when accommodation is overfilled, most commonly during the early and late stages of rift evolution (Fig. 17), continental sequences are upstream-controlled and consist of unconventional systems tracts (e.

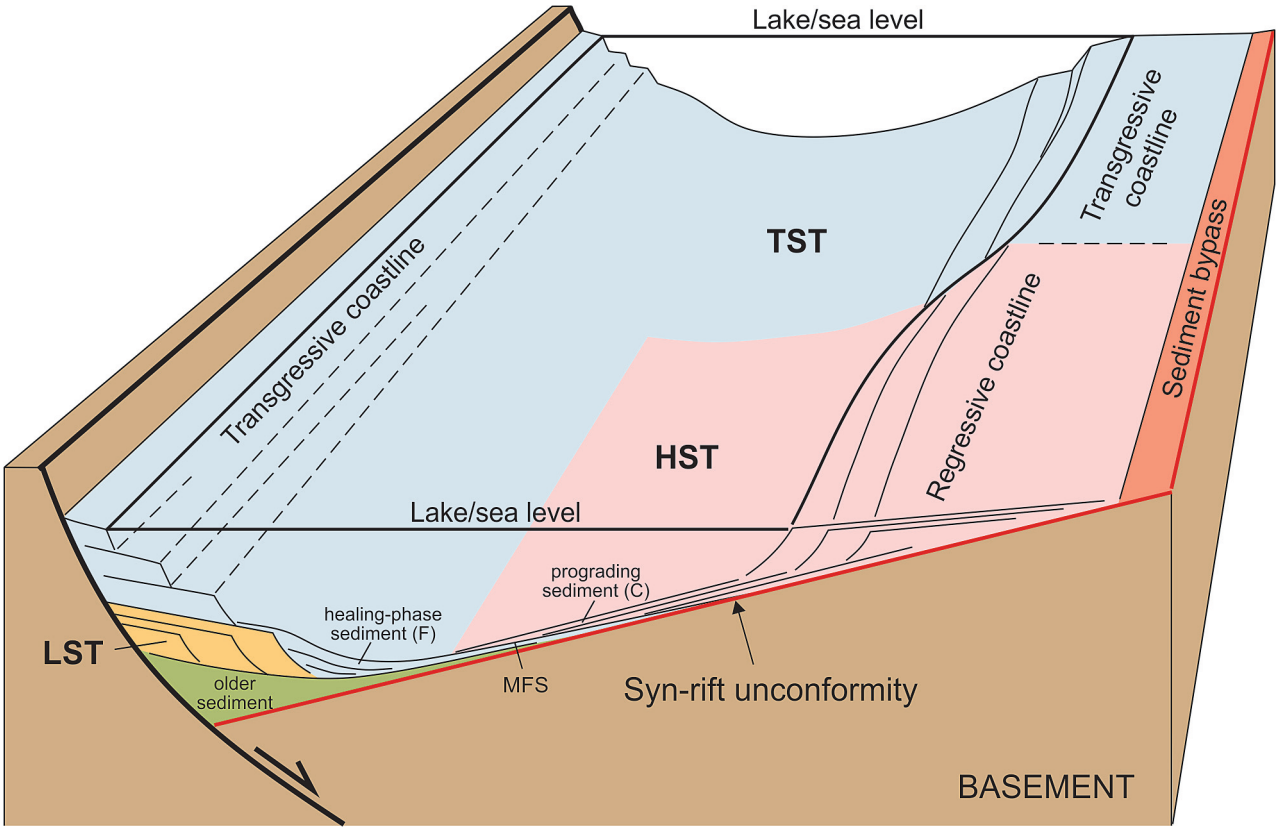

Fig. 19. Stratigraphic variability in an underfilled rift basin: different systems tracts may form at the same time, due to variations in the rates of accommodation and sedimentation along dip and strike directions (from Catuneanu, 2024). Abbreviations: LST – lowstand systems tract; TST – transgressive systems tract; HST – highstand systems tract; F – fining upward; C – coarsening upward; MFS – maximum flooding surface.

g., high- and low-amalgamation systems tracts in fluvial systems). When accommodation is underfilled, which is typically the case during the main stage of rift evolution (Fig. 17), all types of downstream-controlled systems tracts may form in relation to shoreline trajectories, including lowstand, transgressive, highstand, and falling-stage (Catuneanu, 2022). However, the unique tectonic behaviour and subsidence mechanisms that characterize rift systems, which involve rapid addition of accommodation during the reactivation of basin-margin faults, are conducive to a stratigraphic architecture dominated by transgressive and highstand systems tracts (Frostick and Steel, 1993; Catuneanu and Eriksson, 2002; Martins-Neto and Catuneanu, 2010; Catuneanu et al., 2012).

5.2. *Palaeoenvironmental conditions*

During the Late Cretaceous, significant tectonic and climatic changes occurred across West, Central, and East Africa, as well as throughout the African and South American continents (Reyment and Dingle, 1987; Fairhead et al., 2013; Hay, 2017; Barry et al., 2018; Pearson et al., 2024). Several rift systems developed and were filled with thick sedimentary sequences composed of organic-rich mudrocks that formed in marine, brackish, and fluvial environments (Avbovbo et al., 1986; Mao et al., 2016; Qiao et al., 2016; Tan et al., 2017; Morakinyo et al., 2021; Dou et al., 2022a). Consequently, the CARS and WARS are genetically linked, and they are influenced by two primary structural lineaments trending in NW-SE and ENE-WSW (Morakinyo et al., 2021). The regional sedimentation of fine-grained and coarse-grained sequences in the WCARS offers valuable insights into palaeo-sedimentary environmental conditions during sediment formation. The sedimentary infill in these basins was mainly derived from continental sources (Fairhead et al., 2013).

The Cretaceous Trans-Saharan Seaway emerged during the late Cenomanian and early Turonian, stretching from the Tethys in the north, passing through Chad, Niger, and Nigeria, and linking to the South Atlantic Ocean (Fig. 2) (Reyment, 1980; Zhou et al., 2017; Edegbai et al., 2019; Abubakar et al., 2021). During the late Campanian and early Maastrichtian, it underwent a re-establishment phase. Geochemical records and palaeogeographic models reveal that the pre-Santonian Trans-Saharan Seaway was more far reaching, with higher salinity when compared to the more spatially restricted post-Santonian Trans-Saharan Seaway with brackish palaeosalinity (Edegbai et al., 2019). As a result, thick coeval marine to marginal marine sedimentary facies were deposited in Nigeria and throughout the basins of the WARS (Fig. 3) (Zhou et al., 2017; Edegbai et al., 2019). Thus, the sedimentary history, palaeoenvironment, and palaeotectonics of the WARS basins exhibit various similarities (Omietimi et al., 2022). The Benue Trough in Nigeria before the Cretaceous period, similar to other basins within the WARS, comprised a continental landmass of Precambrian crystalline rocks, upon which Cretaceous sedimentary strata were deposited unconformably (Fig. 3). The Benue Trough experienced primary depositional cycles characterised by transgression and regression events. The initial sedimentary cycle began with continental strata deposited from the Aptian to mid-Albian (Lower and Central Benue Trough) and Cenomanian (Upper Benue Trough) arising from the opening of the South Atlantic Ocean, linked with significant tectonic activity characterised by NW-SW-oriented faults (Benkhelil, 1982; Ofoegbu, 1985; Wright, 1985; Abubakar et al., 2021). These strata are on the same stratigraphic level as the 'Continental Intercalaire' described in the Iullemmeden (Nigeria, Niger, and Mali) and Chad basins (Nigeria, Chad, and Cameroon) (Petters, 1982). The first marine ingression, which followed the opening of the Equatorial Atlantic in the mid-Albian, blanketed the continental strata. This marine transgression deposited the Asu River Group in shallow marine to moderately deep marine environments under oxic to

anoxic conditions (Ofoegbu, 1985; Agumanu, 1989; Bolarinwa et al., 2022). A minor regressive phase that followed saw the deposition of the Awe/Keana Formation in the Central Benue Trough (Ofoegbu, 1985; Patrick et al., 2013). In the Upper Benue Trough, this phase is represented by the Yolde Formation, which consists of sandstones and mudrocks formed in a marginal marine environment (Carter et al., 1963). A second marine transgressive phase occurred by the end of the Cenomanian until the Coniacian, initiating the deposition of carbonates, mudrocks, and sandstone strata of the sedimentary cycle (Petters and Ekweozor, 1982; Gebhardt, 1997, 1999, 2001; Edegbai et al., 2019). This transgression led to the deposition of carbonates, mudrocks, sandstones, and mudrocks of the Eze-Aku (older) and Awgu (younger) groups in the Lower and Middle Benue Trough segments (Fig. 3) (Ofoegbu, 1985; Wright, 1985; Rebelle, 1990; Obaje, 2009). This sequence of strata succession depicts a transition from anoxic deep marine conditions to shallow marine dysoxic to oxic-rich palaeoenvironments (Petters and Ekweozor, 1982; Gebhardt, 1997, 1999, 2001; Edegbai et al., 2019). Adedosu et al. (2012) analysed borehole data penetrating coal and carbonaceous shale deposits from the Turonian to Coniacian Awgu Group in the Central Benue Trough. Findings from biomarker and carbon isotope data indicated the presence of both terrestrial and marine palaeoenvironments, depicting a transition to oxic deltaic conditions towards the end of the second depositional cycle (Adedosu et al., 2012). In the Upper Benue Trough, this cycle extended until the Santonian, represented by the Gongila and Fika formations (Pindiga Group) in the Gongola sub-basin and the Dukul, Jessu, Sekuliye, Numanha, and Lamja formations in the Yola sub-basin (Fig. 3). Geochemical analysis from outcrops spanning the late Cenomanian-early Turonian interval (Gongola sub-basin) revealed that sedimentation occurred mostly in suboxic to anoxic conditions (Abubakar et al., 2024). Additionally, the study revealed a brackish environment with limited bioproductivity and strong hydrodynamic water circulation. This second depositional cycle was terminated by the Santonian-Maastrichtian inversion (Edegbai et al., 2019). Post-Santonian lithic fill in the Benue Trough represents the third sedimentary cycle. In the Anambra and Afikpo basins (Lower Benue Trough), the entire succession consists of Nkporo Group, Mamu, Ajali, and Nsukka formations in stratigraphic order representing fluviomarine conditions (Fig. 3). In the Upper and Middle Benue Trough segments, the fluviomarine Gombe and Lafia formations, respectively, represent this sedimentary cycle (Ofoegbu, 1985; Obaje, 2009; Edegbai et al., 2019). The end of the Maastrichtian was marked by a brief inversion episode, represented by a regional unconformity in the WCARS. In the Benue Trough, this event is evinced by the folding of the Gombe Formation as well as an angular unconformity that separates it from the overlying continental Paleogene Kerri-Kerri Formation. Since the Middle Benue Trough emerged in the late Campanian, deltaic processes were common in the Lower Benue Trough, as demonstrated by the diachronous Paleocene to recent sediments of the Niger Delta Basin. Furthermore, the Benue Trough's sedimentary sequences were sourced predominantly from felsic rocks, with minor contributions from mafic and intermediate source rocks as revealed from isotope (i.e., ^{18}O and ^{2}H) and trace element data, indicating widespread extensional tectonic stresses in West Africa during the Cretaceous period (Ofoegbu, 1985; Amajor, 1987; Nwajide, 1987; Odigi and Amajor, 2008; Igwe, 2017; Edegbai and Schwark, 2020; Abubakar et al., 2021, 2024; Bolarinwa et al., 2021, 2022). In addition, deductions from petrographic, mineralogic, and geochemical data point to multiple provenance regions consisting of mafic and felsic rocks with a high degree of chemical alteration (Odigi, 2007; Edegbai and Schwark, 2020). The basin fill in the Southern Benue Trough shows dominant mafic character from Albian–early Turonian, whereas mid-Turonian–Coniacian rocks show a more dominant felsic provenance signature. The foregoing suggests a spatio-temporal variability in the nature of detritus filling the Benue Trough during the pre-Santonian age. Deductions of provenance for the post-Santonian strata from petrographic, mineralogic, and geochemical data reveal a dominant felsic provenance comprising basement and recycled pre-Santonian rocks.

The Termit, Tenere, Tefidet, Gao, Logone-Birni, Bongor, Doba, and Muglad basins were all continental basins during the Early Cretaceous, with marine transgression initiating in the Late Cretaceous in the WARS basins (Fig. 3). In the Niger Termit Basin, the syn-rift Lower Cretaceous K1 Formation, comprising clastic sedimentary strata (i.e., sandstones and mudrocks), was deposited in alluvial and lacustrine fluvial environments (Lai et al., 2018). In the Upper Cretaceous, a marine transgression into the basin led to the deposition of the Donga and Yogou formations (Fig. 3). The Donga Formation consists of mudrocks containing marine fossils (the ostracods *Ovocytheridea nuda* and *Brachycythere* sp.), suggesting deposition in coastal to marine environments (Yuan et al., 2023). In the Upper Cretaceous, based on micropalaeontological data revealing the presence of marine phytoplankton including *Leiosphaeridia*, *Apteodinium*, and *Dinogymnium* as well as the ostracods *Ovocytheridea* cf. *nuda* and *Paracypris* cf. *nigeriensis*, and sedimentary geochemistry, isotopes, and biomarker data from subsurface samples of the Yogou Formation, deposition occurred in dominantly shallow marine environments with minor to intermediate contributions from freshwater and brackish environments (Liu et al., 2015; Tang et al., 2017; Dou et al., 2022a; Yuan et al., 2023). The basin experienced an increase in the input of terrigenous clastic material due to intensified chemical weathering conditions. This was accompanied by a significant increase in the presence of terrigenous organic matter and a high input of nutrients. Deposition took place in an environment characterised by strong primary productivity in freshwater and brackish conditions and marine inflow originating from the Tethys and Atlantic regions. However, the primary productivity was primarily due to marine species and terrestrial organic nutrient supply from land. The presence of marine phytoplankton and freshwater algae (*Apteodinium* and *Pediastrum*) indicates a nearshore environment (Liu et al., 2015). Furthermore, deposition in suboxic to anoxic conditions with varying water depths was identified, thus suggesting good preservation potential for sedimentary organic matter (Dou et al., 2022a). The presence of identical age-diagnostic microfossils in the Cretaceous units within the Termit Basin, Benue Trough, and Bornu Basin supports the hypothesis of the existence of a Trans-Saharan Seaway connecting the Tethys Sea and the South Atlantic during the Cenomanian and Turonian sea incursions (Dou et al., 2022a). During the Maastrichtian, seawater regression from the Termit Basin, along with epeirogenic deformation, caused an inflow of terrigenous material into the basin, resulting in the deposition of fluvial sandstones with high porosity and permeability (Liu et al., 2015). Over time, these sandstones gradually transitioned into a sandy, braided system recognised as the Madama Formation (Fig. 3). In the Paleogene, lacustrine transgression in the basin gave rise to deltaic-to-lacustrine deposits comprising the Sokor-1 and Sokor-2 formations. These formations represent regional seal rocks in the Termit Basin (Yuan et al., 2023). In the Gao Basin in Mali, the fossil content of the Ménaka Formation reveals shallow-marine deposits within the ancient Trans-Saharan Seaway during the Campanian-Maastrichtian. Most facies were interpreted to have been formed in a sublittoral environment with thick fissile and fossiliferous shale and limestone layers.

Limited or no published data exists for the northern Niger basins concerning biostratigraphy, sedimentology, sedimentary geochemistry, and palaeoenvironmental reconstructions. The available information reveals that the stratigraphic succession in the Tefidet Basin primarily comprises Lower and Upper Cretaceous formations, including coarse-grained sandstones, mudrocks, argillaceous fine-grained sandstones, shallow-marine limestones, and aeolian Quaternary sandstones (Konaté et al., 2019). Deposition in the Tefidet Basin commenced during the lower Aptian with the formation of the Angornakeur Formation, interpreted as a sedimentary unit deposited in a continental lacustrine environment (Fig. 3) (Konaté et al., 2019). The presence of coarse-grained sandstones at the base of the formation suggests proximal deposition, likely near the ancient lake shoreline, while finer-grained strata towards the top imply deeper water conditions or increased

distance from the shoreline. Subsequently, the overlying Tagrezou Formation, characterised by mudrocks, indicates deposition in a relatively deeper lacustrine setting (Konaté et al., 2019). On the other hand, the Tanguerat Formation, composed of argillaceous siltstones intermixed with vertebrate bones within calcareous-enriched layers, was deposited in a deltaic to fluvial environment (Konaté et al., 2019). The Upper Cretaceous strata are transgressive on the Lower Cretaceous continental formations. The Alanlara Formation, formed in the lower Cenomanian, marks ongoing transgression in the basin, with predominantly black limestones and thin, fine-grained sandstones, suggesting deposition in a shallow-marine environment (Fig. 3) (Konaté et al., 2019). In the Turonian, identified ammonites in the limestone layers enable a correlation with the Nigerian Benue Trough, implying a connection between the Tenere Mega-system and the Benue Trough during the Cenomanian-Turonian period in West Africa (Konaté et al., 2019).

The lithology and palaeoenvironment of the Tenere Basin are equivalent to those of the Termit Basin (Liu et al., 2017a). Biomarker and stable carbon isotope data from subsurface samples indicate that the Upper Cretaceous Yogou Formation in the Tenere Basin was deposited in a marine environment (Liu et al., 2017a). Sedimentary layers comprising sandstones and mudrocks were laid down in shallow marine to paralic environments. Additionally, organic geochemical data suggest that source rocks within the basin were deposited under anoxic conditions in a high-salinity environment. Furthermore, the carbon isotope compositions of oils from the Tenere and Termit basins are genetically related, indicating a common source (Liu et al., 2017a). In the Logone-Birni Basin, much of the available data is from gravity and seismic surveys. The Lower Cretaceous formations in the basin are made up of continental lacustrine and fluvial deposits. Marine transgressions in the Upper Cretaceous deposited the Gongila Formation in the Logone-Birni Basin (Fig. 3). The formation is distinguished by its thin grey to dark grey calcareous mudrocks and thick sandstone facies.

In the CARS, the Bongor and Muglad basins exhibit complete continental-fluvial sedimentary strata and share similar palynofloras from the Lower Cretaceous (Hu et al., 2023). The Bongor Basin stratigraphic infill consists of Lower Cretaceous continental-fluvial-deltaic system deposits, formed in a freshwater environment (Fig. 9). Palynofacies data from subsurface wells document freshwater algae and ostracods in the Lower Cretaceous sequences (Hu et al., 2023). Samples from the basal Prosopis Formation revealed a high abundance of freshwater ostracods in the NE-1 core, thus suggesting variational precipitation and deposition in deep-water fluvial delta-lacustrine environments (Dou et al., 2020a; Hu et al., 2023). This formation is dominated by a relatively high-gradient arid fan-delta type (Yang et al., 2020). In addition, geochemical proxies support deposition in a freshwater environment, with a Sr/Ba ratio lower than 0.5, while the redox conditions indicate dysoxic to oxic depositional settings (Tan et al., 2017). The overlying Mimosa Formation was deposited in a fluvial environment, as revealed by abundant terrestrial palynomorphs, freshwater algae and non-marine ostracods (Hu et al., 2023). Subsequently, the Kubla-Baobab formations contain primarily freshwater algae such as *Botryococcus* spp. and *Scenedesmus bifidus*, indicating deposition in continental lacustrine and braided-river-deltaic environments with likely minor brackish water incursions (Tan et al., 2017; Hu et al., 2023). In the Muglad Basin, the basal Lower Cretaceous Abu Gabra Formation consists of laminated carbonaceous mudrocks, sandstones, and thin claystone lenses deposited in a fluvial-lacustrine environment (Fig. 9) (Makeen et al., 2015a, 2015b; Leyuan et al., 2021). Based on the interpretation of geochemical and palynofacies data from subsurface cores, particularly low Sr/Ba concentrations and a high abundance of the freshwater algae *Botryococcus*, deposition in a freshwater lacustrine environment under suboxic to anoxic conditions can be proposed (Makeen et al., 2015b). The overlying Bentiu Formation in the Muglad Basin is laterally equivalent (i.e., correlated) to the Cretaceous Baobab Formation in the Bongor Basin. From the Muglad and Bongor basins, a high abundance of freshwater algae is reported. Specifically, in the Muglad Basin, the primary species are *Holmwoodinium notatum* and *Botryococcus* spp. (Hu et al., 2023). Therefore, it can be assumed that the Bentiu Formation was deposited in a freshwater lacustrine environment. The formation is dominated by fluvial, coarse-grained sandstones that serve as the primary reservoir rocks in the Muglad Basin.

In particular, with regards to the Melut and Muglad basins, a continuation of sedimentation between Miocene and Pliocene times in the form of the still highly debated Megalake Sudd is possible (Alvarez, 2023).

5.3. Palaeoclimatic conditions

Global climatic conditions in the Early Cretaceous, spanning from the Berriasian to the Barremian, exhibited characteristics that can be described as an intermediate between an icehouse and a hothouse (Frakes et al., 1992; Scotese et al., 2021). The global average temperature during the Late Cretaceous was ca. 28 °C, whereas the present-day global average is ca. 15 °C (Scotese et al., 2021). When considering the future direction of man-made global warming, one naturally envisions the extreme climate (i.e., hothouse) conditions of the Late Cretaceous and Eocene periods (Scotese et al., 2021). Whether we will increase the Earth's average global temperatures to such levels in the near future remains uncertain. However, we now have a clearer understanding of the characteristics of a warmer world. The African climate, particularly in the context of the WCARS, was affected by the continent's tectonic activity, which varied across different locations. These differences may have been influenced by latitude, elevation, proximity to the sea, etc. Sedimentary deposition in the WARS basins during the Early Cretaceous (Berriasian to Barremian) is recorded in the Termit and Logone-Birni basins. In contrast, the CARS basins recorded widespread Early Cretaceous deposition across the Bongor, Blue Nile, and Anza basins. However, during the Berriasian to Barremian deposition in the WCARS, there is limited palynological, isotope and inorganic geochemistry data to reconstruct climatic conditions. During the deposition of the Valanginian Prosopis Formation in the Bongor Basin, palynofacies data reveals the presence of *Lygodiaceae*, *Araucariaceae* sp. and mainly xenophytes that flourish in the tropical-subtropical regions, suggesting a dominantly arid climate with ephemeral humid pulses (Tan et al., 2017; Hu et al., 2023). The geochemical climate-sensitive Sr/Cu ratios in sampled turbidite beds within the Prosopis Formation range from 4.8 to 58.6, indicating an overall hot and arid climate with brief humid periods. As the overlying Mimosa Formation was being deposited, ferns thrived, particularly Lygodiaceae, Matoniaceae, Schizaeceae, Cyatheaceae, and Lycopodiaceae, all indicative of a hot and humid climate (Hu et al., 2023). The palaeoclimate during the deposition of the Mimosa Formation recorded warmer temperatures and increased rainfall than the Prosopis Formation. Based on PALEOMAP data, the Bongor Basin was suggested to be located at the interface of a humid tropical terrain and an arid region during Berriasian-Aptian times (Boucot et al., 2013; Tan et al., 2017). In the Hauterivian-Aptian, the prevalence of *Classopollis* pollen indicates a warm and dry climate with a Cheirolepidiaceae flora. Across the CARS basins, palynological records from the Bongor, Muglad, Doseo, and Doba basins show similarities, suggesting a temporary transition from a hot to humid environment. All mentioned basins recorded the occurrence of *Afropollis acme*, indicating a uniform climate and flora during the early Aptian (Hu et al., 2023). However, *Sergipea*, typically linked with South American sediments, is solely found in Barremian strata of the Bongor Basin and is absent in the Doba and Muglad basins. In the Muglad Basin, during the formation of the Abu Gabra Formation (Barremian-Aptian interval), the climatic conditions were predominantly arid to semi-arid-semi-humid based on major and trace elements data (Makeen et al., 2015b). The index of compositional variability (ICV) values showed immature sediments, which implies low chemical weathering in an arid climatic environment. Palynological data from subsurface cores of the Melut Basin revealed high abundance

of *Cupliferoidaepollenites*, *Tricolpopollenites*, *Lygodiumsporites*, and *Jiaohepollis* during Barremian-Aptian times. These palynomorphs suggest prevailing warm and humid climates (Dou et al., 2007).

The middle Aptian to early Albian strata in the Doseo Basin, as observed from subsurface cores (i.e., boreholes K-1 and KE-101), indicate a semi-arid to semi-humid, tropical-subtropical climate based on palynomorphs (Dou et al., 2023a). Notably, a transition from relatively dry to humid conditions occurred during the late Aptian to early Albian in the Doseo Basin. This climate shift, evident from palynomorphs in the Doseo Basin and supported by evidence from South America (i.e., Brazil), suggests the establishment of a consistently humid zone extending from east to west across the equatorial region of the southern hemisphere in the late Aptian (Dou et al., 2023a).

The Aptian–Albian period is characterised by a warm greenhouse climate (Huber et al., 2018; O'Brien et al., 2017). However, two cold snaps occurred during this period: one in the earliest Aptian (120–119 Ma) and another in the latest Aptian (115–113 Ma) (Luft-Souza et al., 2022; Steinig et al., 2020). Despite this, a tropical-subtropical climate prevailed in Central Africa, with temperatures generally higher during the middle Aptian to early Albian.

In the WARS, during the early Aptian, the Termit Basin recorded a high abundance of *Classopollis annulatus*, suggesting drier and warmer climates than in the adjacent Doba, Bongor and Muglad basins (Hu et al., 2023). In the late Aptian to early Albian period, the separation of the African and South American continents formed the South Atlantic Ocean (Fairhead, 1988; Benkhelil, 1989). This event significantly impacted the vegetation, leading to a shift from a typically dry to a humid climate in the equatorial region of the southern hemisphere (Chumakov et al., 1995; Hay and Floegel, 2012; Hay, 2017). Geochemistry data (i.e., isotope and major and trace elements) from Albian strata in the Southern Benue Trough from the Asu River Group revealed predominantly warm and humid tropical climatic conditions in the Nigerian arm of the WARS (Bolarinwa et al., 2022). Warm, humid and tropical climates dominated during the Late Cretaceous till the Turonian, marking one of the warmest climates in the last 149 Ma (Hay and Floegel, 2012; Abubakar et al., 2024). Analysis of major and trace elements in the Kanawa shales (Pindiga Group) indicates similar warm and humid conditions in the Gongola arm of the Upper Benue Trough during the late Cenomanian to early Turonian. Petrographic and geochemical data from sandstones and mudrocks in the Lower Benue Trough suggest that the climate was more humid in the post-Santonian time when compared to hotter and drier pre-Santonian palaeoclimate (Odigi, 2007; Edegbai and Schwark, 2020). These findings corroborate the presence of warm and humid climates during this time interval. In the Termit Basin, a hot-humid climatic environment was prevalent during the deposition of the Santonian to Maastrichtian Yogou Formation. Geochemical interpretation of subsurface cores from the Yogou Formation revealed low Sr/Cu ratios, elevated ω(MgO)/ω(CaO) values, and high chemical index of alteration values (CIA) (Tang et al., 2017; Lai et al., 2018). Furthermore, research has shown that the Termit Basin's palaeolatitude during the Late Cretaceous is equivalent to its current geographic location (Guiraud et al., 2005; Lai et al., 2018). Thus, the Late Cretaceous may have been characterised by a hot, humid savanna environment. The climatic conditions of the Tefidet, Gao, and Logone-Birni basins have still not been studied and make further investigations necessary.

Oceanic anoxic events (OAE) are defined as intervals marked by extensive deposition of organic carbon-rich sediments resulting from regional and global marine anoxia (Schlanger and Jenkyns, 1976; Jenkyns, 2010). These events are closely associated with disturbances in the global carbon cycle, shifts in climate, and changes in marine plankton populations (Leckie et al., 2002; Sooraj et al., 2024, and references therein). The OAEs are generally attributed to several causes, including enhanced volcanic activity (along mid-ocean ridges or in large igneous provinces) and CO_2 emissions (e.g., Poulsen et al., 2003; Joo et al., 2020; Lenhardt et al., 2023), the influence of Milankovitch cycles (e.g., Mitchell et al., 2008), sluggish ocean circulation and deep water anoxia (Hay, 2008), and enhanced phosphorus recycling (e.g., Papadomanolaki et al., 2022), among others, or a combination of these factors.

At least seven major and minor OAEs are recorded during the Cretaceous (Jenkyns, 2010) worldwide in terrestrial and marine environments. In Africa, most of the records of Cretaceous OAEs can be found in the strata of the southern Tethys Ocean in Morocco (Kuhnt et al., 2005; Mort et al., 2008; Praus, 2015; Fonseca et al., 2020; Wang et al., 2024), Algeria (Benadla et al., 2018; Salmi-Laouar et al., 2018; Boutaleb et al., 2022), Tunisia (Ben Fadhel et al., 2011; Godet et al., 2014; Touati, 2017; Khalifa et al., 2018; Bouin et al., 2024), and Egypt (El-Sabbagh et al., 2011; Nagm et al., 2014; Kassem et al., 2020; Mansour et al., 2020). Furthermore, there are studies from the Congo Basin (Zhang et al., 2024b; Zeng et al., 2024) and some basins along the Central Atlantic margin (Kuhnt et al., 1990). In the WCARS basins, Petters and Ekweozor (1982), Kuhnt et al. (1990), and Alalade (2016) suggest that the Cenomanian to Coniacian Eze-Aku and Awgu groups (Lower and Middle Benue Trough), together with the Gongila and Fika formations of the Upper Benue Trough (Fig. 3), were deposited under anoxic conditions attributed to an oceanic anoxic event (OAE-II). However, considering the nearly complete Cretaceous sedimentary record within the WCARS basins and the large number of shale units, it can be assumed that a plethora of information on these events in the sedimentary strata of these basins is yet to be discovered.

5.4. Magmatism

So far, there is very little information on the Mesozoic magmatic activity or volcanism within the WCARS basins, with most information stemming from the 1980s and 1990s. In the Benue Trough of Nigeria, volcanic activity is recorded in three magmatic phases that correlate with the major rift phases, i.e. Early Cretaceous (141–106 Ma), Albian-Santonian (95–83 Ma), and Paleocene-Eocene (65–47 Ma) (Baudin, 1991) (Fig. 3). Popoff et al. (1982) describe 147 ± 7 Ma basaltic and rhyolitic lava flows in the Bima Hills (Gongola rift). Furthermore, Umeji and Caen-Vachette (1983) describe 113 ± 3 Ma (Aptian) rhyolites from Yandev (Middle Benue Trough). Additionally, Popoff et al. (1982) describe the occurrence of 100–105 Ma (Albian) transitional tholeiitic basalts in the Gwol region (Upper Benue Trough). The emplacement of these magmatic rocks began with an earlier phase of trachyte-phonolite around 22–11 Ma and a late basaltic phase around 7–2 Ma. It is also important to mention that older magmatic rocks (41–30 Ma) have been reported between the Central and Northern Benue Trough boundary (Wilson and Guiraud, 1992). The Upper Benue Trough is generally characterised by alkaline to tholeiitic basalts and few rhyolites whereas the Lower Benue Trough exhibits a larger variety of igneous rocks such as basalts, lamprophyres, trachytes, and phonolites as lava flows, pyroclastic rocks and dykes, sills, and volcanic necks, with intrusive activity generally dominating (Wilson and Guiraud, 1992). The magmatic activity in the Benue Trough is generally related to crustal thinning due to small-scale asthenospheric upwelling (Eyike and Ebbing, 2015). The Logone Birni Basin, adjacent to the the Benue Trough in northern Cameroon, is characterised by three volcanic episodes that occurred during the first two rift phases of the WCARS, i.e. are associated to the Early Cretaceous, late Albian and Cenomanian–Turonian (Loule and Pospisil, 2013). However, apart from seismic studies, no information on the geochemistry is available on these rocks. The volcanic rocks of the first episode of volcanism rest directly on the basement and maybe an equivalent to the alkaline rhyolites and basalts that directly overlie the Precambrian basement in the Upper Benue Trough (Popoff et al., 1982). The rocks of the second volcanic episode are possibly related to an intense period of volcanic activity in this area. However, also here, no outcrop data are available (Loule and Pospisil, 2013). Nevertheless, they may correspond to basalts and basaltic andesites of that age that have been found along the WARS elsewhere (Genik, 1992, 1993). Finally, the last volcanic or rather magmatic episode, related to the second rifting phase, may correspond to the intrusion of various dykes and sills to this

basin (Loule and Pospisil, 2013). The more intense volcanic/magmatic activity in this area is thought to be related to more intense tectonic activity and potentially to the formation of wrench-induced pull-apart basins and oblique-slip zones (Laville and Petit, 1984; Garfunkel and Ben-Avraham, 2001). The Termit and Tenere basins to the north of the Logone Birni Basin predominantly exhibit magmatic activity from the Early Cretaceous (Wilson and Guiraud, 1992), for instance, with 85–95 Ma basaltic dykes occurring in the southern part of the Termit Basin (Genik, 1992).

In contrast, the basins of the CARS are characterised by lower magmatic activity (Fig. 9). For instance, Lu et al. (2009a, 2009b) describes Barremian tholeiitic basalts in the Kubla Formation of the Bongor Basin. Similarly, Dou et al. (2023b) describe Late Cretaceous (95–75 Ma) sills (olivine tholeiites) from the Doba Basin. The Doseo Basin exhibits ca. 97–101 Ma basaltic sills (Genik, 1992).

In the Sudanese Muglad Basin, aeromagnetic evidence and the occurrence of thin 82 ± 2 Ma basalts (Schull, 1988; Wycisk et al., 1990) suggest that the southwest flank of the structural high connecting the Heglig and Unity fields may be underlain by volcanic rocks (McHargue et al., 1992). As a result, the Muglad Basin exhibits some evidence of Mesozoic volcanic activity, but it is described to be a minor component of its stratigraphy, particularly when compared to the EARS (Fairhead, 1986). In contrast, as previously mentioned, the early Mesozoic intrusive activity in the Muglad Basin (and potentially other WCARS basins) that may have been related to the early stages of crustal extension described by Zhao and Dou (2022) shows a heterogeneous composition of the underlying basement.

Additionally, the occurrence of a Late Cretaceous andesitic tuff was described from the Melut Basin (McHargue et al., 1992).

Possibly, Late Jurassic (ca. 155 Ma) basalts exist in the Blue Nile Basin (Wycisk et al., 1990). Furthermore, the same authors described the occurrence of 143 ± 6 Ma and 125 ± 4 Ma basaltic lava flows in the Khartoum sub-basin.

Since the WCARS is a passive rift environment, the lack of volcanic activity or information thereof during its development is not particularly surprising. Passive rifts commonly arise as a result of regional extension caused by plate boundary forces and/or convective drag at the lithosphere's base, resulting in crustal thinning rather than a mantle plume or hotspot. As can be seen from the few examples above, on rare occasions, thinning may be sufficient to sufficiently lower the lithostatic load on the asthenosphere, resulting in decompression and partial melting. However, drill cores show a strong dominance of intrusive over extrusive rocks. It is reasonable to wonder whether these dykes and sills are evidence that magma never reached the surface or if they are part of a complex magma plumbing system that fed potential volcanic structures at the surface. As of yet, a connection between dykes, sills, and lava flows at the surface has not been established. However, despite the description of the occurrence of these intrusive and extrusive magmatic rocks, basically no research has been done on these rocks for the last 30 years. This can obviously be ascribed to the fact that the occurrence of these rocks is relatively thin and sparse and that there is no surface exposure. Instead they can only be studied in drill cores from oil companies who so far show little interest in the petrology of igneous rocks within these basins.

In contrast, the magmatic activity of the Cameroon Volcanic Line (CVL) is thought to be indirectly related to the formation of the CASZ and, therefore, the formation of the WCARS as a whole (see Njome and de Wit (2014), and Adams (2022) for comprehensive reviews on the formation of the CVL). The CVL is a volcanic chain that is more than 1700 km long and 100 km wide and can be subdivided into an oceanic and a continental segment, stretching from the volcanic islands of Bioko, Principe, Sao Tome, and Annobon in the Gulf of Guinea to the far north of Cameroon (Njome and de Wit, 2014; Lenhardt and Oppenheimer, 2014). While intrusive activity associated with the formation of several alkaline ring complexes along the CVL has been documented since the end of the Maastrichtian (66–30 Ma; Déruelle et al., 1991; Déruelle et al., 2007), volcanic activity is likely to have begun around 42 Ma within the CVL's continental segment. Offshore volcanism began at 30 Ma (Grunau et al., 1975).

5.5. Coal deposits

In the Nigerian section of the WCARS, coal deposition occurred during the Late Cretaceous and Paleogene, with up to 2.75 Gt estimated humic coal resources (Chukwu et al., 2016). The Cretaceous coals are located at two main stratigraphic levels of Coniacian-Santonian and Campanian-Maastrichtian age. The Coniacian-Santonian coals are bituminous and occur as seams interstratified with the sand- and mudstones of the Lamja Formation (Upper Benue Trough) and the Awgu Group (Lower and Middle Benue Trough) (Fig. 3). Coal at this stratigraphic level is prospective but still largely underexplored (Obaje, 2009). The best-known deposit is in the Middle Benue Trough (Lafia-Obi coal) with a seam thickness reaching up to 5 m (Obaje et al., 1994). Similarly, the Campanian-Maastrichtian coals are largely sub-bituminous and occur interbedded with the sand- and mudstones of the Gombe Formation (Upper Benue Trough), the Lafia Formation (Middle Benue Trough), the Nkporo Group, and the Mamu and Nsukka formations (Lower Benue Trough). The coal in the Mamu Formation is the most prospective and widespread, with seam thicknesses ranging from a few centimetres in the western fringes up to over 4 m in deep depocenters in the eastern segment (Obaje, 2009), hosting the largest resources estimated at 1.5 Gt (Orajaka et al., 1990). Cretaceous bituminous and sub-bituminous coals make up 49 % and 39 %, respectively, of Nigeria's coal resources (Chukwu et al., 2016). The type and quality of the Cretaceous coals have been investigated using petrographical and geochemical techniques (e.g., Jimoh and Ojo, 2016; Obaje et al., 2018; Faboya et al., 2019; Mangs et al., 2022). Coal deposits of the Lower Benue Trough have a moderate proportion of liptinite macerals and are rich in vitrinite and inertinite, pointing to a deposition under lacustrine to fluvial conditions. Within the Middle Benue Trough, coals are liptinite-poor, very rich in vitrinite, and rich in inertinite, indicating a lacustrine to swampy environment of deposition. Similarly, coals from the Upper Benue Trough are liptinite-poor but rich in vitrinite and inertinite, suggesting a fluviatile type of deposition (Mangs et al., 2022).

Coal utilisation is determined by its gross calorific value (GCV), which in the Lower Benue Trough is on average 28.39 MJ/kg for its low-rank sub-bituminous coals and can reach up to 30.37 MJ/kg (Mangs et al., 2022). For the Middle Benue Trough, medium-rank bituminous coals with an average GCV of 21.97 MJ/kg, reaching up to 28.7 MJ/kg, have been determined. The Upper Benue Trough yields low-rank sub-bituminous to medium-rank bituminous coals with an average GCV of 24.1 MJ/kg and a maximum of 28.7 MJ/kg.

The sulphur content of the coals proves critical for emissions and air quality, and for most coal seams, it is reported to be less than 1.0 % (Mangs et al., 2022; Obaje et al., 2018). For the Lower Benue Trough, sulphur concentrations in coal were reported to vary from 0.35 to 1.28 % (Obaje et al., 2018), whereas a range of 0.61 to 4.02 % on a dry ash-free basis (daf), averaging 0.73 %, was reported by Mangs et al. (2022). Coals from the Middle Benue Trough show no substantial sulphur enrichment, ranging between 0.64 and 2.08 % and averaging at 0.9 % sulphur (daf). In the Upper Benue Trough, coals exhibit sulphur concentrations of 0.32 to 7.34 % sulphur (daf), averaging at 0.85 % sulphur (daf) when excluding the most sulphur-rich coal. The locally elevated sulphur concentrations in seams from the Upper Benue Trough caution against their utilisation to minimise environmentally detrimental sulphur-oxide emissions.

The coal quality and maturity have been assessed by Rock-Eval pyrolysis (Jimoh and Ojo, 2016; Obaje et al., 2018; Faboya et al., 2019; Mangs et al., 2022), yielding total organic carbon (TOC) values between 71 and 80 %, with an average of 75 % for the Lower Benue Trough (Mangs et al., 2022). This is in contrast to much lower values of 39 to 64 % as reported by Obaje et al. (2018), who did not correct for the

proportion of ash/minerogenic substances. The TOC content of the coals from the Middle Benue Trough ranges between 60 and 83 %, with an average of 72 % (Mangs et al., 2022). Mangs et al. (2022) also reported TOC values ranging from 65 to 78 %, with an average of 74 %, for the Upper Benue Trough. In contrast, Jimoh and Ojo (2016) recorded TOC values ranging from 59 to 65 %, without accounting for ash content.

The hydrogen index (HI) values of Lower Benue Trough coals determined by Rock-Eval pyrolysis yielded comparable values of 206 to 280 mg HC/g TOC (with HC standing for hydrocarbons) as provided by Obaje et al. (2018) and 176 to 187 mg HC/g TOC as determined by Faboya et al. (2019). Rock-Eval-based HI values of only 54 to 59 mg HC/g TOC were determined for the Lafia-Obi coals from the Middle Benue Trough, mainly due to the much advanced degree of coalification, as indicated by a T_{max} value of, on average, 451 °C (Obaje et al., 2018). Coals of the Gombe Formation from the Gongola sub-basin in the Upper Benue Trough yielded HI values between 90 and 165 mg HC/g TOC, as given by Jimoh and Ojo (2016). The relatively low HI values of coals determined for all parts of the Benue Trough indicate the presence of humic coals, deposited under oxic to dysoxic conditions, but argue against the presence of any sapropelic coals, which contain a higher proportion of algal material. Sapropelic coals are assumed to have a higher generation potential for liquid hydrocarbons (oil) as opposed to gaseous hydrocarbons. The petroleum source rock potential of the Benue Trough coals is thus rather low, and coals are supposed to have mainly generated methane, where thermal maturity was sufficient. For further details, see Section 5.6.

The lignitic Paleogene coal, interstratified with the mud- and sandstones of the Ogwashi-Asaba Formation in the Lower Benue Trough (Niger Delta Basin), is the least prospective. It occurs in a 16–20 km wide belt east and west of the Niger River, with an estimated reserve of 300 Mt. This reserve represents 12 % of Nigeria's coal resources and is the largest in Africa (Okezie and Onuogu, 1985; Orajaka et al., 1990; Chukwu et al., 2016). Ogala et al. (2012) conducted a regional assessment of the coals, reporting a GCV of 19.9 to 25.6 MJ/kg (dry basis) and 13.8 to 17.1 MJ/kg (moist, ash-free basis), with moisture content and volatile matter content ranging from 35.3 to 43.6 % (on an as-received basis) and 54.9 to 62.5 % (daf basis), respectively. The HI, carbon, and hydrogen contents vary from 268 to 639 mg HC/g TOC, 42.3 to 67.0 %, and 5.8 to 8.6 % (daf), respectively, while the sulphur content reported was low and generally below the detection limit. The same goes for the ash yield (Ogala et al., 2012; Akande et al., 2015). Organic petrology data categorises the Paleogene coal as humic to cannel coal, with low inertinite (<3 vol%), high huminite (mainly detrohuminite) content (53 to 84 vol%), and significant liptinite (predominantly liptodetrinite and bituminite) content (13 to 44 vol%) (Ogala et al., 2012; Akande et al., 2015). The foregoing characteristics, together with low maturity, i.e., T_{max} ranging from 394 to 425 °C and vitrinite reflectance (R_o) values from 0.36 to 0.42 % (Akande et al., 2015), classify the coal as low-rank coals C to B (Ogala et al., 2012).

Electrical power supply in Nigeria is dominated by gas-fuelled power plants, contributing 90 % of the demand, with the remaining 10 % provided by hydroelectric sources. Coal-fired power plants do not exist in Nigeria, despite the proven coal reserves (Obaje, 2009; Chukwu et al., 2016; Obaje et al., 2018), most of which are exploited locally for domestic coal supply, e.g., the Okaba, Owukpa, Ogboyaga, Odukpuno, and Omelehu coals from the Lower Benue Trough, the Lafia-Obi coals from the Middle Benue Trough, and the Maiganga coals from the Upper Benue Trough (Jimoh and Ojo, 2016; Obaje et al., 2018; Mangs et al., 2022). Intensification of coal utilisation during an energy transition phase before reaching CO_2-free green energy production may help in minimising exploitation of firewood in Nigeria, which leads to deforestation and associated detrimental climatic and environmental effects.

5.6. Implications for petroleum systems/ petroleum geology

Rift basins are known to contain notable hydrocarbon source rocks due to the complex interplay of tectonic activity, stratigraphic succession, and sedimentary filling (Klemme, 1980; Lambiase and Morley, 1999). In fact, 30.9 % of the 877 large oil and gas discoveries identified worldwide are located in rift basins (Mann et al., 2003).

Within the WCARS basins, three plays are apparent (Dou et al., 2020b): the Precambrian basement, the Cretaceous, and the Paleogene (Table 1). Good source rocks within the WCARS basins can primarily be found within the Early Cretaceous lacustrine shale successions, related to the first rift episode. In contrast, reservoir rocks may be found in the Early and Late Cretaceous, as well as the Paleogene successions that are related to all three rift episodes. In the Bongor Basin of the CARS, even the Precambrian basement may act as a reservoir for hydrocarbons. The so-called "buried-hill" fractured reservoirs in the Precambrian basement of the Bongor Basin represent an intriguing location for African oil and gas exploration (Dou et al., 2020b). The basin's proven oil accumulations are primarily concentrated on the so-called Northern Slope of the basin, such as the Great Baobab oilfield (Dou et al., 2015), with approximately 1.5 billion barrels of oil reserves in place (Dou et al., 2020a). Oil exploration in the Bongor Basin began in the 1970s, with the drilling of two wildcat wells, Naramay-1 and Semegin-1, in 1974 and 1976, respectively. However, no oil or gas discoveries occurred until the Ronier-1 well was drilled and tested in the Northern Slope in 2007 (Dou et al., 2020a).

The dark lacustrine mudstones of the Prosopis, Mimosa (and, to a lesser extent, the Kubla) formations (with thicknesses ranging from 500 to 1000 m) (Fig. 9) are considered to be rich in Type I and Type II kerogen (Li et al., 2017; Chen et al., 2018). When subjected to high temperatures, Type I kerogen, which mainly derives from mass blooms of uni-specific algae or cyanobacteria, is the most likely form of kerogen to produce oil (Tissot and Welte, 1984). Type II kerogen, on the other hand, is made up of marine organic materials from a diverse planktonic community, even containing minor admixture of terrestrial biomass, and may produce both oil and gas. The TOC content of sedimentary rocks in the Bongor Basin averages around 3.5 % (Dou et al., 2020b). The Prosopis and Mimosa formations are mature source rocks from which hydrocarbons were expelled and charged downward into the "buried-hill" basement reservoir (Li et al., 2017). The pelitic and low-permeability Prosopis and Mimosa source rocks in parallel provided the seal for the buried-hill traps (Dou et al., 2020b). The geochemical properties of the Bongor Basin oils from different wells are strikingly comparable, implying that they are all derived from the same Lower Cretaceous source rocks (Song et al., 2016). The time of hydrocarbon generation is estimated to have commenced at roughly 89 Ma (Chen et al., 2018), coinciding with the Late Cretaceous uplift, i.e., the Santonian Compressional Event (Chen et al., 2018), but may have lasted to ca. 55 Ma (Dou et al., 2020b).

The Lower Cretaceous rocks of the Doseo Basin towards the south are largely mudrocks of the Mangara Group, as well as the Doba and Kedeni formations (Fig. 9), reported to have produced good quality source rocks (Dou et al., 2022b) with average TOC values of 1.7 % (Zhang et al., 2024a). Here, the mature to highly mature mudrocks of the Kedeni Formation have the highest hydrocarbon potential due to elevated abundance in Type I kerogen, with averaged TOC values of 3.8 % and an averaged HI value of 760 mg HC/g TOC (similar to source rocks from the Mangara Group) (Dou et al., 2022b). As a result, this formation forms the primary source rock in the Doseo Basin. In contrast, the Doba Formation source rock contains Type II kerogen of lower quality and has a relatively low maturity, insufficient for commercial hydrocarbon generation and expulsion.

The majority of the basin's hydrocarbon reservoirs are found in the sandstones of the Kedeni Formation at depths ranging from 1500 to 3000 m (Dou et al., 2022b). However, the upper Mangara Group and the lower Doba Formation are also found to be good reservoirs (Zhang et al., 2024a). The porosity of the primary reservoir of the Lower Cretaceous is 0.16–11 % and the permeability is 81 to 2026 mD, indicating the reservoir is of medium porosity and medium-high permeability (Dou

Table 1
Petroleum system elements of the WCARS basins.

Basin	Main source rock	Age	Thick-ness	Reservoir	Cap rock	Kerogen type	Lithofacies	Maturity	TOC [%]	HI [mgHC/gTOC]
Bongor	Mimosa, Prosopis, Kubla fms.	Early Cretaceous	> 500 m	fractured basement	Prosopis, Mimosa fms.	I, subordinate II	lacustrine shales	early to mid oil window	0.3–16.8; avg. 3.5	50–900; avg. 350
Doseo	Mangara Gp., Doba, Kedeni fms.	Early Cretaceous	> 500 m	Kedeni Fm.	Doba Fm.	I, subordinate II	lacustrine shales	early to mid oil window	0.3–16.8; avg. 3.8	490–980, avg. 760
Muglad	Abu Gabra, Bentiu, Aradeiba, Zarqa, Amal, Ghazal, Nayil, Tendi fms.	Early Cretaceous	> 460 m	Bentiu, Aradeiba fms.	Darfur Fm.	I, subordinate II	lacustrine shales	mature to high mature	2.0–8.3; avg. 3.2	290–870, avg. 538
Melut	Al Renk, Melut fms.	Early Cretaceous	> 800 m	Galhak, Melut, Samma, Yabus fms.	Adar Fm.	II, subordinate I	lacustrine shales	early to mid oil window	2.0–8.3; avg. 3.2	270–580, avg. 430
Blue Nile	Antalo Fm.	Mid to Late Jurassic	> 600 m	Muger shales, Debre Libanos Fm.	Oligocene basalts	I, subordinate II	lacustrine limestone	immature to early oil window	3.4–6.4; avg. 4.8	490–670, avg. 575
Termit	Sokor, Yogou fms.	Eocene, Late Cretaceous	> 1000 m	Sokor-1, Upper Yogour fms.	Yogour, Sokor-2 fms.	mainly II to III	paralic shales, minor marine shales	early mature to main oil window	0.3–23.3; avg. 2.6	<50–822; avg. 192
Upper Benue Trough	Bima Fm.	Early Cretaceous	> 400 m	Bima Fm.	Gongila, Fika fms.	I	lacustrine shales	late to post mature	0.53–0.73; avg. 0.63	10–100; avg. 50
	Gongila Fm.	Late Cretaceous	>400 m	Gongila, Fika fms.	Gongila, Fika fms.	II, III	marine shales, estuarine shales	mid mature to gas window	0.74–1.53; avg. 1.14	43–188 avg. 53
	Fika Fm.	Late Cretaceous	>1500 m	Fika Fm.	Fika Fm.	II, III	marine shales, estuarine shales	early mature to mature	0.08–5.7; avg. 2.89	10–185 avg. 75
	Eze-Aku, Awgu gps.	Late Cretaceous		Eze-Aku, Awgu gps.	Eze-Aku, Awgu gps.	II, III	marine and estuarine shales, subordinate coal	immature to mid oil window	0.24–5.47, avg. 1.87	13–387, avg. 158
Lower Benue Trough	Nkporo Gp., Mamu Fm.	Late Cretaceous		Nkporo Gp., Mamu Fm.	Nkporo Gp., Mamu Fm.	III	estuarine to deltaic shales and coal	immature to early mature	mud: 0.3–2.35, avg. 1.4, coal: 61–77, avg. 69	shale: 55–186. avg. 130; coal: 203–266; avg. 239
	Akata, Agbada fms.	Paleogene	> 500 m	Akata, Agbada fms.	Akata, Agbada fms.	II/III	marine to paralic	early to late mature oil window	0.56–6.11, avg. 2	30–109; avg. 68

Abbreviations used: Fm. - Formation; fms. - formations; Gp. - Group; gps. - groups.

et al., 2022b).

Exploration within the Muglad Basin was started by Chevron in the 1970s, with commercial hydrocarbons discovered in the Unity, Heglig, Kaikang, Abu Gabra, Fula, and Sharaf fields, of which the Unity field (discovered in 1978) is the largest (Schull, 1988). Up to 0.6 billion barrels of recoverable oil have been found in the basin so far (Mohamed et al., 2001), with a daily production ranging from 60,000 to 320,000 barrels (Dou et al., 2013).

Crude oil has been discovered in the Abu Gabra, Bentiu, Aradeiba, Zarqa, Ghazal, Amal, Nayil, and Tendi formations (Dou et al., 2013). However, the Abu Gabra Formation is the most important effective source rock present and has been identified to contain good to excellent oil-prone source rocks (Types I and IIa) (Schull, 1988), with HI values ranging from 290 to 870 mg HC/g TOC and TOC values ranging from 2.0 to 8.3 % (average 3.22 %; Mohamed et al., 2000; Makeen et al., 2015a, 2015c). Kerogen from the Abu Gabra Formation exhibits a vitrinite reflectance of 0.59–0.72 % R_o and T_{max} values of 430–438 °C, indicative of maturities in the early to main oil window (Makeen et al., 2015c). The sandstones in the Bentiu and Aradeiba formations are the primary reservoir targets in the basin, while the rocks of the Darfur Group may form a regional cap rock.

Oil exploration in the Melut Basin began in the 1980s, when Chevron investigated the Adar oilfield in 1981. China National Petroleum Corporation has been operating in this basin since 2003. The Great Palogue Field, discovered in 2003, may contain around 900 million barrels of recoverable oil reserves (Dou et al., 2007). The primary source rocks of the basin are the mudrocks of the Al Renk and Melut formations (Fig. 9), which developed during the first and second rifting events, respectively (Dou et al., 2007; Shi et al., 2021). The Al Renk source rocks have an average TOC content of 2.08 % and reach maximum values of up to 3.24 %. The main kerogen composition is of Type II. The hydrocarbon generation potential (S1 + S2; with S1 characterising free hydrocarbons and S2 characterising hydrocarbons generated from pyrolysis) exhibits a maximum of 19.53 mg HC/g rock, with hydrogen indices ranging from 273 to 579 mg HC/g TOC (with an average of 428 mg HC/g TOC), identifying the Al Renk Formation source rocks as being of high quality (Dou et al., 2007; Mohamed et al., 2016). The Galhak, Melut, Samma, and Yabus formations are considered good reservoirs, with the Samma Formation exhibiting a higher connectivity of sand bodies, potentially forming the better reservoir (Mahgoub et al., 2016). Particularly, the sandstones of the Samma and Yabus formations exhibit average porosities of 30 % and average permeabilities of approximately 1000 mD (Tong et al., 2006). The Eocene Adar Formation with shales and mudstones is considered a regional seal or cap rock (Hakimi et al., 2021).

The Blue Nile Basin's most significant source rock potential is most likely associated with the Middle-Upper Jurassic (Oxfordian-Kimmeridgian) black shales of the Antalo Limestone Formation (Fig. 14), which is composed of marls, shallow marine to deep marine limestones, and intercalated shales (Mohammedyasin et al., 2019). The TOC content of the Antalo Limestone shales and limestones ranges from 3.43 to 6.43 % (average 4.85 %) (Mohammedyasin et al., 2020). According to the same authors, the Antalo Limestone shales have very good to excellent source rock potential, derived from Type I-II kerogen. The Cretaceous Muger Mudstone and Debre Libanos Sandstone generally serve as reservoirs, with the overlying Paleogene and Neogene volcanic rocks forming the seal. The Debre Libanos Sandstone exhibits a maximum porosity of 22.2 % and a permeability of 809.6 mD, with compaction and cementation reducing the primary porosity. Nevertheless, secondary porosity has been formed by the breakdown of unstable framework grains and carbonate cements (Wolela, 2012).

Oil exploration in the Termit Basin commenced in the 1950s with the discovery well Sokor 1 that penetrated the sandstone reservoir of the Paleogene Sokor-1 Formation. Further exploration identified reservoir horizons within sandstones of the Upper Cretaceous Yogou Formation. Both sandstone reservoirs are sealed by low-permeability shales intercalated within the Sokor-2 and Yogou formations (Genik, 1993; Harouna and Philp, 2012; Liu et al., 2015). The main source rock, generating about 90 % of the oils in the basin, is the brackish-marine to fully marine Yogou Formation of Santonian to Campanian age. The strata were deposited in a shallow-water regime under variable but predominantly anoxic conditions and contain preferentially a Type II kerogen (Liu et al., 2017b; Harouna and Philp, 2012). The TOC content of the Yogou Formation varies between 0.36 and 23.3 %, with an average of 2.6 % (Liu et al., 2015; Dou et al., 2024). The HI indices of the source rocks range from 30 to 822 mg HC/g TOC, with an average of 192 mg HC/g TOC. The remaining 10 % of oils in the Termit Basin derive from the Paleogene Sokor-1 Formation shales, which contain 0.3 to 20.3 % TOC, with an average of 2.54 %. The kerogens show HI values ranging between 5 and 562 but mostly remain between 100 and 350 mg HC/g TOC, with an average of 194 mg HC/g TOC (Harouna and Philp, 2012). The dominantly paraffinic oils of the Termit Basin show API (American Petroleum Institute) gravities ranging between 30 and 40°, with a few exceptions at 21 to 23° (Liu et al., 2017b).

In the Benue Trough (Fig. 3), the Upper and Lower Benue Trough segments have been the focus of most exploration efforts in the past 80–90 years. The Paleogene strata in the Lower Benue Trough (Niger Delta Basin) are the most prospective, with oil and gas reserves hovering around 34 billion barrels and 93 TCF (trillion cubic feet), respectively (Tuttle et al., 1999). The first conventional well drilled in the trough in 1951 tested Cretaceous strata in the Lower Benue Trough. There are at least four petroleum systems spanning the Early Cretaceous to Paleogene. The first is an Early Cretaceous syn-rift petroleum system identified so far only in the Upper Benue Trough and Bornu Basin. It consists of a potential lacustrine (Type I) source associated with the Bima Formation (Abubakar, 2019), with present-day TOC varying from 0.53 to 0.73 %, and alluvial to fluvio-deltaic strata (Bima Formation) as potential reservoir units. This petroleum system is hypothesised to exist below the Asu River Group in deep depocenters in the Lower and Middle Benue Trough segments. 3D seismic lines (Suleiman et al., 2019) show tilted fault blocks sealed by Cenomanian to Turonian transgressive marine mudrocks of the Gongila and Fika formations. It is noteworthy that the inversion and magmatism associated with the Campanian-Maastrichtian compression overcooked the source rocks in certain areas, inverted the fault blocks (potentially breaching the traps) and created new anticlinal traps (Suleiman et al., 2019). This petroleum system is not yet proven to work in the Benue Trough and Bornu Basin. However, in the adjoining Benin Basin, it is hypothesised to have sourced a fraction of the oil in the tar sand belt (MMSD (Ministry of Mines and Solid Minerals Development), 2006). The Early to mid-Cretaceous petroleum system is a working system (Coker and Ejedawe, 1987; Bata et al., 2015). It consists of Albian to Turonian marine (pre-maturity Type II) mudstone source rocks (Table 1) of the Eze-Aku and Awgu groups (Lower Benue Trough) and Gongila and Fika formations (Upper Benue Trough), which also function as seals with Albian to Turonian sands and limestones as potential reservoirs. It is also noteworthy that humic coals with up to 72 wt % and Type III are present within Coniacian strata (Awgu Group and Fika Formation), implying some gas-prone potential (Jauro et al., 2007; Sarki Yandoka et al., 2015). Traps are stratigraphic and inversion-related anticlines and faults. The Bima oil sands discovered in the Bornu Basin (Bata et al., 2015) suggest possible downward migration of petroleum, charging the syn-rift strata. Depositional controls on reservoir presence exacerbated by the severity of sediment exhumation resulting from the Campanian-Maastrichtian compression is a key risk limiting the thicknesses of the source, reservoir and seal strata as well as the thermal maturity of the source rocks. In addition, other risk factors related to the Santonian-Maastrichtian compression are the Pb-Zn-Cu-F-Ba mineralisations (see Section 5.6), and Cenozoic magmatic episodes, which need to be fully constrained. These may affect trap integrity evinced by the occurrence of bituminous sands in the Benue Trough and adjoining Benin Basin. Furthermore, the quality of source and reservoir units around magmatic and mineralised bodies are key risk factors that need to be assessed. This is critical, as available burial history models in

the Upper Benue Trough show a post-Santonian critical moment for petroleum generation (Dim et al., 2018; Suleiman et al., 2019). Notwithstanding the aforementioned, it is important to note that in the Lower Benue Trough, the Ihandiagu-1 and Amansiodo-1 wells encountered gas in Turonian reservoirs (Avbovbo and Ayoola, 1981). These gas discoveries underscore the need for more exploration campaigns in order to unlock the hydrocarbon potential of the Albian-Turonian petroleum system.

The Late Cretaceous petroleum system (Table 1), which consists of marine to estuarine mudrocks, coal source rocks, and pelitic seal strata (Fika Formation, Nkporo Group and Mamu Formation) with predominantly gas-prone Type III kerogen, contains commercial and subcommercial petroleum deposits (Nwajide, 2013). Of note is the Anambra River field, which is currently exploited by Orient Petroleum (DPR, pers. comm., 2018) in the Lower Benue Trough (Anambra Basin). The reservoirs are Campanian-Maastrichtian sands facies of the Nkporo Group and Mamu Formation, trapped within growth faults and roll-over anticlinal structures (Nwajide, 2013; Dim et al., 2018).

The Lower Benue Trough (Niger Delta Basin) contains the greatest thickness of Paleogene and Neogene strata, which is up to 12 km (Short and Stauble, 1967). The petroleum system in this basin consists of active marine and paralic source rocks of the Paleogene Akata and Agbada formations (Table 1) with fair to good TOC and Type II/Type III kerogen (Ekweozor et al., 1979; Udo and Ekweozor, 1988; Bustin, 1988; Doust and Omatsola, 1990). The reservoirs are Eocene to Miocene sands and gravels of the Akata and Agbada formations trapped in a plethora of structural traps formed by gravity spreading, stratigraphic traps or a combination thereof (Short and Stauble, 1967; Evamy et al., 1978; Doust and Omatsola, 1990; Chima et al., 2019).

5.7. Pb-Zn-Cu-F-Ba mineralisation

Information on economic mineralisation within the WCARS basins is particularly known from the Benue Trough of Nigeria. Pb-Zn-Cu-F-Ba deposits occur in several mining districts across the Benue Trough. The deposits are characteristically epigenetic, strata-bound, and hosted in carbonaceous mudrocks, carbonates, sandstones, and magmatic rocks (Oha et al., 2017), varying in age from the Aptian to the early Turonian. Mineralisation occurred in three phases, from low to moderate temperature (up to 238 °C) hydrothermal fluids (Akande and Mücke, 1993; Ogundipe, 2017), originating from circulating connate brines present within syn-rift pre-mid-Albian feldspathic alluvial-fluvial sandstones (Olade and Morton, 1985; Maurin and Benkhelil, 1990). The deposits are commonly structurally controlled, especially on faulted broad anticlines with great sediment thickness (Maurin and Benkhelil, 1990). Mineralised fracture trends are typically NW-SE (predominant) and N-S, which are oblique to the regional NE-SW fracture trend of the Benue Trough (Maurin and Benkhelil, 1990; Oha et al., 2017). Dimensions of the mineralised lodes vary, with the largest so far discovered being the Enyigba lode in the southern Benue Trough, extending up to 2000 m with a width of 20 m (Olade and Morton, 1985). Mineralogically, the deposits consist primarily of galena and sphalerite, with minute amounts of chalcopyrite, pyrite, siderite, enargite, quartz, marcasite, tetrahedrite, calcite, fluorite, and barite (Ezepue, 1984; Maurin and Benkhelil, 1990). In the Upper Benue Trough, a significant amount of silver has been extracted from some mining districts (Olade and Morton, 1985). It is noteworthy that the composition of the ore varies from the Lower Benue Trough to the Upper Benue Trough, which may be due to the nature of the host rocks (Akande et al., 1989). Within the Lower Benue Trough, the Pb-Zn concentrations vary within mining districts along a southwest-northeast transect, which also shows an increase in barite from 0 % to almost 100 % (Oha et al., 2017). In the Central Benue Trough, barite and fluorite are the dominant minerals, whereas in the Upper Benue Trough, Pb-Zn-Ba mineralisation persists (Bute et al., 2024).

5.8. Geothermal energy potential

Despite the lack of studies on the WCARS, while the East African Rift System is better known for its geothermal prospects, with an estimated potential of over 20,000 Megawatt electrical (MWe) (Jones, 2020) and approximately 630 MWe of power produced annually (primarily by Kenya and Ethiopia) (Elbarbary et al., 2022a), it is reasonable to assume that the WCARS also has significant potential for geothermal energy development. A first GIS study on the geothermal energy potential of the African continent showed low to moderate potential for the WCARS basins (Elbarbary et al., 2022a). However, considering the scarcity of research wells or available heat flow data from these regions, more studies are needed for a more conclusive answer. Nevertheless, in Nigeria, the Benue Trough shows heat flow values of >90 mW/m^2 and geothermal gradients up to 4.3 °C/100 m (Kwaya et al., 2016; Dopamu et al., 2021; Ijeh et al., 2024). Similar values could also be measured in the CARS basins (Elbarbary et al., 2022b); for instance, in the Melut Basin, where geothermal gradients up to 4.4 °C/100 m and heat flow values of 59 mW/m^2 were recorded (Mohamed et al., 2016). With more data available and applying the thermofacies concept introduced by Sass and Götz (2012) to characterize the geothermal reservoir potential of sedimentary basins, the geothermal potential of these basins may be far greater than previously thought, and the basins could become a viable source of renewable energy for the continent. With the right investments and policies, the region could therefore use its vast renewable energy potential to drive economic growth and enhance energy access for its population.

6. Quo vadis: the way forward

Despite the extent of this article, it is clear that the information provided is far from being complete. The remoteness and political instability of some of the addressed areas made a detailed investigation challenging, if not impossible, in the past and will probably continue to do so in the foreseeable future. One more issue is the apparent lack of surface exposures in several basins, and it is only due to exploration drilling programs from state-owned, American, or Chinese oil companies that limited information from a few boreholes is available to the public. However, very often, too little information is available to establish a coherent stratigraphy or basin-wide correlations. As a result, some of the basins, such as the Anza or Gao basins, still lack general stratigraphy and subdivision into formations. From other WCARS basins, such as the Jonglei or Kafra basins, for instance, virtually no information is available. In consequence, as a first step, additional geophysical analysis could be done on the individual basins in order to establish their exact extent and sedimentary thickness and provide valuable information about the underlying lithospheric structure. A lot of these analyses can be carried out through remote sensing and the use of freely available satellite data, for instance, gravity data, etc. However, these analyses need to be enhanced with multistratigraphic analyses of drill cores and outcrops to establish robust litho- and chronostratigraphic correlation schemes of the basins, which will require the collaboration of academic institutions and industry in the specific countries, a measure that will help both the training of young geologists as well as help to find valuable resources in these basins. Our knowledge of the WCARS could also be enhanced if companies mining ore deposits and industrial rocks grant researchers access to cores, logs, and regional data. In addition, palaeoenvironmental and, particularly, palaeoclimate research in these basins, including integrated sedimentological-geochemical-palynological studies, will undoubtedly yield a wealth of new information to the international scientific community, considering the various oceanic anoxic events that may be recorded by the sedimentary strata of the WCARS basins.

Declaration of competing interest

The authors declare that they have no known competing financial interests or personal relationships that could have appeared to influence the work reported in this paper.

Acknowledgements

This paper emerged after a discussion with Timothy Horscroft and Asfawossen Asrat, who encouraged us to put our ideas into action. In addition, we thank Istvan Csato, John Hancox, and an anonymous reviewer for their very helpful and constructive comments.

Data availability

No data was used for the research described in the article.

References

Abdalla, Y.M., Michael, J.P., William, A.A., 2001. Petroleum maturation modelling, Abu Gabra Sharaf area, Muglad Basin, Sudan. J. Afr. Earth Sci. 35, 331–344.
Abdelhakam, E.M., Ali, S.M., 2008. Stratigraphy and tectonic evolution of the oil producing horizons of Muglad Basin, Sudan. J. Sci. Technol. 9, 1–9.
Abubakar, M.B., 2019. A re-think on the stratigraphy of the Nigerian Chad (Bornu) Basin and its implications on petroleum potential. In: NAPE 2-day Special Workshop on Cretaceous Basins in Nigeria. Extended Abstract, 18-21 (Abuja, May 6-7, 2019). https://nape.org.ng/wp-content/uploads/2019/10/Chad-Basin_Cret.-Wksp-NAPE_MB-Abubakar.pdf.
Abubakar, M.B., Dike, E.F.C., Obaje, N.G., Wehner, H., Jauro, A., 2008. Petroleum prospectivity of Cretaceous formations in the Gongola Basin, Upper Benue Trough, Nigeria: an organic geochemical perspective on a migrated oil controversy. J. Pet. Geol. 31, 387–408.
Abubakar, U., Usman, M.B., Aliyuda, K., Dalha, A., Bello, A.M., Linus, L.N., 2021. Major and trace element geochemistry of the shales of Sekuliye Formation, Yola Sub-Basin, Northern Benue Trough, Nigeria: implications for provenance, weathering intensity, and tectonic setting. J. Sediment. Environ. 6, 473–484.
Abubakar, U., Hohl, S.V., Usman, M.B., Maigari, A.S., Tchouatcha, M.S., Tabale, R.P., Bello, A.M., Dalha, A., Mukkafa, S., 2024. Provenance history, depositional conditions and tectonic settings during late Cenomanian–early Turonian time in the Gongola Sub-Basin of the Upper Benue Trough Nigeria: evidence from major and trace elements geochemistry of the Kanawa shales from the Pindiga Formation. J. Afr. Earth Sci. 211, 105168.
Adams, A., 2022. Insights into the source of Magmatic Hot-Lines: forty years of Geophysical Studies of the Cameroon Volcanic Line. Front. Earth Sci. 10, 838993. https://doi.org/10.3389/feart.2022.838993.
Adedosu, T.A., Sonibare, O.O., Tuo, J., Ekundayo, O., 2012. Biomarkers, carbon isotopic composition and source rock potentials of Awgu coals, middle Benue trough, Nigeria. J. Afr. Earth Sci. 66, 13–21.
Adeleye, D.R., 1975. Nigerian Late Cretaceous stratigraphy and palaeogeography. Am. Assoc. Pet. Geol. Bull. 59, 2302–2313.
Agumanu, A.E., 1989. The Abakaliki and the Ebonyi Formations: sub-divisions of the Albian Asu River Group in the southern Benue trough, Nigeria. J. Afr. Earth Sci. 9, 195–207.
Ahmed, Y., Konaté, M., Harouna, M., 2016. Tectono-magmatic reactivation of Téfidet Cretaceous trough during Cenozoic (Aïr, Niger). Bull. Soc. Géol. Fr. 187, 73–82.
Ahmed, K.S., Liu, K., Fan, Y., Kra, K.L., Harouna, M., Liu, J., Ntibahanana, M., Salim, M. Z., Pidho, J.J., Kouame, M.E., Moussa, H.A., Ahmed, H.A., 2022. Pyrite Dissolution in the Cretaceous Yogou Formation of the Niger (Chad) Basin: Implications for Basin Evolution under a Rift Tectonic Setting. ACS Omega 7, 43411–43420. https://doi.org/10.1021/acsomega.2c03027.
Akande, S.O., Mücke, A., 1993. Coexisting copper sulphides and sulphosalts in the Abakaliki Pb-Zn deposit, lower Benue Trough (Nigeria) and their genetic significance. Mineral. Petrol. 47, 183–192.
Akande, O., Zentelli, M., Reynolds, P., 1989. Fluid inclusion and stable isotope studies of Pb-Zn-fluorite-barite mineralization in the lower and middle Benue Trough, Nigeria. Mineral. Deposita 24, 183–191.
Akande, S.O., Lewan, M.D., Egenhoff, S., Adekeye, O.A., Ojo, O.J., Peterhansel, A., 2015. Source rock potential of lignite and interbedded coaly shale of the Ogwashi-Asaba Formation, Anambra basin as determined by sequential hydrous pyrolysis. Int. J. Coal Geol. 150-151, 224–237. https://doi.org/10.1016/j.coal.2015.09.005.
Akpan, O., Nyblade, A., Okereke, C., Oden, M., Emry, E., Julia, J., 2016. Crustal structure of Nigeria and Southern Ghana, West Africa from P-wave receiver functions. Tectonophysics 676, 250–260.
Alalade, B., 2016. Depositional environments of Late Cretaceous Gongila and Fika formations, Chad (Bornu) Basin, Northeast Nigeria. Mar. Pet. Geol. 75, 100–116.
Allen, P.A., Allen, J.R., 2013. Basin Analysis: Principles and Application to Petroleum Play Assessment, Third edition. Wiley-Blackwell, p. 632.
Allix, P., Popoff, M., 1983. Le Crétacé inférieur de la partie nord-orientale du fossé de la Bénoué (Nigeria); un exemple de relation étroite entre tectonique et sédimentation. Bull. Cent. Rech. Explor. Prod. Elf. Aquit. 7, 349–359.
Alvarez, W., 2023. An enormous Pliocene or Quaternary Megalake Sudd on the River Nile in the Sudan Basin? A review of the dilemma, and a possible solution. J. Afr. Earth Sci. 208, 105016.
Amajor, L.C., 1987. Major and trace element geochemistry of Albian and Turonian shales from the Southern Benue trough, Nigeria. J. Afr. Earth Sci. 6, 633–641.
Avbovbo, A.A., Ayoola, E.O., 1981. Petroleum prospects of southern Nigeria's Anambra Basin. Oil Gas J. 79, 334–347.
Avbovbo, A.A., Ayoola, E.O., Osahon, G.A., 1986. Depositional and structural styles in Chad Basin of Northeastern Nigeria. Am. Assoc. Pet. Geol. Bull. 70, 1787–1798.
Awad, H.M., 2015. Sedimentology and Sequence Stratigraphy of the Paleogene Samma, Yabus and Adar Formations in Rawat Basin, White Nile State, Sudan. MSc thesis. King Fahd University of Petroleum and Minerals, 231 p. https://eprints.kfupm.edu.sa/id/eprint/139920/.
Babai, A.M.A., Gebbayin, O.I.M.F.A., Ehinola, O.A., Ibrahim, M.A.E., 2024. Source rock characterization and biomarkers analysis of Adar and Galhak Formations, Rawat central sub-basin, White Nile basin, Sudan. J. Afr. Earth Sci. 210, 105146.
Babkir, M.D.B.H., Nton, M.E., Eisawi, A.A.M., 2023. Depositional environment and hydrocarbon exploration potential based on sedimentary facies and architectural analysis of the Upper Cretaceous Shendi Formation in Musawwarat-Naga area, Shendi-Atbara Basin, Sudan. Earth Sci. Res. J. 27, 109–128.
Bachari, M., Belkhiria, W., Negra, M.H., Grosheny, D., Soltani, A., 2024. Tectonic controls on Late Cretaceous sedimentation on the southern Tethyan passive margin, Tunisia: new evidence of structural segmentation and early basin inversion. Int. Geol. Rev. 66, 1501–1518. https://doi.org/10.1080/00206814.2023.2243498.
Baranov, A., Tenzer, R., Ghomsi, F.E.K., 2023. A new Moho map of the African continent from seismic, topographic, and tectonic data. Gondwana Res. 124, 218–245.
Barry, A.A., Caesar, J., Klein Tank, A.M.G., Aguilar, E., McSweeney, C., Cyrille, A.M., Nikiema, M.P., Narcisse, K.B., Sima, F., Stafford, G., Touray, L.M., Ayilari-Naa, J.A., Mendes, C.L., Tounkara, M., Gar-Glahn, E.V.S., Coulibaly, M.S., Dieh, M.F., Mouhaimouni, M., Oyegade, J.A., Sambou, E., Laogbessi, E.T., 2018. West Africa climate extremes and climate change indices. Int. J. Climatol. 38, e921–e938. https://doi.org/10.1002/joc.5420.
Bata, T., Parnell, J., Samaila, N.K., Abubakar, M.B., Maigari, A.S., 2015. Geochemical evidence for a Cretaceous oil sand (Bima oil sand) in the Chad Basin, Nigeria. J. Afr. Earth Sci. 111, 148–155.
Baudin, P., 1991. Le magmatisme mesozoique a cenozoique du fosse de la Benoue (Nigeria). Geochronologie, petrogenese, cadre geodynamique. PhD Thesis. Universite Aix—Marseille III.
Beccaluva, L., Bianchini, G., Natali, C., Siena, F., 2020. Plume-related Paranà-Etendeka igneous province: An evolution from plateau to continental rifting and breakup. Lithos 362-363, 105484.
Beil, S., Kuhnt, W., Holbourn, A., Scholz, F., Oxman, J., Wallmann, K., Lorenzen, J., Aquit, M., Chellai, E.H., 2020. Cretaceous oceanic anoxic events prolonged by phosphorus cycle feedbacks. Clim. Past 16, 757–782. https://doi.org/10.5194/cp-16-757-2020.
Ben Fadhel, M., Layeb, M., Hedfi, A., Ben Youssef, M., 2011. Albian oceanic anoxic events in northern Tunisia: Biostratigraphic and geochemical insights. Cretac. Res. 32, 685–699.
Benadla, M., Reolid, M., Marok, A., El Kamali, N., 2018. The Cenomanian–Turonian transition in the carbonate platform facies of the Western Saharan Atlas (Rhoundjaïa Formation, Algeria). J. Iber. Geol. 44, 405–429. https://doi.org/10.1007/s41513-018-0070-6.
Benkhelil, J., 1982. Benue Trough and Benue Chain. Geol. Mag. 119, 155–168. https://doi.org/10.1017/S001675680002584X.
Benkhelil, J., 1989. The origin and evolution of the Cretaceous Benue Trough (Nigeria). J. Afr. Earth Sci. 8, 251–282.
Benoit, M.H., Nyblade, A.A., Pasyanos, M.E., 2006. Crustal thinning between the Ethiopian and East African plateaus from modeling Rayleigh wave dispersion. Geophys. Res. Lett. 33, L13301. https://doi.org/10.1029/2006GL025687.
Bezerra, F.H.R., Ferreira, J.M., Sousa, M.O.M., 2006. Review of seismicity and neogene tectonics in northeastern Brazil. Rev. Asoc. Geol. Argent. 61, 525–535. Retrieved from. https://revista.geologica.org.ar/raga/article/view/1329.
Binks, R.M., Fairhead, J.D., 2019. A plate tectonic setting for Mesozoic rifts of West and Central Africa. Tectonophysics 213, 141–151.
Bolarinwa, A.T., Idakwo, S.O., Bish, D.L., 2021. Source area-weathering, provenance and tectonic setting of the Campanian-Maastrichtian clay sequences in the lower Benue Trough of Nigeria. J. Afr. Earth Sci. 173, 104050.
Bolarinwa, A.T., Faloye, O., Idakwo, S.O., 2022. Geochemical studies of shales from the Asu River Group, lower Benue Trough: Implications for provenance and paleo-environment reconstruction. Solid Earth Sci. 7, 5–18.
Bosence, D.W.J., 1998. Stratigraphic and sedimentological models of rift basins. In: Purser, B.H., Bosence, D.W.J. (Eds.), Sedimentation and Tectonics of Rift Basins, Red Sea – Gulf of Aden. Chapman & Hall, London, pp. 9–25.
Bosworth, W., 1992. Mesozoic and early Tertiary rift tectonics in East Africa. Tectonophysics 209, 115–137.
Bosworth, W., Morley, C.K., 1994. Structural and stratigraphic evolution of the Anza rift, Kenya. Tectonophysics 236, 93–115.
Boucot, A.J., Xu, C., Scotese, C.R., Morley, R.J., 2013. Phanerozoic paleoclimate: an atlas of lithologic indicators of climate. In: SEPM Concepts in Sedimentology and Paleontology 11, Tulsa, OK. https://doi.org/10.2110/sepmcsp.11.
Bouin, M., Soussi, M., Saidi, M., Riahi, S., Boukhalfa, K., Ismail, E., Day, Z., Robert, E., 2024. The early Aptian Oceanic Anoxic event (OAE-1a) of the uppermost M'Cherga formation of northern Tunisia: Geochemical characterization and inferred petroleum potential. J. Afr. Earth Sci. 213, 105238.
Boutaleb, K., Baouche, R., Sadaoui, M., Radwan, A.E., 2022. Sedimentological, petrophysical, and geochemical controls on deep marine unconventional tight

limestone and dolostone reservoir: Insights from the Cenomanian/Turonian oceanic anoxic event 2 organic-rich sediments, Southeast Constantine Basin, Algeria. Sediment. Geol. 429, 106072.
Brownfield, M.E., Charpentier, R.R., 2006. Geology and total petroleum systems of the Gulf of Guinea province of West Africa. U.S. Geol. Surv. Bull. 2207-C, 1–32. https://doi.org/10.3133/b2207C.
Buck, W.R., 1991. Modes of continental lithospheric extension. J. Geophys. Res. 96, 163–168.
Bumby, A.J., Guiraud, R., 2005. The geodynamic setting of the Phanerozoic basins of Africa. J. Afr. Earth Sci. 43, 1–12.
Bunter, M.A.G., Debretsion, T., Woldegiorgis, L., 1998. New developments in the pre-rift prospectivity of the Eritrean Red Sea. J. Pet. Geol. 21, 374–400. https://doi.org/10.1111/j.1747-5457.1998.tb00792.x.
Burke, K.C., Whiteman, A.J., 1973. Uplift, rifting and the break-up of Africa. In: Tarling, D.H., Runcorn, S.K. (Eds.), Implications on Continental Drift to Earth Sciences. Academic Press, London, pp. 735–755.
Burke, K., MacGregor, D.S., Cameron, N.R., 2003. Africa's petroleum systems: Four tectonic 'Aces' in the past 600 million years. In: Arthur, T.J., MacGregor, D.S., Cameron, N.R. (Eds.), Petroleum Geology of Africa: New Themes and Developing Technologies, Geol. Soc. Lond. Spec. Publ, vol. 207, pp. 21–60. https://doi.org/10.1144/GSL.SP.2003.207.3.
Bussert, R., Eisawi, A.A.M., Hamed, B., Babikir, I.A.A., 2018. Neogene palaeochannel deposits in Sudan – Remnants of a trans-Saharan river system? J. Afr. Earth Sci. 151, 9–21.
Bustin, R.M., 1988. Sedimentology and characteristics of dispersed organic matter in Tertiary Niger Delta: origin of source rocks in a deltaic environment. Am. Assoc. Pet. Geol. Bull. 72, 277–298. https://doi.org/10.1306/703C8C18-1707-11D7-8645000102C1865D.
Bute, S.I., Zhou, J., Luo, K., Girei, M.B., Peter, R.T., 2024. Pb-Zn-Ba deposits in the Nigerian Benue Trough: a synthesis on deposits classification and genetic model. Ore Geol. Rev. 166, 1–19.
Carter, J.D., Barber, W.D.F., Tait, E.A., 1963. The geology of parts of Adamawa, Bauchi and Bornu provinces in north-eastern Nigeria. Geol. Surv. Nigeria Bull. 30.
Catuneanu, O., 2022. Principles of Sequence Stratigraphy, Second edition. Elsevier, Amsterdam, p. 494.
Catuneanu, O., 2024. Sequence stratigraphy of rift basins. In: Chiarella, D., Scarselli, N., Adam, J. (Eds.), Regional Geology and Tectonics, Phanerozoic Rift Systems and Sedimentary Basins, Second edition, vol. 2. Elsevier, pp. 147–162.
Catuneanu, O., Eriksson, P.G., 2002. Sequence stratigraphy of the Precambrian Rooihoogte - Timeball Hill rift succession, Transvaal Basin, South Africa. Sediment. Geol. 147, 71–88.
Catuneanu, O., Martins-Neto, M.A., Eriksson, P.G., 2012. Sequence stratigraphic framework and application to the Precambrian. Mar. Pet. Geol. 33, 26–33.
Chavom, B.M., Baudin, F., Kwéa Nzouedjio, J.F., Schnyder, J., Maloum, A., Biouélé, S.E. A., 2022. Neocomian – Barremian lacustrine shales in the Mayo Oulo-Lere Basin, North Cameroon: Depositional environment and petroleum potential. J. Pet. Geol. 45, 201–218.
Chen, L., Ji, H., Dou, L., Du, Y., Xu, Z., Zhang, L., Yang, X., Fu, S., 2018. The characteristics of source rock and hydrocarbon charging time of Precambrian granite reservoirs in the Bongor Basin. Chad. Mar. Pet. Geol. 97, 323–338.
Chima, K.I., Do Couto, D., Leroux, E., Gardin, S., Hoggmascall, N., Rabineau, M., Gorini, C., 2019. Seismic stratigraphy and depositional architecture of Neogene intraslope basins, offshore western Niger Delta. Mar. Pet. Geol. 109, 449–468.
Chorowicz, J., 2005. The East African rift system. J. Afr. Earth Sci. 43, 379–410.
Chukwu, M., Folayan, C.O., Pam, G.Y., Obada, D.O., 2016. Characterization of some Nigerian Coal for Power Generation. J. Comb. 2016, 9728278. https://doi.org/10.1155/2016/97282781-12.
Chumakov, N.M., Zharkov, M.A., Herman, A.B., Doludenko, M.P., Kalandadze, N.N., Lebedev, E.L., Ponomarenko, A.G., Rautian, A.S., 1995. Climatic belts of the Mid-Cretaceous time. Stratigr. Geol. Correl. 3, 42–63.
Cohen, H.A., McClay, K., 1996. Sedimentation and shale tectonics of the northwestern Niger Delta Front. Mar. Pet. Geol. 13, 313–328.
Coker, S.J.L., Ejedawe, J.E., 1987. Petroleum prospects of the Benin Basin. Niger. J. Min. Geol. 23, 27–43.
dePolo, C.M., Anderson, J.G., 2000. Estimating the slip rates of normal faults in the Great Basin, USA. Basin Res. 12, 227–240.
Déruelle, B., Moreau, C., Nkoumbou, C., Kambou, R., Lissom, J., Njonfang, E., Ghogomu, R.T., Nono, A., 1991. The Cameroon Line: a review. In: Kampunzu, A.B., Lubala, R.T. (Eds.), Magmatism in Extensional Structural Settings. Springer, Berlin, Heidelberg. https://doi.org/10.1007/978-3-642-73966-8_12, pp. 274-27.
Déruelle, B., Ngounouno, I., Demaiffe, D., 2007. The 'Cameroon Hot Line' (CHL): a unique example of active alkaline intraplate structure in both oceanic and continental lithospheres. Compt. Rendus Geosci. 339, 589–600. https://doi.org/10.1016/j.crte.2007.07.007.
Dim, C.I.P., Onuoha, K.M., Anyiam, O.A., Okwara, I.C., Oha, I.A., Okonkwo, I.A., Ozumba, B.M., 2018. Analysis of petroleum system for exploration and risk reduction in the South-eastern Inland Basins of Nigeria. Pet. Coal. 60, 305–320.
Dopamu, K.O., Akoshile, C.O., Nwankwo, L.I., 2021. Regional estimation of geothermal resources of the entire Benue Trough, Nigeria using high-resolution aeromagnetic data. Geomech. Geophys. Geo-Energy Geo-Resour. 7, 78. https://doi.org/10.1007/s40948-021-00276-z.
Dou, L., 2005. Formation mechanism and model of oil and gas accumulations in the Melut Basin, Sudan. Bull. Mineral. Petrol. Geochem. 24, 50–57 (in Chinese with English abstract).
Dou, L., Xiao, K., Cheng, D., Shi, B., Li, Z., 2007. Petroleum geology of the Melut Basin and the Great Palogue Field, Sudan. Mar. Pet. Geol. 24, 129–144.
Dou, L., Cheng, D., Li, M., Xiao, K., Shi, B., Li, Z., 2008. Unusual high acidity oils from the Great Palogue Field, Melut Basin, Sudan. Org. Geochem. 39, 210–231.
Dou, L.R., Xiao, K.Y., Hu, Y., Song, H.R., Cheng, D.S., Du, Y.B., 2011. Petroleum geology and a model of hydrocarbon accumulations in the Bongor Basin, the Republic of Chad. Acta Pet. Sin. 32, 379–386 (in Chinese with English abstract).
Dou, L., Cheng, D., Li, Z., Zhang, Z., Wang, J., 2013. Petroleum geology of the Fula sub-basin, Muglad Basin, Sudan. J. Pet. Geol. 36, 43–60.
Dou, L.R., Wei, X.D., Wang, J.C., Li, J.L., Wang, R.C., Zhang, S.H., 2015. Characteristics of granitic basement rock buried-hill reservoir in Bongor Basin, Chad. Acta Pet. Sin. 36, 897–904 (in Chinese with English abstract).
Dou, L., Xiao, K., Wang, J., 2018. Petroleum Geology and Exploration Practice of Strongly-Inverted Rift Basin. Petroleum Industry Press, Beijing, p. 325p.
Dou, L., Cheng, D., Wang, J., Du, Y., Xiao, G., Wang, R., 2020a. Petroleum systems of the Bongor Basin and the Great Baobab Oilfield, southern Chad. J. Pet. Geol. 43, 301–322.
Dou, L., Li, W., Cheng, D., 2020b. Hydrocarbon accumulation period and process in Baobab area of Bongor Basin. J. Afr. Earth Sci. 161, 103673.
Dou, L., Wang, R., Wang, J., Cheng, D., Green, P.F., Wei, X., 2021. Thermal history reconstruction from apatite fission-track analysis and vitrinite reflectance data of the Bongor Basin, the Republic of Chad. Am. Assoc. Pet. Geol. Bull. 105, 919–944. https://doi.org/10.1306/11182019167.
Dou, L., Bai, G., Liu, B., Zhai, G., Zhang, X., Zhang, Y., Yan, G., Chen, G., 2022a. Sedimentary environment of the Upper Cretaceous Yogou Formation in Termit Basin and its significance for high-quality source rocks and Trans-Saharan Seaway. Mar. Pet. Geol. 142, 105732.
Dou, L., Xiao, K., Du, Y., Wang, L., Zhang, X., 2022b. Exploration discovery and hydrocarbon accumulation characteristics of the Doseo strike-slip and inverted basin. Chad. Pet. Explor. Dev. 49, 247–256.
Dou, L., Zhang, X., Xiao, K., Xi, D., Du, Y., Wang, L., Hu, J., Hu, Y., Zheng, Q., 2023a. Early Cretaceous (Aptian to Albian) vegetation and climate change in Central Africa: Novel palynological evidence from the Doseo Basin. Geol. J. 59, 441–467.
Dou, L., Xiao, K., Wang, J., 2023b. Petroleum Geology and Exploration of the Bongor Basin. Springer, Singapore, 486p.
Dou, L., Shi, Z., Pang, W., Ma, F., 2024. Petroleum geological characteristics and exploration targets of the oil-rich sags in the Central and West African Rift System. Pet. Explor. Dev. 51, 1–14.
Doust, H., Omatsola, E., 1990. Niger Delta. In: Edwards, J.D., Santogrossi, P.A. (Eds.), Divergent/Passive Margins, Amer. Assoc. Petrol. Geol. Mem, vol. 48, pp. 201–338.
Eagles, G., 2007. New angles on South Atlantic opening. Geophys. J. Int. 168, 353–361.
Edegbai, A.J., Schwark, L., 2020. Differentiation of Sediment Source Regions in the Southern Benue Trough and Anambra Basin, Nigeria: Insights from Geochemistry of Upper Cretaceous Strata. Geol. Earth Marine Sci. 2, 1–37. https://doi.org/10.31038/GEMS.2020224.
Edegbai, A.J., Schwark, L., Oboh-Ikuenobe, F.E., 2019. A review of the latest Cenomanian to Maastrichtian geological evolution of Nigeria and its stratigraphic and paleogeographic implications. J. Afr. Earth Sci. 150, 823–837.
Eisawi, A.A.M., Babikir, I.A.A., Ali, O.E., Khalil, M.A., Adam, A.E., Bussert, R., 2015. Atbara Basin. In: Awad, M.Z. (Ed.), Petroleum Geology and Resources of the Sudan. Geozon Science Media, Berlin, Germany, pp. 309–319.
Ekweozor, C.M., Okogun, J.I., Ekong, D.E.U., Maxwell, J.R., 1979. Preliminary organic geochemical studies of samples from the Niger delta (Nigeria) I. Analyses of crude oils for triterpanes. Chem. Geol. 27, 11–28.
El Hassan, W.M., El Nadi, A.-H.H., 2015. Impact of inversion tectonics on hydrocarbon entrapment in the Baggara Basin, western Sudan. Mar. Pet. Geol. 68, 492–497.
El Hassan, W.M., Farwa, A.G., Awad, M.Z., 2017. Inversion tectonics in Central Africa Rift System: evidence from the Heglig Field. Mar. Pet. Geol. 80, 293–306.
El Tahir, N., Nyblade, A., Julià, Durrheim R., 2013. Crustal structure of the Khartoum Basin, Sudan. Tectonophysics 593, 151–160.
Elbarbary, S., Zaher, M.A., Saibi, H., Fowler, A.-R., Saibi, K., 2022a. Geothermal renewable energy prospects of the African continent using GIS. Geotherm. Energy 10, 8. https://doi.org/10.1186/s40517-022-00219-1.
Elbarbary, S., Zaher, M.A., Saibi, H., Fowler, A.-R., Ravat, D., Marzouk, H., 2022b. Thermal structure of the African continent based on magnetic data: Future geothermal renewable energy explorations in Africa. Renew. Sust. Energ. Rev. 158, 112088.
El-Sabbagh, A., Tantawy, A.A., Keller, G., Khozyem, H., Spangenberg, J., Adatte, T., Gertsch, B., 2011. Stratigraphy of the Cenomanian-Turonian Oceanic Anoxic Event OAE2 in shallow shelf sequences of NE Egypt. Cretac. Res. 32, 705–722.
Etim, O., Louis, P., Maurin, J., 1988. Interpretation of electrical soundings on the Abakaliki lead-zinc and brine prospects, SE Nigeria: geological and genetic implications. J. Afr. Earth Sci. 7, 743–747.
Evamy, B.D., Haremboure, P., Kamerling, W.A., Knaap, F., Molloy, A., Rowlands, M.H., 1978. Hydrocarbon habitat of Tertiary Niger Delta. Am. Assoc. Pet. Geol. Bull. 62, 1–39.
Eyike, A., Ebbing, J., 2015. Lithospheric structure of the West and Central African Rift System from regional three-dimensional gravity modelling. S. Afr. J. Geol. 118, 285–298. https://doi.org/10.2113/gssajg.118.3.285.
Eyike, A., Werner, S.C., Ebbing, J., Dicoum, E.M., 2010. On the use of global potential field models for regional interpretation of the West and Central African Rift System. Tectonophysics 492, 25–39.
Ezepue, M., 1984. The geologic setting of lead-zinc deposits at Ishiagu, southeastern Nigeria. J. Afr. Earth Sci. 2, 97–101.
Faboya, O.L., Sonibare, O.O., Xu, J.B., Cheng, B., Deng, Q., Weil, Z.W., Olowookere, A., Liao, Z.W., 2019. Geochemical characterisation of lower Maastrichtian Mamu Formation kerogens, Anambra Basin, Nigeria. IOP Conf. Ser. Earth Environ. Sci. 360, 012015. https://doi.org/10.1088/1755-1315/360/1/012015.

Fadul, M.F., El Dawi, M.G., Abdel-Fattah, M.I., 2020. Seismic interpretation and tectonic regime of Sudanese Rift System: Implications for hydrocarbon exploration in Neem field (Muglad Basin). J. Pet. Sci. Eng. 191, 107223.
Fairhead, J.D., 1986. Geophysical controls on sedimentation within the African Rift Systems. In: Frostick, L.E., Renaut, R.W., Reid, I., Tiercelin, J.-J. (Eds.), Sedimentation in the African Rifts, Geol. Soc. Spec. Publ, vol. 25, pp. 19–27.
Fairhead, J.D., 1988. Mesozoic plate tectonic reconstructions of the central South Atlantic Ocean: the role of the West and Central African rift system. Tectonophysics 155, 181–191.
Fairhead, J.D., 2020. Regional tectonics and basin formation: The role of potential field studies - an application to the Mesozoic West and Central African Rift System. In: Scarselli, N., Adam, J., Chiarella, D., Roberts, D.G., Bally, A.W. (Eds.), Regional Geology and Tectonics: Principles of Geologic Analysis Volume 1: Principles of Geologic Analysis. Elsevier, Amsterdam, pp. 541–556. https://doi.org/10.1016/B978-0-444-64134-2.00018-3.
Fairhead, J.D., 2023. The Mesozoic West and Central Africa Rift System (WCARS) and the older Kandi Shear Zone (KSZ): Rifting and tectonics of North Africa and South America and fragmentation of Gondwana based on geophysical investigations. J. Afr. Earth Sci. 199, 104817.
Fairhead, J.D., Binks, R.M., 1991. Differential opening of the Central and South Atlantic Oceans and the opening of the West African rift system. Tectonophysics 187, 191–203.
Fairhead, J.D., Green, C.M., 1989. Controls on rifting in Africa and the regional tectonic model for the Nigeria and East Niger rift basins. J. Afr. Earth Sci. 8, 231–249.
Fairhead, J.D., Okereke, C.S., 1987. A regional gravity study of the West African rift system in Nigeria and Cameroon and its tectonic interpretation. Tectonophysics 143, 141–159.
Fairhead, J.D., Green, C.M., Masterton, S.M., Guiraud, R., 2013. The role that plate tectonics, inferred stress changes and stratigraphic unconformities have on the evolution of the West and Central African Rift System and the Atlantic continental margins. Tectonophysics 594, 118–127.
Finthan, B., Mamman, Y.D., 2020. The lithofacies and depositional paleoenvironment of the Bima Sandstone in Girei and Environs, Yola arm, Upper Benue Trough, Northeastern Nigeria. J. Afr. Earth Sci. 169, 103863.
Fonseca, C., Mendonça Filho, J.G., Lézin, C., Duarte, L.V., 2020. Organic facies variability and paleoenvironmental changes on the Moroccan Atlantic coast across the Cenomanian—Turonian Oceanic Anoxic Event (OAE2). Int. J. Coal Geol. 230, 103587.
Foulger, G.R., 2018. Origin of the South Atlantic igneous province. J. Volcanol. Geotherm. Res. 355, 2–20.
Frakes, L.A., Francis, J.E., Syktus, J.I., 1992. Climate Modes of the Phanerozoic. Cambridge University Press, Cambridge, 288 p.
Frostick, L.E., Steel, R.J., 1993. Sedimentation in divergent-plate basins. In: Frostick, L. E., Steel, R.J. (Eds.), Tectonic Controls and Signatures in Sedimentary Successions, IAS Spec. Publ, vol. 20, pp. 111–128.
Gani, N.D.S., Abdelsalam, M.G., Gera, S., Gani, M.R., 2009. Stratigraphic and structural evolution of the Blue Nile Basin, Northwestern Ethiopian Plateau. Geol. J. 44, 30–56.
Gao, H., Du, Y., Wang, L., Gao, S., Hu, J., Bai, J., Ma, H., Wang, Y., Zhang, X., Liu, H., 2023. Tectonic features, genetic mechanisms and basin evolution of the eastern Doseo Basin. Chad. Petrol. Explor. Dev. 50, 1151–1166.
Garfunkel, Z., Ben-Avraham, Z., 2001. Basins along the Dead Sea Transform. In: Ziegler, P.A., Cavazza, M., Robertson, A.H.F., Crasquin-Soleau (Eds.), Peri-Tethys Memoir 6: Peri-Tethyan Rift/Wrench Basins and Passive Margins, 186, pp. 607–627.
Gebhardt, H., 1997. Cenomanian to Turonian foraminifera from Ashaka (NE Nigeria): quantitative analysis and palaeoenvironmental interpretation. Cretac. Res. 18, 17–36.
Gebhardt, H., 1999. Cenomanian to Coniacian ostracodes from the Nkalagu area (SE Nigeria): biostratigraphy and palaeoecology. Palaontol. Z. 73, 77–98.
Gebhardt, H., 2001. Calcareous nannofossils from the Nkalagu Formation type locality (Middle Turonian to Coniacian, southern Nigeria): biostratigraphy and palaeo-ecologic implications. J. Afr. Earth Sci. 32, 391–402.
Genik, G.J., 1992. Regional framework, structural and petroleum aspects of rift basins in Niger, Chad and the Central African Republic. Tectonophysics 213, 169–185.
Genik, G.J., 1993. Petroleum geology of Cretaceous-Tertiary rift basins in Niger, Chad, and Central African Republic. Am. Assoc. Pet. Geol. Bull. 77, 1405–1434. https://doi.org/10.1306/BDFF8EAC-1718-11D7-8645000102C1865D.
George, R., Rogers, N., Kelley, S., 1998. Earliest magmatism in Ethiopia: evidence for two mantle plumes in one flood basalt province. Geology 26, 923–926.
Ghomsi, F.E.K., Tenzer, R., Njinju, E., Steffen, R., 2022. The crustal configuration of the West and Central African Rift System from gravity and seismic data analysis. Geophys. J. Int. 230, 995–1012. https://doi.org/10.1093/gji/ggac089.
Globig, J., Fernàndez, M., Torne, M., Vergés, J., Robert, A., Faccenna, C., 2016. New insights into the crust and lithospheric mantle structure of Africa from elevation, geoid, and thermal analysis. J. Geophys. Res. Solid Earth 121, 5389–5424. https://doi.org/10.1002/2016JB012972.
Godet, A., Hfaiedh, R., Arnaud-Vanneau, A., Zghal, I., Arnaud, H., Ouali, J., 2014. Aptian palaeoclimates and identification of an OAE1a equivalent in shallow marine environments of the southern Tethyan margin: evidence from Southern Tunisia (Bir Oum Ali section, Northern Chott Chain). Cretac. Res. 48, 110–129.
Gomes, A.S., Vasconcelos, P.M., 2021. Geochronology of the Paraná-Etendeka large igneous province. Earth Sci. Rev. 220, 103716.
Grunau, H.R., Lehner, P., Cleintuar, M.R., Allenbach, P., Bakker, G., 1975. New radiometric ages and seismic data from Fuerteventura (Canary Islands), Maio (Cape Verde Islands), and Sao Tome (Gulf of Guinea). In: Borradaile, G.J., Ritsema, A.R., Rondeel, H.E., Simon, O.J. (Eds.), Progress in Geodynamics. Royal Academy of Arts and Sciences, Amsterdam, pp. 90–118.
Guiraud, R., Bellion, Y., 1995. Late Carboniferous to recent geodynamic evolution of the West Gondwanian, Cratonic, Tethyan margins. In: Nairn, A.E.M., Ricou, L.-C., Vrielynck, B., Dercourt, J. (Eds.), The Ocean Basins and Margins, vol. 8. The Tethys Ocean, Plenum, New York, pp. 101–124. https://doi.org/10.1007/978-1-4899-1558-0_3.
Guiraud, R., Bosworth, W., 1997. Senonian basin inversion and rejuvenation of rifting in Africa and Arabia: synthesis and implications to plate-scale tectonics. Tectonophysics 282, 39–82.
Guiraud, R., Maurin, J.-C., 1992. Early Cretaceous rifts of Western and Central Africa: an overview. Tectonophysics 213, 153–168.
Guiraud, R., Issawi, B., Bellion, Y., 1985. The Guineo Nubian Lineaments, a major structural Zone of the African Plate. C. R. Acad. Sci. 11, 17–20.
Guiraud, R., Bellion, Y., Benkhelil, J., Moreau, C., 1987. Post-Hercynian tectonics in Northern and Western Africa. Geol. J. 22, 433–466.
Guiraud, R., Bosworth, W., Thierry, J., Delplanque, A., 2005. Phanerozoic geological evolution of Northern and Central Africa: An overview. J. Afr. Earth Sci. 43, 83–143.
Hakimi, M.H., Abas, A.N., Hadad, Y.T., Al Faifi, H.J., Kinawy, M., Lashin, A., 2021. Bulk pyrolysis and biomarker fingerprints of Late Cretaceous Galhak Shale Formation in the northern Melut Basin, Sudan: implications on lacustrine oil-source rock. Arab. J. Geosci. 14, 520.
Hakimi, M.H., Abass, A.N., Lashin, A., Gharib, A.F., Radwan, A.E., Rahim, A., Ahmed, A., Asiwaju, L., Afify, W.E., 2022. Geochemical investigation and basin modelling of the Al renk shale formation in the Melut Basin, South Sudan: Implications for estimation of thermogenic gas generation potential. Mar. Pet. Geol. 146, 105926.
Harouna, M., Philp, R.P., 2012. Potential petroleum source rocks in the Termit Basin, Niger. J. Pet. Geol. 35, 165–185.
Hassan, A.H.O., Osinowo, O.O., Zayed, M.A., 2024. Application of seismic sequence stratigraphy and seismic facies analyses for identifying stratigraphic trap system within Rawat central sub-basin, White Nile State, Sudan. Arab. J. Geosci. 17, 25. https://doi.org/10.1007/s12517-023-11826-y.
Hay, W.W., 2008. Evolving ideas about Cretaceous climate and ocean circulation. Cretac. Res. 29, 725–753.
Hay, W.W., 2017. Toward understanding Cretaceous climate—An updated review. Sci. China Earth Sci. 60, 5–19.
Hay, W.W., Floegel, S., 2012. New thoughts about the Cretaceous climate and oceans. Earth Sci. Rev. 115, 262–272.
Heine, C., Zoethout, J., Müller, R.D., 2013. Kinematics of the South Atlantic rift. Solid Earth 4, 215–253.
Hofmann, C., Courtillot, V., Feraud, G., Rochette, P., Yirgu, G., Ketefo, E., Pik, R., 1997. Timing of the Ethiopian flood basalt event and implications of Plume birth and global change. Nature 389, 838–841.
Holz, M., Vilas-Boas, D.B., Troccoli, E.B., Carnairo Santana, V., Vidigal-Souza, P.A., 2017. Conceptual models for sequence stratigraphy of continental rift successions. In: Montenari, M. (Ed.), Stratigraphy and Timescales, vol. 2. Academic Press, UK, pp. 119–186.
Hu, Y., Hu, J., Du, Y., Lu, H., Yang, N., Wang, L., Xu, H.-H., 2023. Early Cretaceous palynofloras from the Bongor basin, Chad, and their palaeoenvironmental and palaeoclimatic significances. J. Afr. Earth Sci. 198, 104792.
Huber, B.T., MacLeod, K.G., Watkins, D.K., Coffin, M.F., 2018. The rise and fall of the Cretaceous Hot Greenhouse climate. Glob. Planet. Chang. 167, 1–23.
Igwe, E.O., 2017. Composition, provenance and tectonic setting of Eze-Aku sandstone facies in the Afikpo Synclinorium, Southern Benue Trough, Nigeria. Environ. Earth Sci. 76, 1–12.
Ijeh, B.I., Anyadiegwu, F.C., Onwubuariri, C.N., Eze, M.O., 2024. Evaluation of geothermal resource potential of the lower Benue Trough using aeromagnetic and radiometric data. Model. Earth Syst. Environ. 10, 695–721.
Izart, A., Stephenson, R.A., Vai, G.B., Vachard, D., Nindrfe, Y.L., Vaslet, D., Sues, P., Fauvel, P.J., Kossovaya, O., Chen, Z., Maslo, A., Stovba, S., 2003. Sequence stratigraphy and correlation of late Carboniferous and Permian in the CIS, Europe, Tethyan area, North Africa, Arabia, China, Gondwanaland and the USA. Palaeogeogr. Palaeoclimatol. Palaeoecol. 196, 59–84.
Jauro, A., Obaje, N.G., Agho, M.O., Abubakar, M.B., Tukur, A., 2007. Organic geochemistry of Cretaceous Lamza and Chikila coals, Upper Benue Trough, Nigeria. Fuel 86, 520–532.
Jenkyns, H.C., 2010. Geochemistry of oceanic anoxic events. Geochem. Geophys. Geosyst. 11, Q03004. https://doi.org/10.1029/2009GC002788.
Jimoh, A.Y., Ojo, O.J., 2016. Rock-Eval pyrolysis and organic petrographic analysis of the Maastrichtian coals and shales at Gombe, Gongola Basin, Northeastern Nigeria. Arab. J. Geosci. 9, 443. https://doi.org/10.1007/s12517-016-2467-x.
Jones, D.J.R., 2020. A Summary of the East Africa Rift Temperature and Heat Flow Model (EARTH). British Geological Survey Open Report, OR/20/006. 24pp.
Joo, Y.J., Sageman, B.B., Hurtgen, M.T., 2020. Data-model comparison reveals key environmental changes leading to Cenomanian-Turonian Oceanic Anoxic Event 2. Earth Sci. Rev. 203, 103123.
Jorgensen, G.J., Bosworth, W., 1989. Gravity modeling in the Central African Rift System, Sudan: rift geometries and tectonic significance. J. Afr. Earth Sci. 8, 283–306.
Kassem, A.A., Sharaf, L.M., Baghdady, A.R., El-Naby, A.A., 2020. Cenomanian/Turonian oceanic anoxic event 2 in October oil field, central Gulf of Suez, Egypt. J. Afr. Earth Sci. 165, 103817.
Kazmin, V., 1975. Explanation of the Geological Map of Ethiopia. Ethiopian Geol. Surv. Bull. 1, 1–15.
Keller, G.R., Wendlandt, R.F., Bott, M.H.P., 2006. Chapter 13 West and Central African rift system. In: Olsen, K.H. (Ed.), Developments in Geotectonics 25. Elsevier, pp. 437–449. https://doi.org/10.1016/S0419-0254(06)80021-2.

Khain, V.Y., 1992. The role of rifting in the evolution of the Earth's crust. Tectonophysics 215, 1–7.
Khalifa, Z., Affouri, H., Rigane, A., Jacob, J., 2018. The Albian oceanic anoxic events record in central and northern Tunisia: Geochemical data and paleotectonic controls. Mar. Pet. Geol. 93, 145–165.
Klemme, H.D., 1980. Petroleum Basins-Classifications and Characteristics. J. Pet. Geol. 3, 187–207.
Konaté, M., Ahmed, Y., Harouna, M., 2019. Structural evolution of the Téfidet trough (East Aïr, Niger) in relation with the West African Cretaceous and Paleogene rifting and compression episodes. Compt. Rendus Geosci. 351, 355–365.
Korme, T., Acocella, V., Abebe, B., 2004. The role of pre-existing structures in origin, propagation and architecture of faults in the Main Ethiopian Rift. Gondwana Res. 7, 467–479.
Kress, P.R., Catuneanu, O., Gerster, R., Bolatti, N., 2021. Tectonic and stratigraphic evolution of the Cretaceous western South Atlantic. Mar. Pet. Geol. 134, 105197.
Kuhnt, W., Herbin, J.P., Thurow, T., Wiedmann, J., 1990. Distribution of Cenomanian–Turonian organic facies in the western Mediterranean and along the adjacent Atlantic margin. In: Huc, A.Y. (Ed.), Depositional of Organic Facies, Am. Assoc. Pet. Geol. Stud. Geol, vol. 30, pp. 133–160.
Kuhnt, W., Luderer, F., Nederbragt, S., Thurow, J., Wagner, T., 2005. Orbital-scale record of the late Cenomanian–Turonian oceanic anoxic event (OAE-2) in the Tarfaya Basin (Morocco). Int. J. Earth Sci. 94, 147–159.
Kwaya, M.Y., Kurowska, E., Arabi Suleiman, A., 2016. Geothermal gradient and heat flow in the Nigeria sector of the Chad basin, Nigeria. Comput. Water Energy Environ. Eng. 5, 70–78. https://doi.org/10.4236/cweee.2016.52007.
Lai, H., Li, M., Liu, J., Mao, F., Xiao, H., He, W., Yang, L., 2018. Organic geochemical characteristics and depositional models of Upper Cretaceous marine source rocks in the Termit Basin, Niger. Palaeogeogr. Palaeoclimatol. Palaeoecol. 495, 292–308.
Lambiase, J.J., Morley, C.K., 1999. Hydrocarbons in rift basins: the role of stratigraphy. Phil. Trans. R. Soc. Lond. A 357, 877–900.
Laville, E., Petit, P., 1984. Role of synsedimentary strike-slip faults in the formation of Moroccan Triassic basins. Geology 12, 424–427.
Lawver, L.A., Roger, J.Y., Sandwell, D.T., Scotese, C.R., 1991. Evolution of the Antarctic continental margins. In: Thomson, M.R.A., Crame, J.A., Thomson, J.W. (Eds.), Geological Evolution of Antarctica. Proceedings of the Fifth International Symposium on Antarctic Earth Sciences. Cambridge University Press, Cambridge, UK, pp. 533–539.
Leckie, R.M., Bralower, T.J., Cashman, R., 2002. Oceanic anoxic events and plankton evolution: Biotic response to tectonic forcing during the mid-Cretaceous. Paleoceanography 17, 13-1–13-29. https://doi.org/10.1029/2001PA000623.
Leleu, S., Hartley, A.J., van Oosterhout, C., Kennan, L., Ruckwied, K., Gerdes, K., 2016. Structural, stratigraphic and sedimentological characterisation of a wide rift system: the Triassic rift system of the Central Atlantic Domain. Earth Sci. Rev. 158, 89–124.
Lenhardt, N., Oppenheimer, C., 2014. Volcanism in Africa: Geological perspectives, hazard assessment and societal implications. In: Ismail-Zadeh, A., Urrutia-Fucugauchi, J., Kijko, A., Takeuchi, K., Zaliapin, I. (Eds.), Extreme Natural Hazards, Disaster Risks and Societal Implications, IUGG Special Publication Series 1. Cambridge University Press, pp. 169–199.
Lenhardt, N., Galerne, C., Le Roux, P., Götz, A.E., Lötter, F.J.P., 2023. Geochemistry of dolerite intrusions of the southeastern Karoo Basin, South Africa: Magma evolution, evidence for thermogenic gas sequestration, and potential implications for the Toarcian anoxic event. Gondwana Res. 113, 144–162.
Leyuan, F., Jiapeng, W., Wan, D., Yang, L.I., 2021. Sedimentary characteristics of the shallow water delta in rifted lacustrine basin: a case study in the Aradeiba Formation, Unity Sag, Muglad Basin. Earth Sci. Front. 28, 155.
Li, W., Dou, L., Wen, Z., Zhang, G., Cheng, D., 2017. Use of a geochemical method to analyze the hydrocarbon accumulation process in the Bongor Basin. Chad. Pet. Sci. Technol. 35, 2133–2138.
Liu, G.H., Chen, Q.H., 2014. Structure and sedimentary-filling evolution of Anza Basin of East Africa. J. Xi'an Univ. Sci. Technol. 34, 326–330 (in Chinese with English abstract).
Liu, B., Wan, L., Mao, F., Liu, J., Lü, M., Wang, Y., 2015. Hydrocarbon potential of Upper Cretaceous marine source rocks in the Termit Basin, Niger. J. Pet. Geol. 38, 157–175.
Liu, B., Zhang, G., Mao, F., Liu, J., Cheng, D., Lü, M., 2017a. The petroleum system of the Tenere Basin: oil geochemistry from the SH-1 wildcat well in eastern Niger. Pet. Geosci. 23, 427–439. https://doi.org/10.1144/petgeo2015-067.
Liu, B., Zhang, G., Mao, F., Liu, J., Lü, M., 2017b. Geochemistry and origin of Upper Cretaceous oils from the Termit Basin, Niger. J. Pet. Geol. 40, 195–207.
Loule, J.-P., Pospisil, L., 2013. Geophysical evidence of Cretaceous volcanics in Logone Birni Basin (Northern Cameroon), Central Africa, and consequences for the West and Central African Rift System. Tectonophysics 583, 88–100.
Lowell, J.D., Genik, U.J., 1972. Sea floor spreading and structural evolution of Southern Red Sea. Am. Assoc. Pet. Geol. Bull. 56, 247–259.
Lu, Y., Liu, J., Dou, L., Guo, Z., Xiao, K., Hu, Y., Du, Y., 2009a. Geochemistry and petrogenesis of volcanic rocks from Chad basins, Africa. Acta Petrol. Sin. 25 (1), 109–123.
Lu, Y., Liu, J., Dou, L., Guo, Z., Xiao, K., Hu, Y., Du, Y., Meng, F., 2009b. K-Ar and 39Ar-40Ar geochronology of basalts from the chad basins, Africa and its geodynamics setting. Acta Petrol. Sin. 83 (8), 1125–1133.
Luft-Souza, F., Fauth, G., Bruno, M.D., Mota, M.A.D.L., Vázquez-García, B., Santos Filho, M.A., Terra, G.J., 2022. Sergipe-Alagoas Basin, Northeast Brazil: a reference basin for studies on the early history of the South Atlantic Ocean. Earth Sci. Rev. 229, 104034.
Mahgoub, M.I., Padmanabhan, E., Abdullatif, O.M., 2016. Sedimentological reservoir characteristics of the Paleocene fluvial/lacustrine Yabus Sandstone, Melut Basin, Sudan. J. Afr. Earth Sci. 123, 75–88.
Makeen, Y.M., Abdullah, W.H., Hakimi, M.H., Elhassan, O.M.A., 2015a. Organic geochemical characteristics of the Lower Cretaceous Abu Gabra Formation in the Great Moga oilfield, Muglad Basin, Sudan: Implications for depositional environment and oil-generation potential. J. Afr. Earth Sci. 103, 102–112.
Makeen, Y.M., Abdullah, W.H., Hakimi, M.H., 2015b. Biological markers and organic petrology study of organic matter in the Lower Cretaceous Abu Gabra sediments (Muglad Basin, Sudan): origin, type and palaeoenvironmental conditions. Arab. J. Geosci. 8, 489–506.
Makeen, Y.M., Hakimi, M.H., Abdullah, W.H., 2015c. The origin, type and preservation of organic matter of the Barremian–Aptian organic-rich shales in the Muglad Basin, Southern Sudan, and their relation to paleoenvironmental and paleoclimate conditions. Mar. Pet. Geol. 65, 187–197.
Makeen, Y.M., Shan, X., Ayinla, H.A., Adepehin, E.J., Ayuk, N.E., Yelwa, N.A., Yi, J., Elhassan, O.M.A., Fan, D., 2021. Sedimentology, petrography, and reservoir quality of the Zarga and Ghazal formations in the Keyi oilfield, Muglad Basin, Sudan. Sci. Rep. 11, 743. https://doi.org/10.1038/s41598-020-80831-y.
Makris, J., Rihm, R., 1991. Shear controlled evolution of the Red Sea: pull apart model. Tectonophysics 198, 441–468.
Maluski, H., Coulon, C., Popoff, M., Baudin, P., 1995. 40Ar/39Ar chronology, petrology and geodynamic setting of Mesozoic to early Cenozoic magmatism from the Benue Trough, Nigeria. J. Geol. Soc. Lond. 152, 311–326.
Manga, C.S., Loule, J.-P., Koum, J.-J., 2001. Tectonostratigraphic evolution and prospectivity of the Logone Birni Basin, North Cameroon–Central Africa. Am. Assoc. Pet. Geol. Bull. 85, 1–6.
Mangs, A.D., Wagner, N.J., Moroeng, O.M., Lar, U.A., 2022. Petrographic composition of coal within the Benue Trough, Nigeria and a consideration of the paleodepositional setting. Int. J. Coal Sci. Technol. 9, 35. https://doi.org/10.1007/s40789-022-00500-5.
Mann, P., Gahagan, L., Gordon, M.B., 2003. Tectonic setting of the World's Giant Oil and Gas Fields. In: Halbouty, M.T. (Ed.), Giant Oil and Gas Fields of the Decade 1990–1999, Am. Assoc. Pet. Geol. Mem, vol. 78, pp. 15–105.
Mansour, A., Wagreich, M., Gentzis, T., Ocubalidet, S., Tahoun, S.S., Elewa, A.M.T., 2020. Depositional and organic carbon-controlled regimes during the Coniacian-Santonian event: first results from the southern Tethys (Egypt). Mar. Pet. Geol. 115, 104285.
Mao, F., Liu, R., Liu, B., Jiang, H., Liu, J., Wang, X., Tang, W., Zheng, F., Li, Z., 2016. Palaeogeographic evolution of the Upper Cretaceous in Termit Basin and its adjacent areas, Niger. Earth Sci. Front. 23, 186–197 (in Chinese with English abstract).
Martins-Neto, M.A., Catuneanu, O., 2010. Rift sequence stratigraphy. Mar. Pet. Geol. 27, 247–253.
Maurin, J., Benkhelil, J., 1990. Model of Pb/Zn mineralization genesis in the Cretaceous Benue Trough (Nigeria): Structural, geophysical and geochemical constraints. J. Afr. Earth Sci. 11, 345–349.
Maurin, J.-C., Guiraud, R., 1993. Basement control in the development of the early cretaceous West and Central African rift system. Tectonophysics 228, 81–95.
Mbafor, P.U., Fon, N.N., Njoh, O.A., Agbor-Taku, J., Bessong, M., 2023. A new lithostratigraphic profile for cretaceous to Paleogene successions in the West and Central African Rift System, Koum Basin, northern Cameroon. Stratigraphy 20, 109–128.
McHargue, T.R., Heidrick, T.L., Livingston, J.K., 1992. Tectono-stratigraphic development of the interior Sudan rifts, Central Africa. Tectonophysics 213, 187–202.
McKenzie, D., 1978. Some remarks on the development of sedimentary basins. Earth Planet. Sci. Lett. 40, 25–32.
Meert, J.G., Lieberman, B.S., 2008. The Neoproterozoic assembly of Gondwana and its relationship to the Ediacaran–Cambrian radiation. Gondwana Res. 14, 5–21.
Mengesha, T., Tadiwos, C., Workineh, H., 1996. Explanation of the geological map of Ethiopia, scale 1:2,000,000. Ethiopian Inst. Geol. Surv. Bull. 3, 1–79.
Merabet, O., Klotchko, V., Timonine, L., Lvannikov, A., 1971. Précision sur l'age de la transgression du Cénomano-Turonien inferieur au Sahara central. Publ. Serv. Géol. Algerie 41, 217–223.
Michon, L., Famin, V., Quidelleur, X., 2022. Evolution of the East African Rift System from trap-scale to plate-scale rifting. Earth Sci. Rev. 231, 104089. https://doi.org/10.1016/j.earscirev.2022.104089.
Min, G., Hou, G., 2019. Mechanism of the Mesozoic African rift system: Paleostress field modelling. J. Geodyn. 132, 101655.
Mitchell, R.N., Bice, D.M., Montanari, A., Cleaveland, L.C., Christianson, K.T., Coccioni, R., Hinnov, L.A., 2008. Oceanic anoxic cycles? Orbital prelude to the Bonarelli Level (OAE 2). Earth Planet. Sci. Lett. 267, 1–16.
MMSD (Ministry of Mines and Solid Minerals Development), 2006. Technical Overview Nigeria's Bitumen Belt and Development Potential, 27 p.
Mohamed, A.Y., Iliffe, J.E., Ashcroft, W.A., Whiteman, A.J., 2000. Burial and maturation history of the Heglig field area, Muglad Basin, Sudan. J. Pet. Geol. 23, 107–128.
Mohamed, A.Y., Ashcroft, W.A., Whiteman, A.J., 2001. Structural development and crustal stretching in the Muglad Basin, southern Sudan. J. Afr. Earth Sci. 32, 179–191.
Mohamed, A.Y., Whiteman, A.J., Archer, S.G., Bowden, S.A., 2016. Thermal modelling of the Melut basin Sudan and South Sudan: Implications for hydrocarbon generation and migration. Mar. Pet. Geol. 77, 746–762.
Mohammed, I.A., 1997. Geology and structures of the area west of the White Nile as deduced from gravity measurements. (Unpublished) M.Sc. Thesis Khartoum Univ.
Mohammedyasin, M.S., Wudie, G., 2019. Provenance of the Cretaceous Debre Libanos Sandstone in the Blue Nile Basin, Ethiopia: evidence from petrography and geochemistry. Sediment. Geol. 379, 46–59.

Mohammedyasin, M.S., Wudie, G., Anteneh, Z.L., Bawoke, G.T., 2019. Paleoredox conditions of the Middle-Upper Jurassic black shales in the Blue Nile Basin, Ethiopia. J. Afr. Earth Sci. 151, 136–145.
Mohammedyasin, M.S., Littke, R., Wudie, G., Ziege, L., 2020. Source rock potential and depositional environment of Middle – Upper Jurassic sedimentary rocks, Blue Nile Basin, Ethiopia. J. Pet. Geol. 43, 401–418.
Mohd Sumery, N.F., Lo, S.Z., Salim, A.M.A., 2017. Lacustrine environment reservoir properties on sandstone minerals and hydrocarbon content: a case study on Doba Basin, Southern Chad. IOP Conf. Ser. Earth Environ. Sci. 88, 012005.
Moody, R.T.J., Sutcliffe, P.J.C., 1991. The Cretaceous deposits of the Iullemmeden Basin of Niger, central West Africa. Cretac. Res. 12, 137–157.
Moody, R.T.J., Sutcliffe, P.J.C., 1993. The sedimentology and palaeontology of the Upper Cretaceous-Tertiary deposits of central West Africa. Mod. Geol. 18, 459–474.
Morakinyo, A.M., Mohamed, A.Y., Bowden, S.A., 2021. The release of petroleum from Central Africa rift basins over geological time as deduced from petroleum systems modelling. J. Afr. Earth Sci. 183, 104319.
Moretti, I., Colletta, B., 1987. Spatial and temporal evolution of the Suez rift subsidence. J. Geodyn. 7, 151–168.
Mort, H.P., Adatte, T., Keller, G., Bartels, D., Föllmi, K.B., Steinmann, P., Berner, Z., Chellai, E.H., 2008. Organic carbon deposition and phosphorus accumulation during Oceanic Anoxic Event 2 in Tarfaya, Morocco. Cretac. Res. 29, 1008–1023.
Moulin, M., Aslanian, D., Unternehr, P., 2010. A new starting point for the South and Equatorial Atlantic Ocean. Earth Sci. Rev. 98, 1–37.
Mustafa, A.A., Tyson, R.V., 2002. Organic Facies of Early Cretaceous Syn-rift Lacustrine Source Rocks from the Muglad Basin, Sudan. J. Pet. Geol. 25, 351–366. https://doi.org/10.1111/j.1747-5457.2002.tb00013.x.
Mustafa, M.K.M., Farwa, A.G., Salim, A.M.A., 2022. 3D Seismic data interpretation in Gumry Field, Melut Basin. Earth Sci. 11, 109–120. https://doi.org/10.11648/j.earth.20221103.17.
Nagm, E., El-Qot, G., Wilmsen, M., 2014. Stable-isotope stratigraphy of the Cenomanian–Turonian (Upper Cretaceous) boundary event (CTBE) in Wadi Qena, Eastern Desert, Egypt. J. Afr. Earth Sci. 100, 524–531.
Nguimbous-Kouoh, J.J., Ngos III, S., Mbarga, T.N., Manguelle-Dicoum, E., 2017. Use of the Polynomial Separation and the Gravity Spectral Analysis to Estimate the Depth of the Northern Logone Birni Sedimentary Basin (CAMEROON). Int. J. Geol. 8, 1442–1456.
Njome, M.S., de Wit, M.J., 2014. The Cameroon Line: Analysis of an intraplate magmatic province transecting both oceanic and continental lithospheres: Constraints, controversies and models. Earth Sci. Rev. 139, 168–194.
Nkodia, H.M.D.-V., Miyouna, T., Kolawole, F., Boudzoumou, F., Loemba, A.P.R., Bazebizonza Tchiguina, N.C., Delvaux, D., 2022. Seismogenic fault reactivation in western Central Africa: Insights from regional stress analysis. Geochem. Geophys. Geosyst. 23, e2022GC010377. https://doi.org/10.1029/2022GC010377.
Nürnberg, D., Müller, R.D., 1991. The tectonic evolution of the South Atlantic from Late Jurassic to present. Tectonophysics 191, 27–53.
Nwajide, C.S., 1987. Provenance and palaeogeographic history of the Turonian Makurdi sandstones in the benue trough of Nigeria. Palaeogeogr. Palaeoclimatol. Palaeoecol. 58, 109–119.
Nwajide, C.S., 2013. Geology of Nigeria's Sedimentary Basins. CSS Bookshop Ltd., Lagos, p. 565.
Obaje, N.G., 2009. Geology and Mineral Resources of Nigeria. Springer-Verlag, Berlin Heidelberg, 221 p.
Obaje, N.G., Ligouis, B., Abaa, S.I., 1994. Petrographic composition and depositional environments of Cretaceous coals and coal measures in the Middle Benue Trough of Nigeria. Int. J. Coal Geol. 26, 233–260.
Obaje, N.G., Amadi, A.N., Aweda, A.K., Umar, U.M., Shuaibu, I., 2018. Processing Nigerian coal deposits for energy source. Environ. Earth Sci. 77, 176. https://doi.org/10.1007/s12665-018-7362-1.
O'Brien, C.L., Robinson, S.A., Pancost, R.D., Sinninghe Damsté, J.S., Schouten, S., Lunt, D.J., Alsenz, H., Bornemann, A., Bottini, C., Brassell, S.C., Farnsworth, A., Forster, A., Huber, B.T., Inglis, G.N., Jenkyns, H.C., Linnert, C., Littler, K., Markwick, P., McAnena, A., Mutterlose, J., Naafs, B.D.A., Püttmann, W., Sluijs, A., van Helmond, N.A.G.M., Vellekoop, J., Wagner, T., Wrobel, N.E., 2017. Cretaceous sea-surface temperature evolution: Constraints from TEX86 and planktonic foraminiferal oxygen isotopes. Earth Sci. Rev. 172, 224–247.
Odigi, M.I., 2007. Facies Architecture and Sequence Stratigraphy of Cretaceous Formations, Southeastern Benue Trough, Nigeria. Unpublished PhD thesis. University of Portharcourt, Nigeria, 288p.
Odigi, M.I., Amajor, L.C., 2008. Petrology and geochemistry of sandstones in the southern Benue Trough of Nigeria: Implications for provenance and tectonic setting. Chin. J. Chem. 27, 384–394. https://doi.org/10.1007/s11631-008-0384-8.
Offodile, M.E., 1980. A mineral survey of the Cretaceous of the Benue Valley, Nigeria. Cretac. Res. 1, 101–124.
Ofoegbu, C.O., 1984. A model for the tectonic evolution of the Benue Trough of Nigeria. Geol. Rdsch. 73, 1009–1020.
Ofoegbu, C.O., 1985. A review of the geology of the Benue Trough, Nigeria. J. Afr. Earth Sci. 3, 283–291.
Ogala, J., Siavalas, G., Christanis, K., 2012. Coal petrography, mineralogy and geochemistry of lignite samples from the Ogwashi–Asaba Formation, Nigeria. J. Afr. Earth Sci. 66-67, 35–45.
Ogundipe, I.E., 2017. Thermal and chemical variations of the Nigerian Benue Trough lead-zinc-barite-fluorite deposits. J. Afr. Earth Sci. 132, 72–79.
Oha, I.A., Onuoha, K.M., Dada, S.S., 2017. Contrasting styles of lead-zinc-barium mineralization in the lower Benue Trough, Southeastern Nigeria. Earth Sci. Res. J. 21, 7–16. https://doi.org/10.15446/esrj.v21n1.39703.
Okezie, C.N., Onuogu, S.A., 1985. The Lignites of Southeastern Nigeria: a summary of available information. Geol. Surv. Nigeria Occ. Pap. 10, 28 pp.
Olade, M.A., 1976. On the genesis of lead-zinc deposits in Nigeria's Benue rift (aulacogen): a re-interpretation. Nig. J. Min. Geol. 13, 20–27.
Olade, M.A., Morton, R.D., 1985. Origin of lead zinc mineralization in the southern Benue Trough, Nigeria, fluid inclusion and trace element studies. Mineral. Deposita 20, 76–80.
O'leary, M.A., Bouaré, M.L., Claeson, K.M., Heilbronn, K., Hill, R.V., Mccartney, J., Sessa, J.A., Sissoko, F., Tapanila, L., Wheeler, E., Roberts, E.M., 2019. Stratigraphy and paleobiology of the Upper Cretaceous-lower Paleogene sediments from the trans-Saharan seaway in Mali. Bull. Am. Mus. Nat. Hist. 436, 1–183.
Omietimi, E.J., Lenhardt, N., Yang, R., Götz, A.E., Bumby, A.J., 2022. Sedimentary geochemistry of Late Cretaceous-Paleocene deposits at the southwestern margin of the Anambra Basin (Nigeria): Implications for paleoenvironmental reconstructions. Palaeogeogr. Palaeoclimatol. Palaeoecol. 600, 111059. https://doi.org/10.1016/j.palaeo.2022.111059.
Orajaka, I.P., Onwemesi, G., Egboka, B.C.E., Nwankor, G.I., 1990. Nigerian coal. Min. Mag. 162, 446–451.
Papadomanolaki, N.M., Lenstra, W.K., Wolthers, M., Slomp, C.P., 2022. Enhanced phosphorus recycling during past oceanic anoxia amplified by low rates of apatite authigenesis. Sci. Adv. 8, eabn2370. https://doi.org/10.1126/sciadv.abn2370.
Patrick, N.O., Fadele, S.I., Adegoke, I., 2013. Stratigraphic Report of the Middle Benue Trough, Nigeria: Insights from Petrographic and Structural Evaluation of Abuni and Environs Part of Late Albian-Cenomanian Awe and Keana Formations. Pac. J. Sci. Technol. 14, 557–570.
Patton, T.L., Moustafa, A.R., Nelson, R.A., Abdine, S.A., 1994. Tectonic evolution and structural setting of the Suez rift. In: Landon, S.M. (Ed.), Interior Rift Basins, Am. Assoc. Pet. Geol. Mem, vol. 59, pp. 9–55.
Pearson, M., Casson, M., Millar, I., Charton, R., Redfern, J., 2024. Cretaceous climate change evidenced in the Senegalese rock record, NW Africa. J. Afr. Earth Sci. 211, 105166.
Petters, S.W., 1982. Central West African Cretaceous-Tertiary benthic foraminifera and stratigraphy. Palaeogeographica 179, 1–104.
Petters, S.W., Ekweozor, C.M., 1982. Origin of mid-cretaceous black shales in the benue through, Nigeria. Palaeogeogr. Palaeoclimatol. Palaeoecol. 40, 311–319.
Peyve, A.A., 2015. The Role of Mantle Plumes in the Evolution of the African Segment of Pangea and the Formation of the Atlantic Ocean. Geotectonics 49, 379–394.
Popoff, M., Kampunzu, A.B., Coulon, C., Esquevin, J., 1982. Découverte d'un volcanisme mésozoïque dans le NE du Nigéria: datations absolues, caractères magmatiques et signification dans l'évolution du rift de la Bénoué. In: Popoff, M., Tiercelin, J.J. (Eds.), Rifts et Fosses Anciens. Résumés Commun, 819. Trav. Lab. Sci. Terre St.-Jerome, Marseille, pp. 47–49.
Poulsen, C.J., Gendaszek, A.S., Jacob, R.L., 2003. Did the rifting of the Atlantic Ocean cause the Cretaceous thermal maximum? Geology 31, 115–118.
Praus, M.L., 2015. Marine palynology of the Oceanic Anoxic Event 3 (OAE3, Coniacian –Santonian) at Tarfaya, Morocco, NW Africa – transition from preservation to production controlled accumulation of marine organic carbon. Cretac. Res. 53, 19–37.
Prodehl, C., Jacob, A.W.B., Thybo, H., Dindi, E., Stangl, R., 1994. Crustal structure on the northeastern flank of the Kenya rift. Tectonophysics 236, 271–290.
Prodehl, C.K., Fuchs, K., Mechie, J., 1997. Seismic-refraction studies of the Afro-Arabian rift system — a brief review. Tectonophysics 278, 1–13.
Qiao, J., Liu, L., An, F., Xiao, F., Wang, Y., Wu, K., Zhao, Y., 2016. Hydrocarbon potential evaluation of the source rocks from the Abu Gabra Formation in the Sufyan Sag, Muglad Basin, Sudan. J. Afr. Earth Sci. 118, 301–312.
Radier, H., 1959. Contribution à l'étude géologique du Soudan oriental (A.O.F.), II. Le bassin Crétacé et Tertiaire de Gao. Bull. Serv. Géol. Prospect. Min. 26, 309–556.
Rebelle, M., 1990. The marine transgression in the Benue Trough (NE Nigeria): a palaeogeographic interpretation of the Gongila Formation. J. Afr. Earth Sci. 10, 643–655.
Reeves, C.V., Karanja, F.M., Macleod, I.N., 1987. Geophysical evidence for a failed Jurassic Rift and triple junction in Kenya. Earth Planet. Sci. Lett. 81, 299–311.
Reyment, R.A., 1980. Biogeography of the Saharan Gretaceous and Paleocene epicontinental transgressions. Cretac. Res. 1, 299–327.
Reyment, R.A., Dingle, R.V., 1987. Palaeogeography of Africa during the Cretaceous period. Palaeogeogr. Palaeoclimatol. Palaeoecol. 59, 93–116.
Reyment, R.A., Tait, E.A., 1972. Biostratigraphical dating of the early history of the South Atlantic. Philos. Trans. R. Soc. B 264, 55–95.
Reynolds, D.J., Jones, C.R., 2004. Tectonic evolution of the Doba and Doseo basins, Chad: controls on trap formation and depositional setting of the three fields area. Chad. Am. Assoc. Pet. Geol. Bull. 88, 15–16.
Salman, G., Abdula, I., 1995. Development of the Mozambique and Ruvuma sedimentary basins, offshore Mozambique. Sediment. Geol. 96, 7–41.
Salmi-Laouar, S., Ferré, B., Chaabane, K., Laouar, R., Boyce, A.J., Fallick, A.E., 2018. The oceanic anoxic event 2 at Es Souabaa (Tebessa, NE Algeria): bio-events and stable isotope study. Arab. J. Geosci. 11, 182. https://doi.org/10.1007/s12517-018-3509-3.
Sarki Yandoka, B.M., Abdullah, W.H., Abubakar, M.B., Hakimi, M.H., Adegoke, A.K., 2015. Geochemical characterisation of Early Cretaceous lacustrine sediments of Bima Formation, Yola Sub-basin, Northern Benue Trough, NE Nigeria: Organic matter input, preservation, paleoenvironment and palaeoclimatic conditions. Mar. Pet. Geol. 61, 82–94.
Sarki Yandoka, B.M., Abdullah, W.H., Abubakar, M.B., Adegoke, A.K., Maigari, A.S., Haruna, A.I., Yaro, U.Y., 2017. Hydrocarbon potential of Early Cretaceous lacustrine sediments from Bima Formation, Yola Sub-basin, Northern Benue Trough, NE

Nigeria: Insight from organic geochemistry and petrology. J. Afr. Earth Sci. 129, 153–164.
Sass, I., Götz, A.E., 2012. Geothermal reservoir characterization: a thermofacies concept. Terra Nova 24, 142–147.
Schlanger, S.O., Jenkyns, H., 1976. Cretaceous oceanic anoxic events: causes and consequences. Geol. Mijnb. 55, 179–184.
Schull, T.J., 1988. Rift Basins of Interior Sudan: petroleum exploration and discovery. Am. Assoc. Pet. Geol. Bull. 72, 1128–1142.
Scotese, C.R., 2014. Atlas of Paleogene Paleogeographic Maps (Mollweide Projection), Maps 8–15, Volume 1, The Cenozoic. PALEOMAP Atlas for ArcGIS, PALEOMAP Project, Evanston, IL.
Scotese, C.R., Song, H., Mills, B.J., van der Meer, D.G., 2021. Phanerozoic paleotemperatures: the earth's changing climate during the last 540 million years. Earth Sci. Rev. 215, 103503.
Seton, M., Müller, R.D., Zahirovic, S., Gaina, C., Torsvik, T., Shephard, G., Talsma, A., Gurnis, M., Turner, M., Maus, S., Chandler, M., 2012. Global continental and ocean basin reconstructions since 200 Ma. Earth Sci. Rev. 113, 212–270.
Sewe, C., 1995. Optimization Analysis of Organic Carbon Concentration and Sedimentation Rate in the Anza Graben, Kenya. MSc thesis. University of Nairobi, Kenya, p. 99.
Shellnutt, J.G., Lee, T., Yang, C., Hu, S., Wu, J., Wang, K., Lo, C., 2015. Late Permian mafic rocks identified within the Doba Basin of southern Chad and their relationship to the boundary of the Saharan Metacraton. Geol. Mag. 152, 1073–1084.
Shellnutt, J.G., Lee, T.-Y., Yang, C.-C., Hu, S.-T., Wu, J.-C., Iizuka, Y., 2016. A mineralogical investigation of the late Permian Doba gabbro, southern Chad: Constraints on the parental magma conditions and composition. J. Afr. Earth Sci. 114, 13–20.
Shellnutt, J.G., Pham, N.H.T., Denyszyn, S.W., Yeh, M.-W., Lee, T.-Y., 2017. Timing of collisional and post-collisional Pan-African Orogeny silicic magmatism in south-Central Chad. Precambrian Res. 301, 113–123.
Shi, B., Li, Z., Xue, L., Yuan, S., Su, Y., Li, Z., 2014. Petroleum accumulation pattern and exploration targets in hydrocarbon rich sags of Melut Basin, southern Sudan. Xinjiang Pet. Geol. 35, 481–485 (in Chinese with English abstract).
Shi, Z.S., Xue, L., Niu, H.Y., Wang, G.L., Chen, B.T., He, W.W., Ma, L., 2017. Accumulation conditions of far-source lithologic reservoirs and exploration strategy in Melut Basin, Central Africa. China Petrol. Explor. 22, 41–49.
Shi, Z.S., Wei, P.S., Wang, L., Xue, L., Pang, W.Z., Chen, B.T., Ma, L., Shi, J.L., Zhao, Y.J., 2021. Formation of the stratigraphic hydrocarbon accumulations of the upper Yabus Formation in the northern sub-basin of the Melut Basin, South Sudan. J. Afr. Earth Sci. 177, 1–13.
Short, K.C., Stauble, A.J., 1967. Outline of geology of Niger delta. Am. Assoc. Pet. Geol. Bull. 15, 761–779.
Song, H.X., Wen, Z.G., Bao, J.P., 2016. Influence of biodegradation on carbazole and benzocarbazole distributions in oils from the Bongor Basin. Chad. Org. Geochem. 100, 18–28.
Sooraj, C.P., Gupta, S., Punekar, J., 2024. Spatio-temporal variability in microfossil and geochemical records of Cenomanian-Turonian oceanic anoxic event-2: a review. J. Palaeogeogr. 13, 646–674.
Srivastava, S.K., 1976. The fossil pollen genus Classopollis. Lethaia 9, 437–457.
Steinig, S., Dummann, W., Park, W., Latif, M., Kusch, S., Hofmann, P., Flögel, S., 2020. Evidence for a regional warm bias in the Early Cretaceous TEX86 record. Earth Planet. Sci. Lett. 539, 116184.
Stuart, G.W., Fairhead, J.D., Dorbath, L., Dorbath, C., 1985. A seismic refraction study of the crustal structure associated with the Adamawa Plateau and Garoua Rift, Cameroon, West Africa. Geophys. J. R. Astron. Soc. 81, 1–12.
Suleiman, A.A., Bomai, A.D., Umaru, A.F., Ali, M.S., Zanna, M., Tarka, A.N., Kaumi, M., Dauda, R.S., Kigbu, L.J., 2019. Understanding the petroleum systems of the Cretaceous Basins: insights from the hydrocarbon exploration records. In: NAPE 2-day Special Workshop on Cretaceous Basins in Nigeria, Extended Abstract, 18-21 (Abuja, May 6-7, 2019).
Tan, M., Zhu, X., Geng, M., Zhu, S., Liu, W., 2017. The occurrence and transformation of lacustrine sediment gravity flow related to depositional variation and paleoclimate in the Lower Cretaceous Prosopis Formation of the Bongor Basin. Chad. J. Afr. Earth Sci. 134, 134–148.
Tang, W.X., Jiang, Z.X., Liu, R.H., Wang, X.Y., 2017. Geochemical characteristics and deposition environment of the Yogou Formation mudstone in the Termit Basin, Niger. Oil Gas Geol. 38, 592–601.
Tissot, B.P., Welte, D.H., 1984. Petroleum Formation and Occurrence, 2nd ed. Springer Verlag, Berlin. 699 p.
Tokam, A.P.K., Tabod, C.T., Nyblade, A.A., Julia, J., Weins, D.A., Pasyanos, M.E., 2010. Structure of the crust beneath Cameroon, West Africa, from the joint inversion of Rayleigh wave group velocities and receiver functions. Geophys. J. Int. 183, 1061–1076.
Tong, X.G., Xu, Z.Q., Shi, B.Q., Dou, L.R., Xiao, K.Y., 2006. Petroleum geologic property and reservoir forming pattern of Melut Basin in Sudan. Acta Pet. Sin. 27, 1–10.
Torsvik, T., Rousse, S., Labails, C., Smethurst, M., 2009. A new scheme for the opening of the South Atlantic Ocean and the dissection of an Aptian salt basin. Geophys. J. Int. 177, 1315–1333.
Touati, Z., 2017. Evidence of bottom-redox conditions during oceanic anoxic event 2 (OAE2) in Wadi Bazina, Northern Tunisia (Southern Tethyan margin). Arab. J. Geosci. 10, 291. https://doi.org/10.1007/s12517-017-3053-6.
Tuttle, M.L.W., Charpentier, R.R., Brownfield, M.E., 1999. The Niger Delta Petroleum System: Niger Delta Province, Nigeria, Cameroon, and Equatorial Guinea, Africa. U. S. Geological Survey Open-File Report 99-50-H, 65.
Udo, O.T., Ekweozor, C.M., 1988. Comparative source rock evaluation of Opuama Channel complex and adjacent producing areas of Niger delta, 3. Nigerian Association of Petroleum Explorationists Bulletin, pp. 10–27.
Umeji, A.C., Caen-Vachette, M., 1983. Rb-Sr isochron from Gboko and Ikuyen rhyolites and its implication for the age and evolution of the Benue Trough, Nigeria. Geol. Mag. 20, 529–533.
Unternehr, P., Curie, D., Olivet, J.L., Goslin, J., Benzarty, P., 1988. South Atlantic fits and intraplate boundaries in Africa and South America. Tectonophysics 155, 169–179.
Unternehr, P., Péron-Pinvidic, G., Manatschal, G., Sutra, E., 2010. Hyper-extended crust in the South Atlantic: in search of a model. Pet. Geosci. 16, 207–215. https://doi.org/10.1144/1354-079309-904.
Vail, J.R., 1989. Ring complexes and related rocks in Africa. J. Afr. Earth Sci. 8, 19–40.
Van Wees, J.D., Stephenson, R.A., Stovba, S.M., Shymanovskyi, V.A., 1996. Tectonic variation in the Dnieper-Donets Basin from automated modelling of backstripped subsidence curves. Tectonophysics 268, 257–280.
Wagreich, M., 2012. "OAE 3" – regional Atlantic organic carbon burial during the Coniacian–Santonian. Clim. Past 8, 1447–1455. https://doi.org/10.5194/cp-8-1447-2012.
Wang, T., Yuan, S., Li, C., Mao, F., Pang, S., Jiang, H., Zheng, F., 2022. Geological structure and dynamic mechanism of the Termit rift basin in West African rift system. Pet. Explor. Dev. 49, 1339–1350.
Wang, J., Bulot, L.G., Taylor, K.G., Redfern, J., 2024. Carbon isotope sratigraphy and biostratigraphy, and associated organic carbon deposition during the late Cenomanian to early Turonian in the Tarfaya Basin, Morocco. Palaeogeogr. Palaeoclimatol. Palaeoecol. 654, 112446.
Wernicke, B., 1985. Uniform-sense normal simple shear of the continental lithosphere. Can. J. Earth Sci. 22, 547–8369. https://doi.org/10.1139/e85-009.
Whiteman, A.J., 1971. The Geology of the Sudan Republic. Clarendon Press, Oxford, UK, 290 pp.
Whiteman, A.J., 1973. Geology and Hydrocarbon Prospects of Nigeria, vols. 1 and 2, pp. 1–257.
Whiteman, A., 1982. Nigeria: Its Petroleum Geology, Resources and Potential, vol. 2. Graham and Trotman, London, United Kingdom, p. 394.
Wilson, M., Guiraud, R., 1992. Magmatism and rifting in Western and Central Africa, from Late Jurassic to recent times. Tectonophysics 213, 203–225.
Winn Jr., R.D., Steinmetz, J.C., Kerekgyarto, W.L., 1993. Stratigraphy and Rifting history of the Mesozoic-Cenozoic Anza Rift, Kenya. Am. Assoc. Pet. Geol. Bull. 77, 1989–2005.
Wolela, A., 2007. Source rock potential of the Blue Nile (Abay) Basin, Ethiopia. J. Pet. Geol. 30, 389–402.
Wolela, A., 2008. Sedimentation of the Triassic–Jurassic Adigrat Sandstone Formation, Blue Nile (Abay) Basin, Ethiopia. J. Afr. Earth Sci. 52, 30–42.
Wolela, A., 2009. Sedimentation and depositional environments of the Barremian-Cenomanian Debre Libanose Sandstone, Blue Nile (Abay) Basin, Ethiopia. Cretac. Res. 30, 1133–1145.
Wolela, A., 2012. Reservoir potential of the Barremian–Cenomanian Debre Libanose sandstone, Blue Nile (Abay) Basin, Ethiopia. J. Cretaceous Res. 36, 83–95.
Wright, J.B., 1985. The Benue Trough and coastal basins. In: Geology and Mineral Resources of West Africa, pp. 98–113.
Wycisk, P., Klitzsch, E., Jas, C., Reynolds, O., 1990. Intracratonal sequence development and structural control of Phanerozoic strata in Sudan. Berl. Geowiss. Abh. 120, 45–86.
Yang, X., Ji, H., Dou, L., Du, Y., Jia, H., Chen, L., Xiang, P., 2020. Tectono-sedimentary characteristics in the area with distributed normal faults: Lower Cretaceous Prosopis Formation in the northern slope of Bongor Basin. Chad. J. Pet. Sci. Eng. 190, 107081.
Yassin, M.A., Hariri, M.M., Abdullatif, O.M., Korvin, G., Makkawi, M., 2017. Evolution history of transtensional pull-apart, oblique rift basin and its implication on hydrocarbon exploration: a case study from Sufyan Sub-basin, Muglad Basin, Sudan. Mar. Pet. Geol. 79, 282–299.
Ye, J., Chardon, D., Rouby, D., Guillocheau, F., Dall'asta, M., Ferry, J.-N., Broucke, O., 2017. Paleogeographic and structural evolution of northwestern Africa and its Atlantic margins since the early Mesozoic. Geosphere 13, 1254–1284. https://doi.org/10.1130/GES01426.1.
Yuan, S., Zhai, G., Mao, F., 2022. Risk exploration in superimposed rift basin: Case studies of Agadem/Bilma/Tenere blocks in Termit Basin, Niger. China Pet. Explor. 27, 63–74.
Yuan, S., Dou, L., Cheng, D., Mao, F., Pan, C., Zheng, F., Jiang, H., Pang, W., Li, Z., 2023. New understanding and exploration direction of hydrocarbon accumulation in Termit Basin, Niger. Pet. Explor. Dev. 50, 238–249.
Zanguina, M., Bruneton, A., Gonnard, R., 1998. An introduction to the petroleum potential of Niger. J. Pet. Geol. 21, 83–103.
Zeng, Z., Zhu, H., Yang, X., Ji, S., Zhang, Z., Huang, X., 2024. Depositional characteristics of fine-grained sedimentary rocks and the links to OAE-3 and PETM of the Upper Cretaceous-Paleogene Madingo Formation, lower Congo Basin, West Africa. Mar. Geol. 467, 107206.
Zhang, X., Zhu, L., Wang, T., Shi, X., Han, B., Shen, J., Gao, H., 2024a. Fluid property identification of the Lower Cretaceous reservoirs with complex oil-water contacts in Deseo Basin. Chad. Energy Geosci. 5, 100219.
Zhang, B., Zhu, H., Yang, X., Zeng, Z., Sun, Z., Pang, L., Yao, T., 2024b. Depositional characteristics in the lower Congo Basin during the Cenomanian-Turonian stage: Insights from fine-grained sedimentary rocks. Mar. Pet. Geol. 170, 107151.
Zhao, J., Dou, L., 2022. Discovery of early Mesozoic magmatism in the northern Muglad Basin (Sudan): Assessment of its impacts on basement reservoir. Front. Earth Sci. 10, 853082. https://doi.org/10.3389/feart.2022.853082.

Zhao, W., Shi, Z., Li, S., Chen, B., Luo, X., Pang, W., 2020. Petroleum geological characteristics and hydrocarbon accumulation patterns in the Melut Basin, South Sudan. Arab. J. Geosci. 13, 1149.

Zhou, L., Su, J., Dong, X., Shi, B., Sun, Z., Qian, M., Lou, D., Liu, A., 2017. Controlling factors of hydrocarbon accumulation in Termit rift superimposed basin, Niger. Pet. Explor. Dev. 44, 358–367.

Ziegler, P.A., Cloetingh, S., 2004. Dynamic processes controlling evolution of rifted basins. Earth Sci. Rev. 64, 1–50.